UNIVERSITETET I AGDER

Voltage Regulation of a Distribution Grid with Distributed Generation

Kim-Rune Kastet

June, 2013

Supervisor:
Stein Bergsmark, UIA

Co-supervisors:
Mohan Lal Kolhe, UIA
Bjarne Tufte,Agder Energy
Rolf Håkan Josefsen, Agder Energy

Department of Engineering Sciences
Faculty of Engineering and Science
University of Agder

Summary

The expansion of distributed generation has seen a significant increase over the last decade, and has lead to an increase of two-way power flow in the power-grid. These DG units are often built in areas where the power-grid has low transmission capability. As a result, the introduction of DG units causes the voltage to rise in the given area, and the total voltage variation increases. This report focuses on the reactive co-operation of DG units to reduce the voltage variations, and compares this to the common measure of replacing power lines.

The distribution grid under study, Øie-Kvinesdal, contains 4 main radials, Kvinesdal, Guseland, Høylandsfoss and Gyland, which are located in the southern part of Norway. The Kvinesdal radial is currently experiencing high voltage variations due to 7 installed DG units, which have a total output of about 27 MW. Moreover, there are plans for 12 new DG units, with a total output of about 32MW. As shown with simulations by Norconsult [10], the DG units will cause a voltage variation which significantly violates the given limits even when a new production radial is introduced.

In this report two main cases have been studied, one main case to assess the effects of reactive co-operation of the DG units. Here 9 different subcases were simulated, to fully show the effect of reactive power upon the grid voltage. The second main case in the report deals with the change of feeder in the radial, and compares this to the reactive co-operation. Here 3 subcases where simulated, to show the benefits of changing feeder segments.

Simulation results clearly show that reactive co-operation of DG units alone can only reduce the voltage variations by some 1-2 percent. As a result, additional measures have to be taken to further reduce the voltage variation. By adding a shunt reactor of 1,30 MVAr running at full capacity at the end of the radial, it is possible to reduce the voltage variation down to about 8,3 %. By changing the main feeder in the radial from FeAl 120 to 454-Al-59, the voltage variation is reduced to 7,6 %.

The conclusion is that it is preferable to change the feeder in the Kvinesdal radial, as this will give a smaller voltage variation, a more robust grid and lower transmission losses. In addition, further work is recommended on the characteristics of the 454-Al-59 feeder, as it is considered to be more easily influenced by reactive power, as compared to the common FeAl 120 feeder.

Preface

This report *"Voltage Regulation of a Distribution Grid with Distributed Generation"* is the result of the finishing work in the course ENE500 at the 2 year duration masters program at the University of Agder. The master thesis was done in the spring of 2013 by Kim-Rune Kastet, in collaboration with Agder Energy and RFF Agder. As the thesis will be a part of the project *"Grid Operation and Distributed Energy Storage: Potential for improved grid-operation efficiency"* by RFF Agder.

The thesis deals with the reactive co-operative of DG units, and the grid simulated is a genuine distribution grid located in the southern part of Norway, and is called the Kvinesdal grid. The report shows how the reactive co-operation of the DG units in this radial can help diminish the voltage variation in the grid, and compares this to the common measure of changing the main feeder in the grid.

The thesis could not have been done without the excellent guiding from the following people:

- Stein Bergsmark, Head of ICT, University of Agder
- Rolf Håkan Josefsen, Engineer, Agder Energy AS
- Bjarne Tufte, Manager Grid Strategies Department, Agder Energy AS
- Mohan Lal Kolhe, Professor in Electrical Power Engineering, University of Agder
- Kjell Morgan Ose, Engineer, Agder Energy AS
- Jørgen Tingstveit, Teacher, Tertiary Vocational School of Southern Norway

Definitions

Symbol	
δ	Torque angle of synchronous generator
θ	Angle between generator output voltage V_ϕ and internal generated voltage E_A
E_A	Internal generated voltage in synchronous generator
f_e	Power system frequency
n_{sync}	Speed of magnetic field in a asynchron generator
n_m	Mechanical speed $\frac{r}{min}$
N_P	Number of windings on primary side of transformer
N_S	Number of windings on secondary side of transformer
P	Active Power
P_m	Number of poles in a generator
PF	Powerfactor($cos\theta$)
Q	Reactive power
R_A	Stator resistance in synchronous generator
S	Apparent power
U_N	Nominal voltage
V_F	DC voltage supplying the rotor field on synchronous generator
V_P	Voltage of primary side of transformer
V_ϕ	Output voltage from synchronous generator
V_S	Voltage of secondary side of transformer
X_S	Synchronous reactance of synchronous generator
Abbreviation	
AEN	Agder Energy grid division
AVR	Automatic Voltage Regulator
BL	Circuit breaker
BS	Circuit breaker
CVVC	Central Volt Var Control
DG	Distributed Generation
DSSE	Distribution System State Estimator
HLLP	Heavy Load Light Production
KA	Cable
LV	Low Voltage
OLTV	On Load Tap Changer
POC	Point Of Connection
PV	Photovoltaics
REN	Rational Electrical Network operations
SCADA	Supervisory Control and Data Acquisition
SI	Fuse
TC	Current transfomer
TSO	Transmission System Operator
UNFCCC	United Nations Framework Convention on Climate Change
VVC	Volt Var Control

Contents

List of Figures

List of Tables

Chapter 1

Introduction

As the worlds electricity demand increases, more environmental constraints is given to conventional energy sources such as fossil or nuclear energy. This comes as a direct result of the problem with global warming, where the emissions from energy production from fossil fuels are a big contributor. Which is clearly emphasized by the fact that in 2008, 81% of the worlds energy was produced by fossil fuels [18]. As a counter-reaction in Europe, the EU have launched a climate and energy package, known as the 20-20-20 targets. Where the following goals have been established:

1. 20% reduction in EU greenhouse gas emissions from 1990 levels
2. Raising the total share of EU energy consumption produced from renewable resources to 20
3. 20 % improvement in the EU's energy efficiency

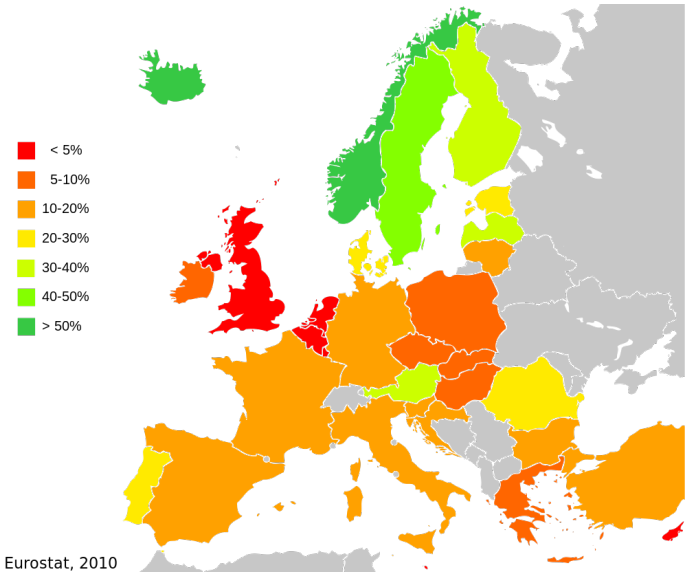

Figure 1.1: Proportion of renewable energy in the EU, candidate countries and Norway as percentage of total energy consumption, 2010 [19]

As shown in Figure 1.1 one can see that there is a considerable way to go to fulfill the 20% portion of renewable. As the demand for alternative renewable energy sources rise, an outburst of distributed generators (DGs) and smartgrid concepts can be observed [17]. This especially in Norway, due to the fact that over

99% of electricity produced on the mainland is covered by hydropower already. Therefore, to increase the production of electricity even more, additional sources are needed. However, due to the fact that most of the main watercourses already are exploited, one have now turned to distributed generators like on and off-shore windpower and small scale hydropower [20].

1.1 Motivation

Distributed generation (DG) of electric power has in recent years become more and more common, due to the large increase in generation from renewable energy sources such as small hydropower stations, wind turbines, photovoltaics (PV) etc. The definition for such units can be as described by T.Ackermann [3] :

> In general, DG can be defined as electric power generation within distribution networks or on the customer side of the network .

These units vary in size in the range of ≤ 10 MW [1], and are often connected to fragile distribution grids. Thus, causing a rise in voltage which in worst case can cause electrical components to fail. By coordination of reactive power production/consumption of DG units in the same distribution grid, it is possible to lower the voltage as described in citec15.

Originally the power grid was designed for a one-way power flow, where reactive and active power was to be distributed to consumers from the central grid and down to the distribution grid. This grid in turn works as a link between the regional grid and the low voltage network (<1kV) as shown in Figure 1.2.

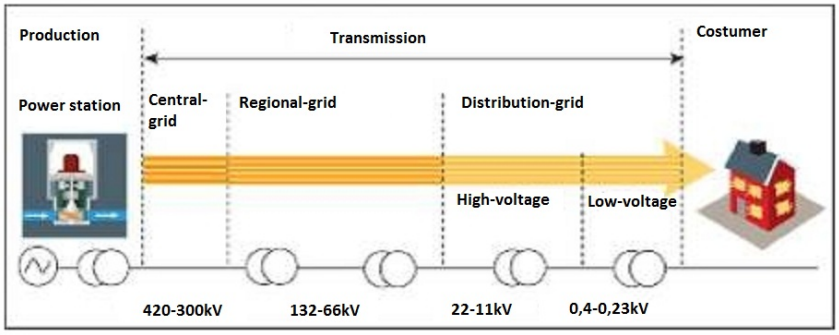

Figure 1.2: Classical power grid overview [2]

Being the last link to the consumer, the distribution grid was built in a radial structure, where the cross section of cables and power lines are reduced as the load decreases. Since DG units often are connected at this level the characteristics of the distribution grid change from being a "passive" grid to a more and more "active" grid.

In a "passive" grid the power is one-way directed and the voltage is decided by the load. In an "active" grid one has two-way power flow. DG units which produce active and/or reactive power or consumes reactive power, will in such an active grid influence the voltage, power flow, power quality, power system stability and fault situations [4].

The distribution grid under study, Øie-Kvinesdal, contains 4 main radials (Kvinesdal, Gusedal, Høylandsfoss and Gyland) and are located in the southern part of Norway. The main focus will be on the Kvinesdal radial, since it has the highest DG concentration. presently there are six synchronous and one asynchronous generators installed on this radial, where the largest generator has a rated output of 10,00 MW and smallest has 0,35 MW. However, there are plans for twelve additional DG units, with rated output ranging from 13,60 MW to 0,10 MW. Currently one has a critical situation in the Kvinesdal radial with regards to high fluctuations in voltage, this due to the high voltage rise caused by the all ready existing DG units [10].

1.2 Problem Statement

This MSc thesis focuses on the voltage control of distributed generation (DG) units through reactive co-operation, and how this control can help keeping the voltage within legal limits in grids with high density of distributed generation. The thesis also covers renewal of power lines in order to compare traditional measures to the mentioned voltage control.

The Kvinesdal distribution grid, located in Vest-Agder county in Norway will be the basis for simulations and calculations. The voltage in this grid is 22 kV, and it has 4 main radials (Kvinesdal, Gusedal, Høylandsfoss and Gyland). Currently there are 10 DG units connected to the grid, with a total output of 41,0 MW. Furthermore, there are plans for 21 new DG units, with a total output of 52,3 MW.

A description of the current situation in the grid, with and without new DG units will be based on a study made by Norconsult. This description will be used as a basis for comparison to the two main cases in the thesis, which are:

1. Reactive co-operation of DG units.
    - Feasibility
    - Cost
    - Voltage quality
    - Load levels
2. Renovation or renewal of the transmission lines.
    - Feasibility
    - Costs
    - Voltage quality
    - Load level

The project work will mainly address steady state analysis, where the key scenarios are High Load Low Production (HLLP) and Low Load High Production (LLHP).

Furthermore, if time allows, the following case can be included.

3. Dynamic analysis of faults such as drop out of generators or transmission lines.

The simulation tool will be NetBas.

1.3 Key Assumptions and Limitations

The following assumptions and limitations have been made for this thesis:

- Case 1
    - All DG units with the exception of Oksefjell are assumed to be able to operate at -0,33 $\leq tan\phi \leq$ 0,48.

  - Thermal limits of components are not included
  - The economic aspect will only deal with the expenses related to the upgrade of communication.
  - The control of the DG units will not be simulated. However, a suggestion for control system based upon a report from Salzburg Netz [16] will be included.
  - The practical implementation of the control system is not considered.

- Case 2
  - All DG units are able to run at PF=1, regardless of the voltage levels being too high/low.
  - Thermal limits of the components are not included.
  - The practical issues regarding the replacement of the feeder is not considered.
  - The economic aspect will only deal with the cost of the feeder, and the demolition of the old line.

1.4 Methods and Tools

All simulations in this report will be done with NetBas, which is a power system analysis program developed by Powel. Models used will be developed on the basis of former models supplied by Norconsult, and simulations will be done in the module Maske in NetBas. The simulations will be of trial and error type, this due to the fact that the simulations will be of steady state.

1.5 Report Outline

This report starts by introducing important basic principles in chapter 2 Power System Theory, as these principles are key to fully understanding the thesis. Chapter 3 deals with a prior study of the network radial under study, and gives an overview over the current operating situation. Chapter 4 deals with the first case, which is reactive co-operation of DG units. Presented in this chapter is a suggestion for control of the DG units, and multiple simulations cases to show how reactive power influences the voltage in the grid. Chapter 5 deals with renewal of power lines, and shows how changing the current FeAl 120 feeder with a 454-Al-59 feeder influences the voltage in the radial. Chapter 6 presents a discussion of the findings in chapter 4 and 5. Where chapter 7 gives a conclusion on the findings. Other relevant material is presented in appendices.

Chapter 2

Power System Theory

This chapter explains the basic principles of generators, regulators and load situations. Moreover, some selected parts of the legislation will be reviewed, as all this information is key to fully understanding this work.

2.1 Generators used in DG units

2.1.1 The Synchronous Generator

The theory in section 2.1.1 is taken from Chapman [5], and concerns three-phase machines. As the term synchronous implies, the generator operates at synchronous speed, and the relation between the system frequency and mechanical frequency is shown in Equation. 2.1.

$$f_e = \frac{n_m \cdot P_m}{120} \tag{2.1}$$

$n_m =$ Mechanical speed $[\frac{r}{min}]$
$f_e =$ System frequency [Hz]
$P_m =$ Number of poles in the machine

Furthermore, the rotor in such a generator can have two different designs. The magnetic poles on the rotor can be salient or nonsalient, where salient means sticking out. Hence, a salient pole, is a pole that sticks out from the surface of the rotor as shown in Figure 2.1

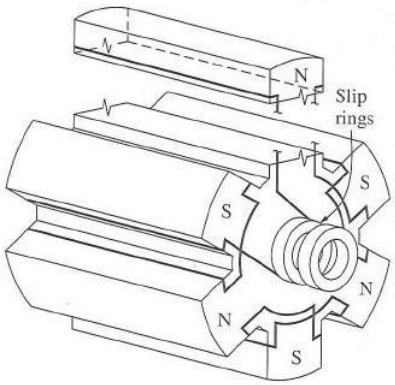

Figure 2.1: A salient six-pole rotor of a synchronous machine [5]

Nonsalient rotors have the opposite design, in other words the poles are not sticking out. As one can see from Figure 2.2 the poles are aligned such that the surface of the rotor is uniform.

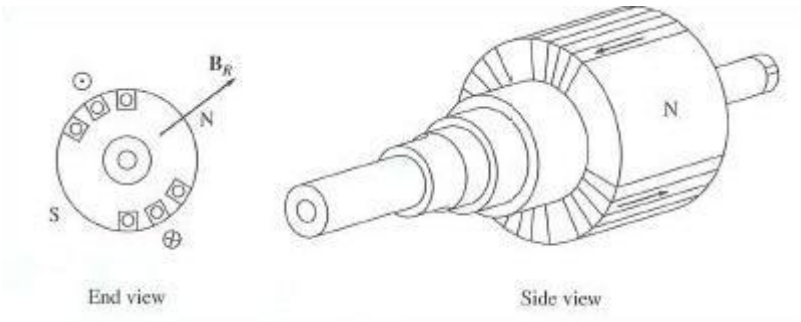

Figure 2.2: A nonsalient two-pole rotor of a synchronous machine [5]

While nonsalient rotors are used for two to four pole rotors, salient rotors on the other hand are usually used for rotors with four or more poles. Hence, large generators are usually salient.

Figure 2.3 shows the per-phase equivalent circuit of a synchronous generator. Here one has combined the internal field circuit resistance and the external variable resistance into a single resistor R_F. R_A in the figure is the stator resistance, and X_S the synchronous reactance of the machine. Furthermore, E_A represents the internal generated voltage, V_ϕ is the output voltage, and V_F the dc voltage supplying the rotor field circuit. I_A represents the stator current, and I_F the magnetizing current.

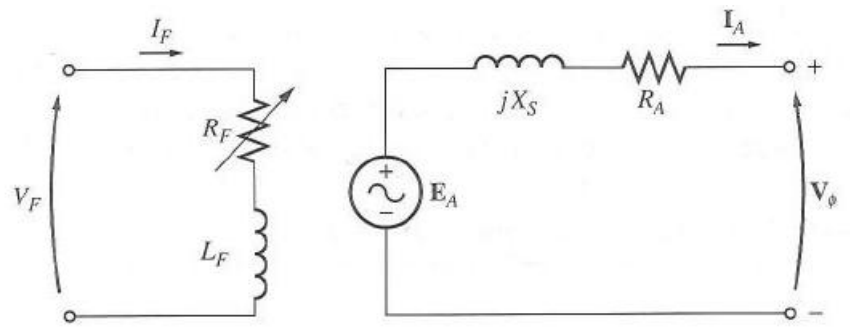

Figure 2.3: The per-phase equivalent circuit of a synchronous generator. [5]

The relation between V_ϕ and E_A is shown in Equation 2.2.

$$V_\phi = E_A - jX_S I_A - R_A I_A \tag{2.2}$$

$V_\phi =$ Output voltage [V]
$E_A =$ Internal generated voltage [V]
$X_S =$ Synchronous reactance of the machine
$I_A =$ Stator current [A]
$R_A =$ Stator resistance [Ω]

Moreover, the synchronous generator can operate in overexcited mode or under-exited mode. The difference is that in overexcited mode the generator produces reactive power, where in the under-exited mode the generator consumes reactive power. The phasor diagram for a synchronous generator is shown in figure 2.4. Here one can see the phasor angle, θ, which shows the angle between the generators output voltage and internal generated voltage. The generators power factor (PF) is decided by this angle, by the relation $PF = cos\theta$. The angle θ can also be calculated on the basis of the generators production/consumption of reactive power and production of active power as shown in Equation 2.3.

$$\theta = \arctan \frac{Q}{P} \tag{2.3}$$

When I_A is lagging V_ϕ the generator is running overexcited, and when I_A is leading V_ϕ the generator is running underexcited. Hence, when the generator runs at PF=1, it doesn't produce or consume reactive power.

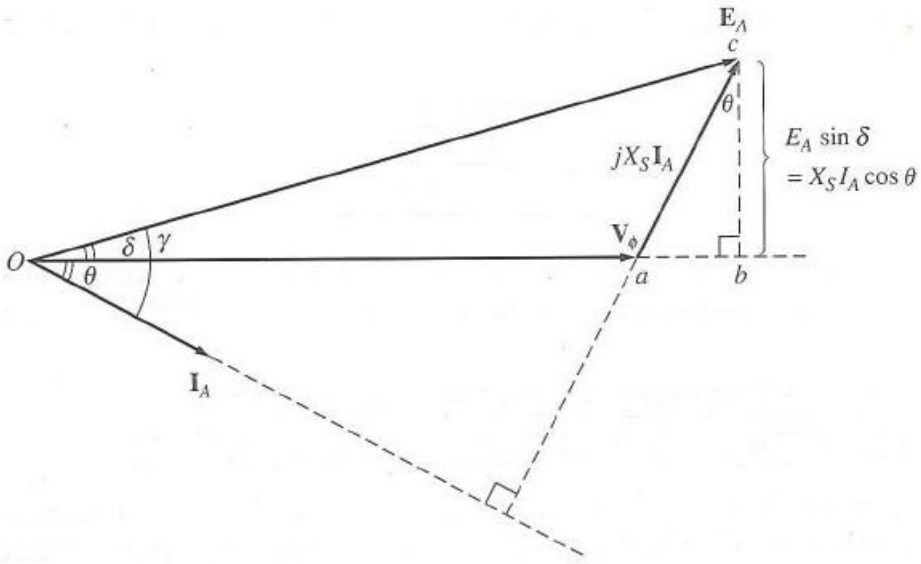

Figure 2.4: Simplified phasor diagram with armature resistance ignored. [5]

The angle δ is know as the torque angle, and from equation 2.4 one can see that maximum power occurs at $\delta = 90\,°$.

$$P = \frac{3 \cdot V_\phi \cdot E_A \cdot sin\delta}{X_S} \tag{2.4}$$

The magnetizing system for a synchronous generator deliveres dc current to the field windings, which in turn generates the magnetic field in the rotor. There are 2 different ways of generating this DC power:

1. Supply the DC power from an external DC source to the rotor by means of slip rings and brushes.
2. Supply the DC power from a special DC power source mounted directly on the shaft of the synchronous machine.

The brushes used in this external feeding are of course worn down eventually, and hence they need replacement after a while. As a result, the brushless type of DC power is preferred by many, since this system doesn‘t need as much maintenance. Figure 2.5 illustrates a brushless magnetizing system for a synchronous generator. As one can see a three phase current is rectified and used to supply the field circuit of the exciter, this again is located on the stator. The output of the armature circuir of the exciter (on the rotor) is then rectified and usted to supply the field current of the main machine.

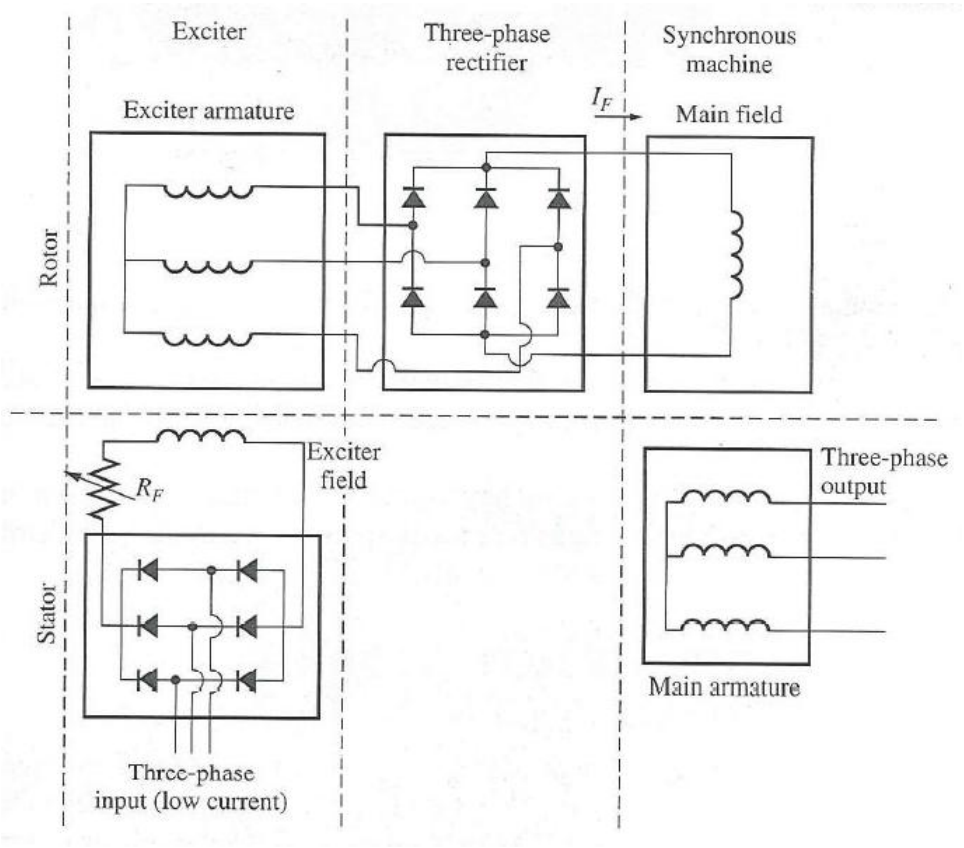

Figure 2.5: A brusless exciter circuit [5]

Furthermore, to supply the DC current one usually has a small pilot exciter included in this system. As explained by Chapman [5]:

> To make the excitation of a generator completely independent of any external power sources, a small pilot exciter is often included in the system. A pilot exciter is a small AC generator with permanent magnets mounted on the rotor shaft and a three-phase winding on the stator. It produces the power for the field circuit of the exciter, which in turn controls the field circuit of the main machine. If a pilot exciter is included on the generator shaft, then no external power is required to run the generator.

2.1.2 The Asynchronous Generator

Explanations and equations in this section are taken from Chapman [5]. In an asynchronous generator the physical stator is the same as that of a synchronous generator, but with a different rotor construction. A three phase set of stator currents produces a magnetic field which rotates with synchronous speed (n_{sync}). The speed of the rotating field n_{sync} is a function of the system frequency (f_e) and number of poles in the machine (P) as shown in equation 2.5.

$$n_{sync} = \frac{120 \cdot f_e}{P_m} \tag{2.5}$$

$n_{sync} =$ Speed of magnetic field's rotation $[\frac{r}{min}]$
$f_e =$ System frequency [Hz]
$P_m =$ Number of poles in the machine

Furthermore, an advantage with the asynchronous generator is that no DC field current is needed to run the generator. The rotor voltage is induced in the rotor windings, as opposed to the being connected by wires. Hence, these machines is commonly known as induction machines. In addition to not being in need of an DC field current, the asynchronous generator automatically synchronizes with the power system. Which in turn makes the controls simpler and low cost. Moreover, the asynchronous generator is also more readily available on the market than the synchronous generator and less expensive.

As one can see from the points made, this type of generator has many advantages. But the reasons why it's not commonly used on larger power plants are the following:

1. The asynchronous generator can only run in inductive mode. Hence, it is unable to produce reactive power.
2. It is unable to contribute to system stability, in other words the maintenance of system voltage levels. Hence one can call the asynchronous generator a voltage following machine.
3. As a result of point nr 2, it is not suitable for separate, isolated operation.
4. The efficiency of the asynchronous generator is generally lower than that of the synchronous generator.

As a result of these points, the asynchronous generator are commonly used for small DG units where private investors are mostly interested in cost and availability. Hence, for DG units of the size $\geq$ 1MW, synchronous generator is the preferred choice

2.2 Stability in Distribution Grids with DG Units

2.2.1 Voltage supporting and voltage following Machines

In power systems one can have two types of generators, voltage supporting or voltage following. These two categories are defined in [6] as follows:

- *Voltage supporting generators* are those which would be expected to aid in the regulation of the system voltage. Generators in this group are large machines with large rotating mass.

- *Voltage following generators* are those which would not be expected to aid in the regulation of the system voltage, but rather follow the variations of the system voltage. Generators in this group are small machines with a small rotating mass.

Synchronous generators working as voltage supporting generators, instead of voltage following generators, improve the system voltage stability. However, in distribution grids with all ready installed voltage regulation devises such as tap changers, capacitor banks etc, one can experience problems when the control of the voltage is not coordinated properly.

2.2.2 Voltage Regulator

The definition of a voltage regulator is described in IEEE standard 421.1 [7]:

> A synchronous machine regulator that functions to maintain the terminal voltage of a synchronous machine at a predetermined value, or to vary it according to a predetermined plan.

To maintain the desired voltage, the voltage regulator adjusts the magnetizing current I_F which is supplied to the generator. An illustration of a synchronous generator with a brushless magnetizing system and automatic voltage regulator (AVR).

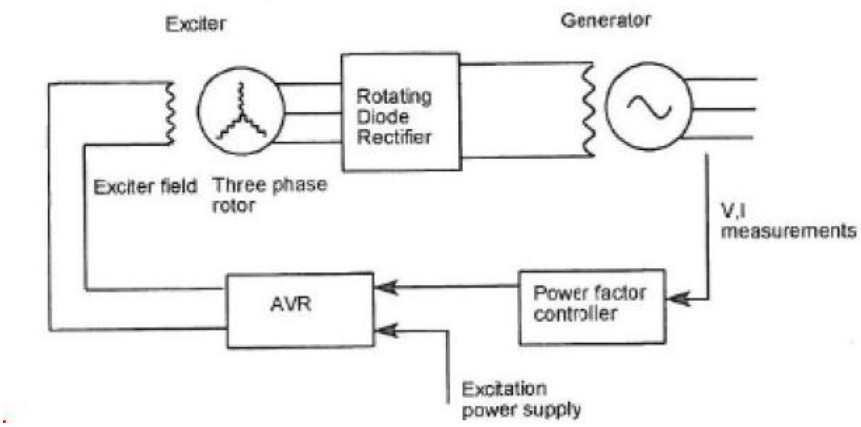

Figure 2.6: Brushless magnetizing system with AVR [4]

A voltage regulator can be set at two different operation modes, automatic control (AVR) or manual control. When set to manual control, the excitation level is held constant and adjusted by the operator directly. When set to automatic control, the excitation is automatically adjusted. This in turn holds the generator terminal voltage at the reference level which is predetermined by the operator or plant controls. If the controller experiences a drop in generator terminal voltage, it will increase the magnetizing current I_F. This increase is followed by a increase in the generator reactive power output, as an excitation system cannot control voltage and reactive power independently. And of course the opposite will happen if the generator terminal voltage increases .

As a result of this dependency, voltage regulators are typically equipped with overexcitation limiters. This to prevent the excitation system output from exceeding the thermal limit of the generator field, which in turn also limits the maximum reactive power output.

Moreover, to obtain the best support possible, one should have AVR in all voltage supporting generators as stated in [6]:

> Voltage regulator control should be utilized on all voltage supporting machines, since it provides superior voltage support during changing system voltage conditions. Underexcitation and overexcitation limiters are typically utilized to prevent excessive excursions in excitation.

2.2.3 VAr/PF control

Some regulators has Var/PF control as an optional setting, this makes it possible to set the regulator to a predetermined value of reactive power or PF. The definition of the Var/PF control is described in IEEE standard 421.1-2007 [7]:

> A function that acts through the adjuster to modify the voltage regulator set point so as to maintain the synchronous machine steady-state reactive power at a predetermined value.

This type of control has the downside of preventing excitation systems from providing voltage support during system disturbance. As a result, one should not use this type of control on voltage supporting generators as stated in [6]:

> Var/PF controllers should generally not be specified or utilized on generators intended to operate as voltage supporting machines, since they prevent needed steady state voltage support during periods of prolonged system voltage excursion.

2.2.4 Distribution System State Estimation (DSSE)

To control DG units one need a full overview over the situation in the distribution grid. By implementing DSSE one can get an approximation on the grid situation and act accordingly.

As stated in Section 1.1 *Motivation*, the current distribution grid is a passive one. And as a result, the network can only allow a restricted amount of DG capacity. To increase this capacity one need to have a significant reinforcement of the communication network, such that a more active grid is established.
The transmission systems today operate with state estimation (SE), as SE is a fairly routine task there exist a number of established methodologies. However, these methodologies can‘t be directly transferred into DSSE due to the difference in network topology and characteristics [8].
As the measurement data for the distribution system are purely statistical, DSSE have to rely on measurements of the pseudo type. Hence, the performance of a DSSE is based on the quality of these statistical measurements [8].

2.3 Legislation

2.3.1 Rational Electrical Network operations (REN)

REN has formulated the standard agreement that is used when new DG units are to be built. In this report Appendix 3 is of special interest as it deals with the technical requirements [9].

For the synchronous generator, there are several special technical requirements regarding production or drawing of reactive power. Firstly, the generator should be dimensioned for PF in the in the range of 0,95-1,0 when drawing reactive power. When supplying reactive power, the generator should be dimensioned for PF in the range 0,9-1,0. This is equivalent of $\tan\phi$ in the range -0,33 up to 0,48. This range is shown in figure 2.7.

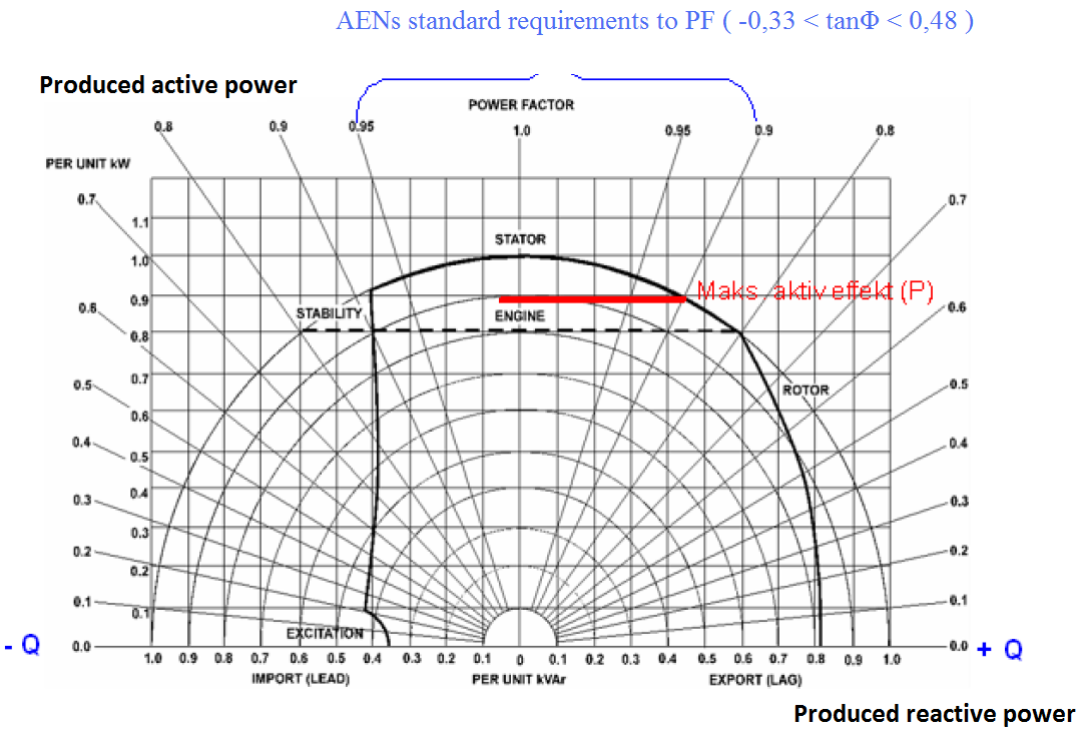

Figure 2.7: Capabilitycurve of synchronous generator[9]

Secondly, the DGs generator should be dimensioned for a wider range of PF if analyses of the grid showsuch a necessity. However, the generator is not allowed to drawn more reactive power than $\tan\phi <$ -0,5, this due to the interests of stability and reactive power backup in the grid.

Thirdly, for the generator to be able to produce maximum active power in the range of -0,33 $\leq \tan\phi \leq$ 0,48 , one has to run the generator at 90 % of rated output (S_N).

Lastly, for all DG-units with synchronous generator of size > 1,0 MVA, its mandatory to install regulator of type AVR. VAr/PF control can only be implemented is this has been discussed with the Transmission System Operator (TSO). For DG-units with synchronous generator of size < 1,0 MVA VAr/PF control can be implemented, but if system analysis show that there is a need for better control, then AVR is once again mandatory.

For asynchronous generators there are technical requirements regarding reactive power. As mentioned in section 2.1.2 asynchronous generators draw reactive power from the grid. As a result, automatic compensation of reactive power has to be installed if challenges arise in keeping the voltage in the grid within required limits. This compensation will ensure that the delivered power at point of connection (POC) is within the span of $\tan\phi =$ -0,33 to 0,48, at full production.

2.3.2 AEN defined requirements

As stated in Norconsult's report, AEN has defined the following requirements regarding the voltage quality in the high voltage part of the distribution grid [10].

1. The voltage fluctuation is not to exceed 7 %. The deviation is measured as the difference between the maximum and minimum voltage level in every single point in the grid.
2. The maximum drop in voltage in radials is not to exceed 8 %, when the point of reference is the substation which the radials are connected.

Furthermore, AEN has also stated the following limits for termal loading of components:

Table 2.1: Thermal limits for Distribution Grid components [10].

Component	Under normal conditions	Under abnormal conditions
Kables	80 %	100 %
Power lines	100 %	120 %
Transfomer (winter)	120 %	120 %
Transfomer (summer)	100 %	100 %

Moreover, reinforcement measures are recommended if the connection of DG units cause these limits to be exceeded.

2.3.3 Regulations of quality of supply in the power system

In this act, §3-3 and §3-5 are of special interest, since they cover the slow voltage variations and limits for quick step changes in the grid [11].

> As stated in § 3-3: The grid company is responsible for keeping the voltage value within ± 10% of the nominal voltage. Measured as an average over the time span of one minute, in the POC in the low voltage (LV) grid.

> As stated in § 3-5: The grid company is to make sure that step changes in voltage do not exceed the following values in POC, with the nominal voltage of $U_N[kV]$ as show in table 2.2.

Table 2.2: Maximum allowed rapid step changes in voltage per day [10].

	0,23 $\leq U_N[kV] \leq$ **35**	**35** $< U_N$
$\triangle U_{stationary} \geq 3$ %	24	12
$\triangle U_{max} \geq 5$ %	24	12

2.3.4 The Energy Act

The energy act is the overarching legislation for grid companies in Norway. In this thesis it is important to emphasize §3-4, as it deals with the connection of DG units:

> Anyone who have licenses for transmission facilities as stated in this act, are obliged to connect new production installations and new installations for the extraction of electrical energy which is not covered by §3-3, and if necessary invest in grid installations. The same requirement applies when an increase of production and consumption leads to a need for investment in grid installations. The obligation to make necessary investments in transmission grids as stated in this act applies to all concessionaires, where the connection triggers a need for grid investment. The ministry may grant exemptions from the duty of connection- and investment for production, if the initiative isn‘t beneficial for society. Moreover, the ministry can also in exceptional cases grant exemptions from the duty of connection- and investment for consumption.

2.4 Voltage Variation

2.4.1 Seasonal Voltage Variation

At normal operation of the grid, one can expect to have voltage variation according to the load at a designated area. Furthermore, this load will generally be high in the winter, when additional power for heating is needed. Hence one get a plot like Figure 2.8, showing the seasonal voltage variation, were Heavy Load No Production (HLNP) usually occurs in winter time.

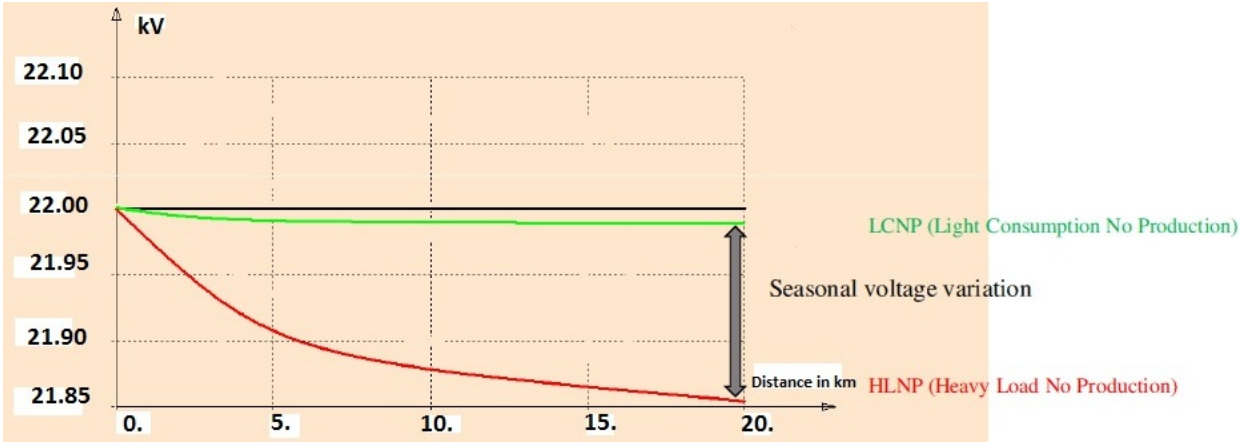

Figure 2.8: Example of voltage profile for distribution grid without DG units [12]

When implementing DG units, one will have the challenge of dealing with a higher seasonal voltage as shown in figure 2.9.

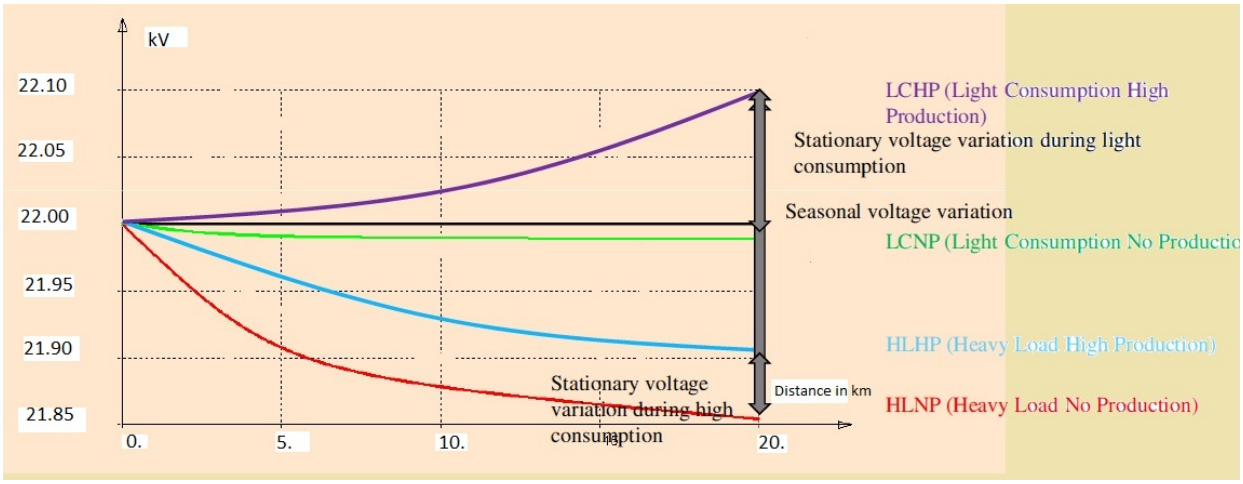

Figure 2.9: Example of voltage profile for distribution grid with DG units [12]

Before implementing the DG units, the seasonal voltage variation was the difference between LCNP and HLNP. But after the implementation, one can clearly see that there is a considerable higher difference between LCHP and HLNP. This additional change in seasonal voltage variation can cause challenges, especially regarding the regulations mentioned previously [11].

2.4.2 Variations on the Distribution Grids low voltage (LV) Side

The variations experienced in on the high voltage (HV) side, will directly influence the voltage on the LV side. Since the transformer transforms voltage according to equation 2.6 [5].

$$\frac{V_S}{V_P} = \frac{N_S}{N_P} \tag{2.6}$$

$V_S =$ Voltage of secundary side of the transfomer
$V_P =$ Voltage of primary side of the transfomer
$N_S =$ Number of windings on the secondary side of the transfomer
$N_P =$ Number of windings on the primary side of the transfomer

Hence one can get voltage variation in the households, which in worst case can exceed the legal limits as shown in Figure 2.10 and 2.11.

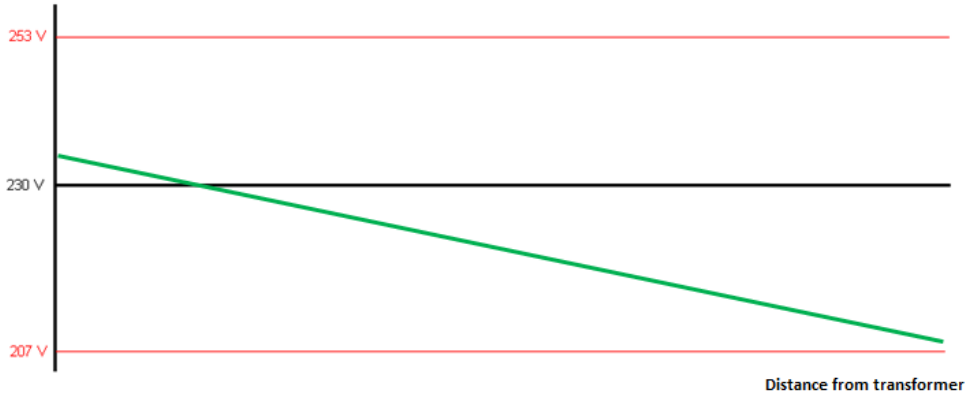

Figure 2.10: Example of voltage profile for LV distribution grid without DG units on HV side [13]

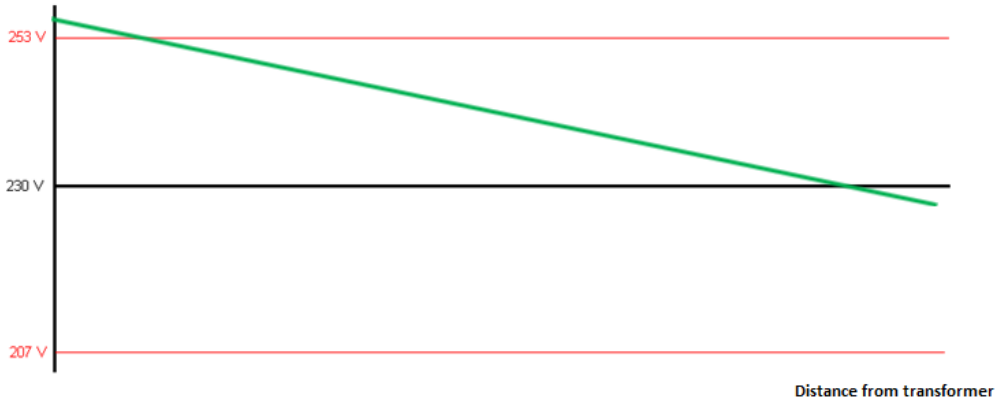

Figure 2.11: Example of voltage profile for LV distribution grid with DG units on HV side [13]

As one can see from these figures, before implementing the DG in the distribution grid one had an acceptable voltage profile. However, after implementation one can see that the legal limit of ± 10% is exceeded. The households closest to the transformer has a voltage higher than 253 V.

2.5 On-Load Tap Changer Transformer

Keeping the voltage within the legal limits mentioned in section 2.3 is a difficult task indeed. The distribution transformers between HV and LV have the possibility of regulating this voltage through a series of taps in the windings, which in turn allows for small changes in the turn ratio of the transformer. However, these transformers cannot normally be changed while the transformer is loaded, and the taps need to be tuned manually. As a result, one usually sets the taps once and then leave it be.

Even so, there are transformers that are able to change taps while loaded. Such transformers are called On-Load Tap Changer (OLTC) transformers, and often such transformers have built-in voltage sensing circuitry which automatically changes taps to keep the system voltage constant [5]. A simple illustration of this concept is shown in figure 2.12.

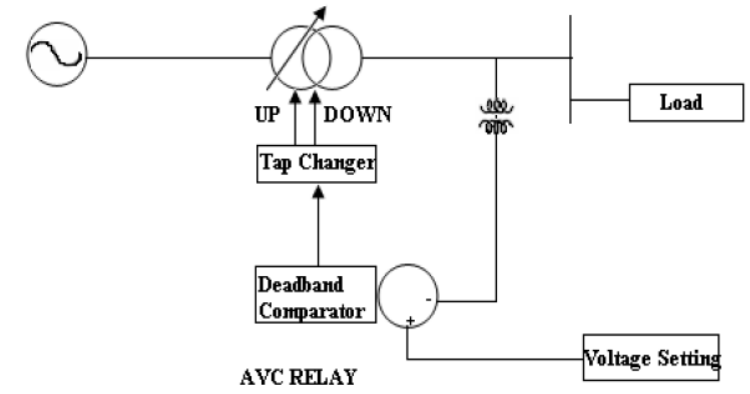

Figure 2.12: Simple illustration of ONTC transformer scheme [14]

As one can see from this simple block diagram, it illustrates the basic operation of the OLTC and a simple Automatic Voltage Control(AVR) relay. By having a measurement of the voltage on the secondary side of the transformer, and comparing this to a reference voltage setting the transformer can adjust the voltage accordingly.

However, such transformers are usually used to transform from 22 kV down to 11 kV or 6,6 kV. As a result, the whole radial connected to the transformer gets the voltage shifted when the transformer initiates a tap change.

Chapter 3

Prior study of Network Radial

To fully see the benefits of the implementation of DG units in co-operative reactive power mode, a reference is needed. This chapter gives such a reference and is based on a study made by Norconsult [10]. It contains detailed descriptions of relevant DG units, point of connection(POC), localizations, voltage profiles and load conditions.

3.1 Background

The distribution grid discussed in this thesis is located in Kvinesdal municipality in Vest-Agder county, Norway. and has a nominal operating voltage of 22 kV. The grid is of radial type, which is common for distribution grids in such regions. The POC to the central grid is located in Øye substation, which in turn is powered from Feda. Currently there are 4 main radials in the grid, the Kvinesdal radial, the Gusedal radial, the Høylandsfoss raidal and the Gyland Radial. However, for this thesis the Kvinesdal radial is the one beeing analysed. A full overview over the transmission lines dimensions and length is shown in table 3.1.

Table 3.1: Overview over dimensions and length of power lines in the Kvinesdal radial [10]

Sub radial	Dimension	Length
Øye substation to Liknes	FeAl 120	5,8 km
Liknes to Sindland	FeAl 120	14,1 km
Sindland to Kvinlog	FeAl 120	12,2 km
Kvinlog to Netland	FeAl 50	13,3 km

3.2 Overview of DG units located in the Kvinesdal radial

3.2.1 Currently installed DG units

On the radial in question, there are currently connected 7 DG units and one shunt reactor. These DG units have a installed power of 26,64 MW in total, however, there are only made connection agreements for 17,68 MW. Figure 3.1 shows the connection points for the DG units while table 3.2 and 3.3 shows key numbers.

Table 3.2: Overview over DG units in the Kvinesdal radial [10]

Name	Rated power of turbine [MW]	Connection agreement rated power [MW]	Rated power of generator [MVA]
Bergesli	0,81	0,78	0,90
Hisvatn	3,60	3,60	4,00
Eftestøyl	0,18	0,40	0,18
Kvinesdal	1,35	1,35	1,50
Oksefjellet	0,35	0,35	0,35
Røylandsfoss	1,55	1,20	1,55
Trælandsfoss	18,90	10,00	21,40
Summation	26,64	17,68	29,88

Table 3.3: Overview over reactors in the Kvinesdal radial [10]

Name	Rated power of reactor [MWr]	Number of steps	Power per step [MVAr]
Hisvatn shunt reactor	1,30	2	0,65

As one can see there is a big difference between rated power and connection agreement rated power for Trælandsfoss, and one do not know for sure if all the generators at this power plant are still operative.

3.2.2 Envisaged DG units

In total there are planned 12 new DG units in the radial. These will have a total rated output of 31,55 MW, and a production of 87,30 $\frac{GWh}{year}$. The placement of these units is shown in figure 3.1, and as one can see they lie in close proximity of the 22 kV distribution grid. Table 3.4 shows the key numbers for these units.

Table 3.4: Overview over planned DG units in the Kvinesdal radial [10]

Name	Rated power of turbine [MW]	Yearly production [GWh]	Status
Kjilen	0,35	1,60	Concession is applied for
Kvinlog	1,20	3,10	
Lindland	1,40	2,80	
Narvestad	0,70	1,60	
Omland	0,40	1,00	
Rafoss	13,60	34,50	Concession is applied for
Røyland	0,10	0,20	
Røylandsfoss	0,60		
Røynebu	1,00	2,00	
Selandsåne	2,00	7,00	Concession given 10.09.2008
Stakkeland	9,70	31,50	
Åråna	0,50	2,00	
Summation	31,55	87,30	

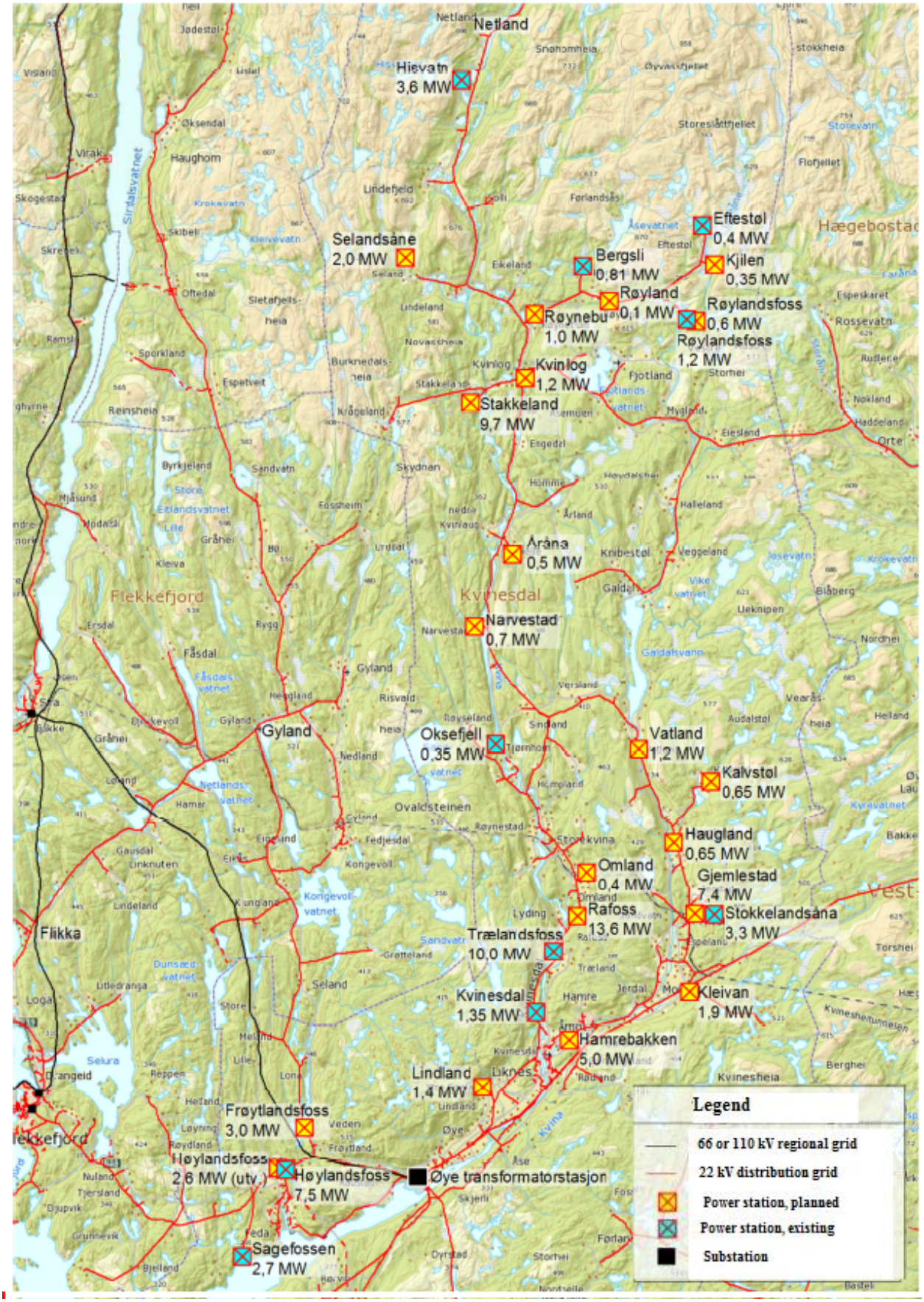

Figure 3.1: Overview over Kvinesdals distribution grid [10]

3.3 Topography

The total length of this radial is 45,4 km, and has four sub radials as shown in table 3.1.

Furthermore, the radial has its POC to the central grid is located in Øye substation, which in turn gets its power supplied from Feda. Figure 3.2 shows a overview over the Kvinesdal radial. As one can see the Kvinesdal radial stretches from Øye substation in the south to Trælandsfoss, past Kvinlog and to Netland.

Figure 3.2: Overview Kvinesdal radial [10]

There are currently 7 DG units (Hisvatn, Bergsli, Eftestøl, Røylandsfoss, Oksefjell, Trælandsfoss and Kvinesdal) connected to the radial, as marked by a small green square in figure 3.2. Additionally there is

connected a shunt reactor connected at Hisvatn, this have a capability of drawing 1,3 MVAr and is divided between two reactors of equal size (0,65 MVAr).

3.4 Current Operating Situation

Currently this radial has a medium high load level. The highest stress arises during LLHP where a line located between substation Stampebekken and node 82043-Helsehuset reaches 67 % of its capacity. At HLLP the situation is almost the same, with the highest load occurring is 66 % of capacity in a cable from Øye TS. The cable is of type TXSE 3X1X240 and have a length of 82 meters.

In the radial one usually experiences voltage drop as the distance to the substation increases, however as there are installed a great amount of DG units one will experience the difficulties mentioned in section 2.4.1. If the voltage is held constant at 22kV at the busbar in Øye TS, one will experience a voltage of approximately 24,1 kV at Hisvatn during LLHP. During HLLP one would on the other hand get a voltage of 20,9 kV at the same location. Hence one has a overall variation of 13,9 % on a yearly basis. The variation at the other DG units will be somewhat smaller than that of Hisvatn as shown in figure 3.3.

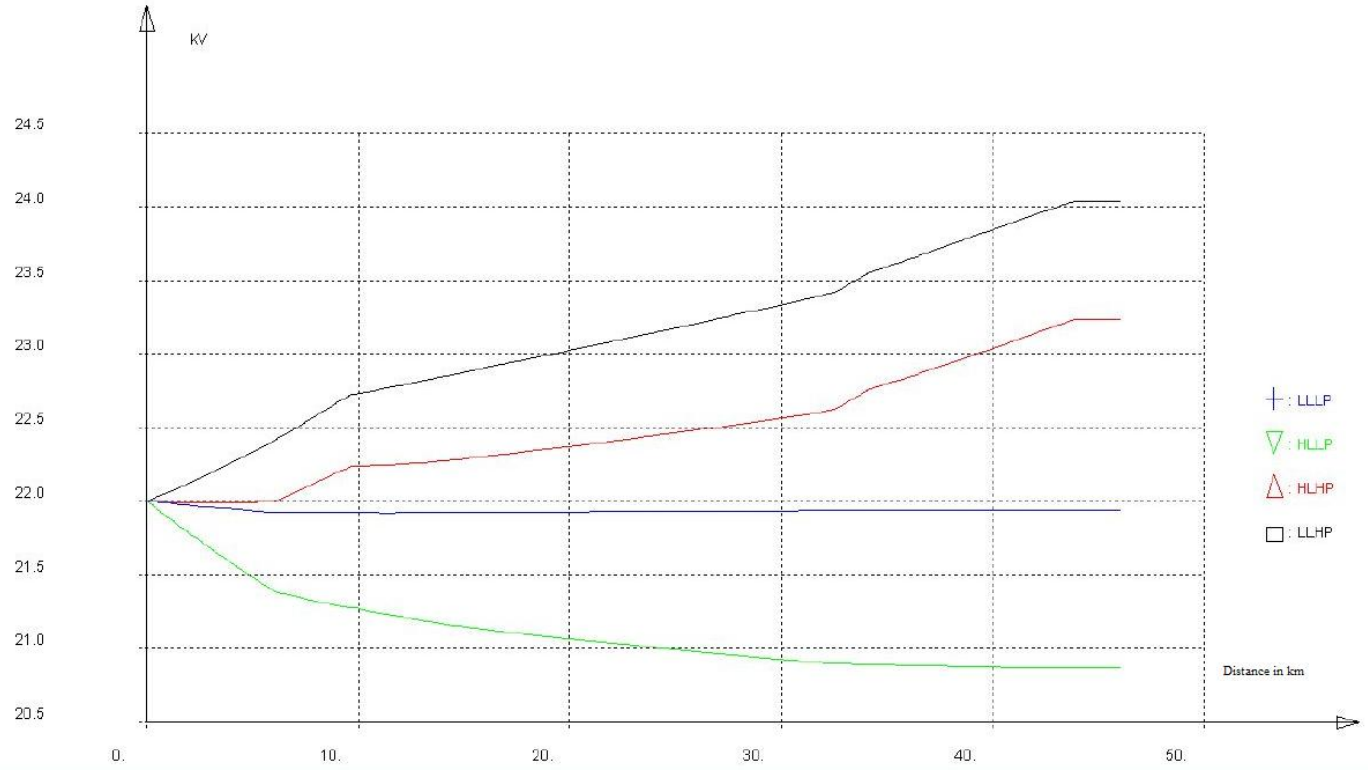

Figure 3.3: Voltage rise from Øye substation (distance =0) to the end of the radial at Netland. [10]

As one can see, the maximal voltage drop will be 10,33 %, and hence be somewhat higher than the 8 % limit mentioned in section 2.3.2. Moreover, the voltage variations exceeds the limit mentioned in section 2.3.2 by far.

3.5 Current Operating Situation with DG Units in Underexited Mode

By letting the shunt reactor running at full power and the current DG units run underexited, it's possible to somewhat improve the voltage situation. However, the DG units have small or no possibility of producing reactive power, and are only able to produce 0,5 MVAr in total. If the voltage is held constant at 22kV at the busbar in Øye TS, one will experience a voltage of approximately 23,0 kV at Hisvatn during LLHP. During HLLP one would on the other hand get a voltage of 20,9 kV at the same location. Hence one has a overall variation of 9,1 % at Hisvatn on a yearly basis. However, the largest variation will occur at Eftestøl, which will be 9,5 %. As one can see from figure 3.4, the situation has improved somewhat.

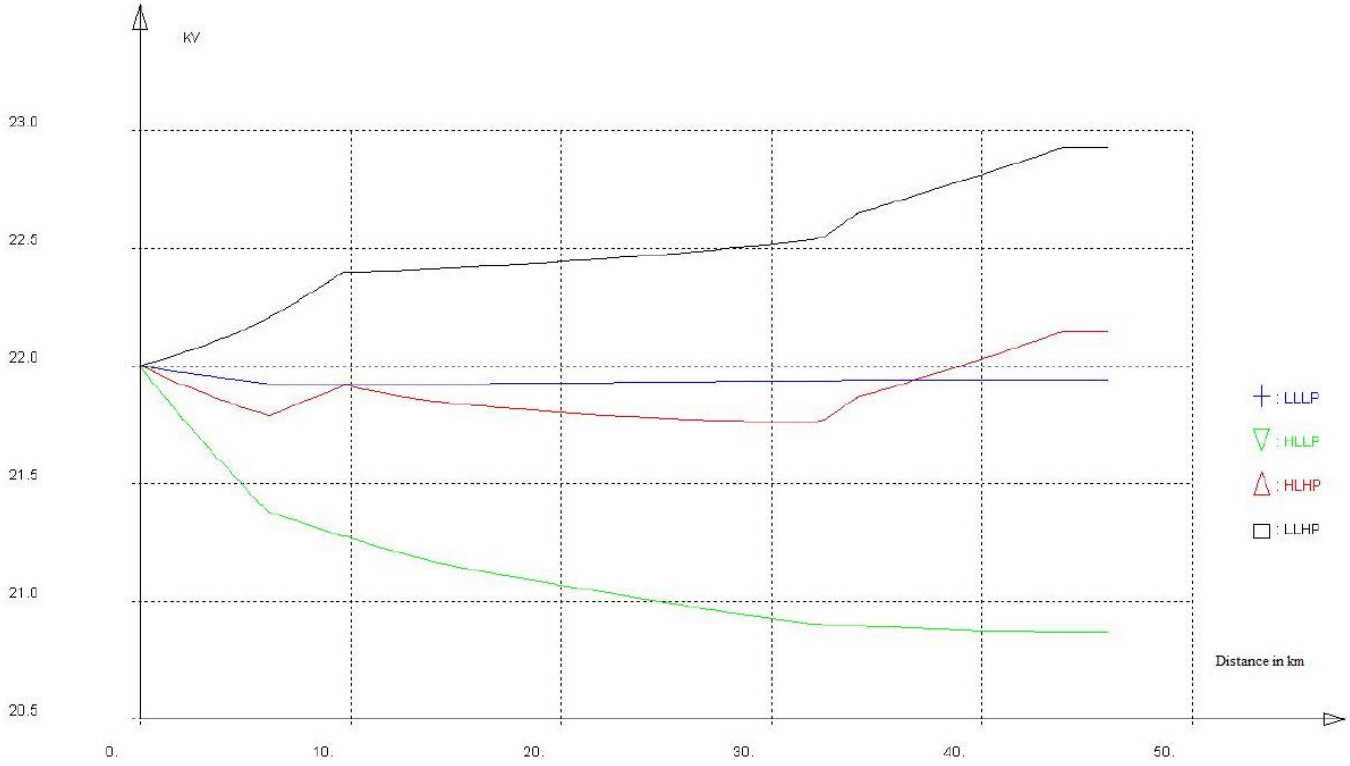

Figure 3.4: Voltage rise from Øye substation while running DG units underexited, (distance =0) to the end of the radial at Netland. [10]

As one can see, the maximal voltage drop will be 9,5 %, and hence be somewhat higher than the 8 % limit mentioned in section 2.3.2. Furthermore, even with the DG units running in underexicted mode, the voltage variations exceeds the limit mentioned in section 2.3.2 by far.

3.6 New production radial from Øye substation to Rafoss

Due to the fact that the voltage variations are too high as mentioned in previous section, a new production radial from Øye substation to Rafoss is suggested. This also to make is possible to connect the new DG units, as this is impossible with the current grid. Two (Rafoss and Lindland) of the twelve planned DG units in the Kvinesdal radial will be connected to this radial, together with two of the current DG units (Kvinesdal and Trælandsfoss). All other units stay connected as discussed previously as shown in Figure 3.5

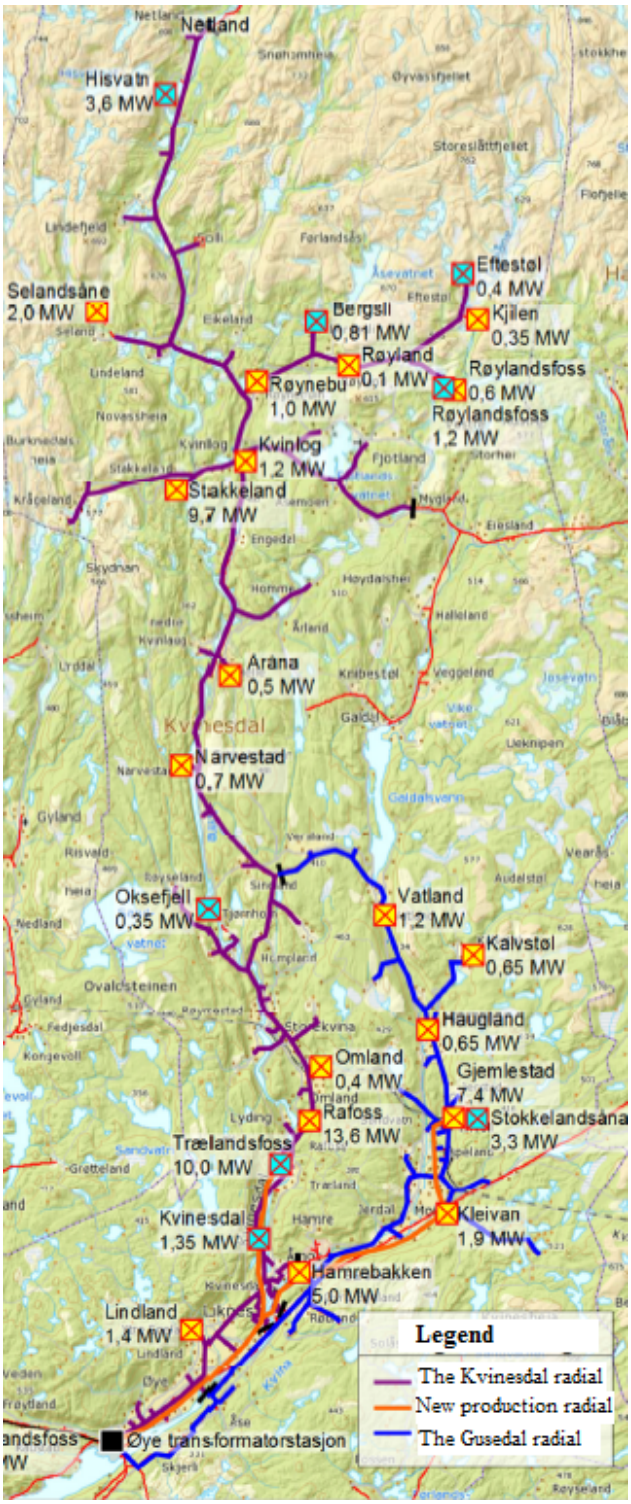

Figure 3.5: Overview over new production radial[10]

With this new radial in place the load situation improves somewhat, and it is possible to connect more units. However, at LLHP with the new DG units installed, the whole radial from Øye substation to Kvinlog will have a load of 85-90 % of the feeders capacity.

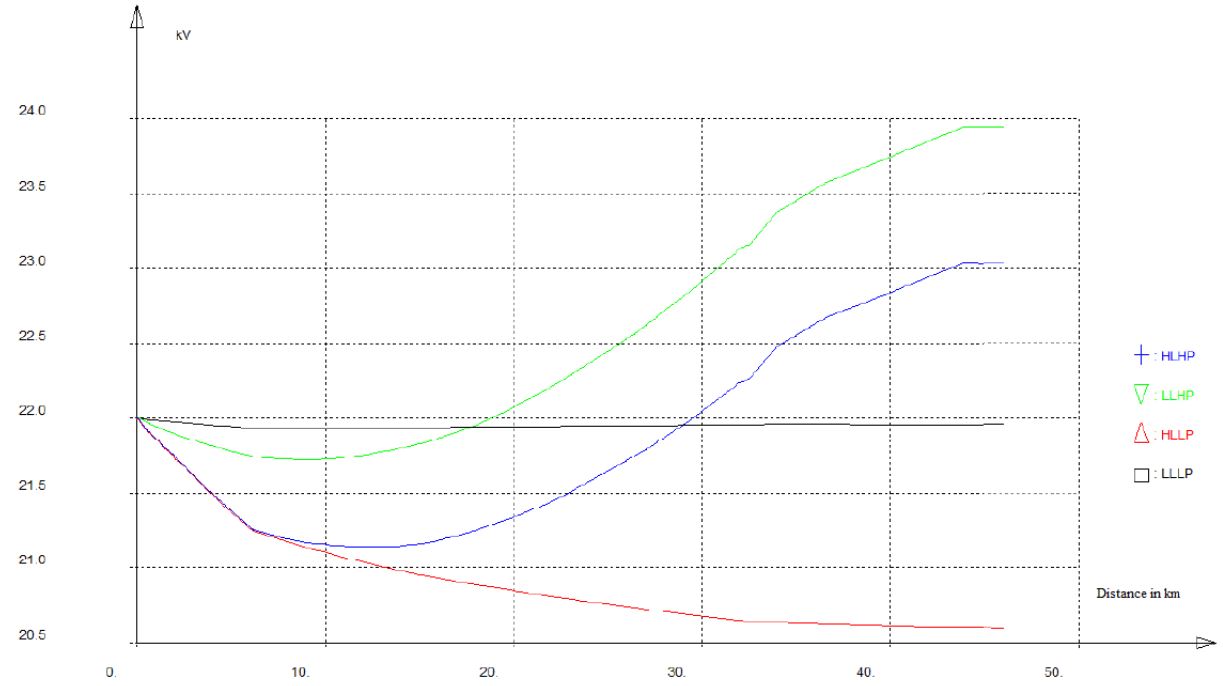

Figure 3.6: Voltage rise in the Kvinesdal radial from Øye substation, (distance =0) to the end of the radial at Netland. [10]

As one can see, the radial has a considerable voltage rise. At Hisvatn the voltage is approximately 24,0 kV at LLHP. In HLLP the voltage is 20,6 kV at the same location. This gives a total variation of 14,7 %, which is exceeds the limit discussed in 2.3.2. Furthermore, the voltage drop is approximately 6,4 % at from Øie to Hisvatn, which is within the given limits.

Chapter 4

Voltage Regulation through reactive co-operation of DG Units

As DG units become more and more common, problems arise when grids get saturated with power from such units. Voltage outside of given limits and overloaded components are example of such problems. In this chapter the focus will be on the impact some of the DG units have by running underexited, hence drawing reactive power and lowering the voltage at the site. Some of the DG units will run overexited to supply these units with reactive power. This is done to avoid reactive power flow from Øye substation, as this is unwanted due to the strain it puts on the regional grid.

In addition, the control system for such a system will be described based on work done by Salzburg Netz. The costs related to the communication will be briefly shown, this to give a rough idea of the cost of such a project.

4.1 Control of DG units

This section covers the control of the DG units, and will be based on the work made by Salzburg Netz in [16]. To control the voltage in the Kvinesdal radial, one needs to know the different voltages at the different locations. However, as there are little measurements of the grid one needs to use a DSSE as mentioned in section 2.2.4, and combine this with actual measurements which in total gives a feasible solution. Furthermore, one also need a voltage and reactive power control (VVC), which is connected to the DSSE, as shown in Figure 4.1.

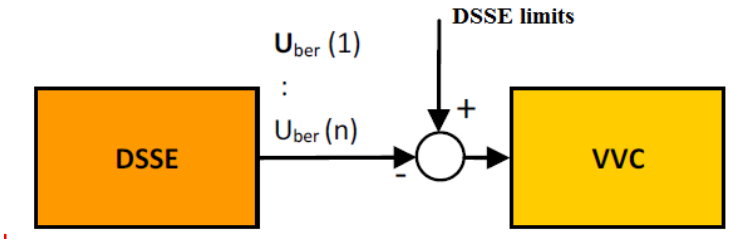

Figure 4.1: DSSE and VVC cooperation [16]

The software package included in the VVC works as a Distribution Management System (DMS), which has the necessary means of processing the complexity of the voltage and reactive power in today‘s distribution grid. Moreover, it allows the VVC to control tap changers of transformers, AVR units and switchable reactive

power producers as shown in Figure 4.2. By controlling these components in an optimal way, one can achieve the following:

1. Avoiding violations of voltage limits values
2. Minimization of transmission loss

The VVC's primary objective is to keep the voltage within given limits. When this primary objective is satisfied, the VVC will initiate the secondary objectives, which are mainly to minimize losses. Furthermore, the VVC only calculates a portion of the distribution grid at a time, which may consist of a single or multiple branches. And the algorithm used in in this VVC is a gradient algorithm, which regulates with regard to discrete and continuous control variables as described in [16].

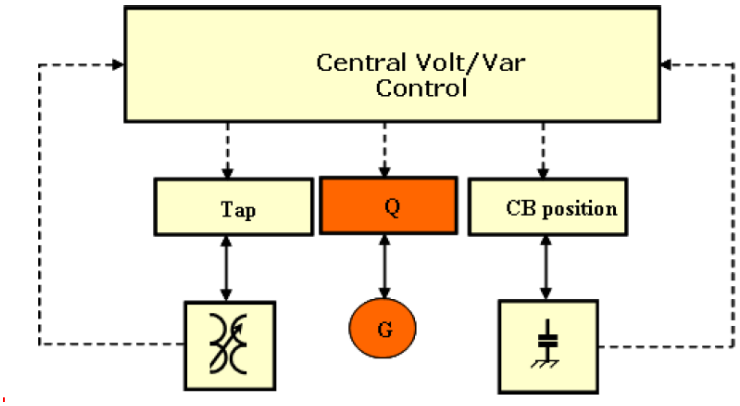

Figure 4.2: Central control of voltage and reactive power by VVC [16]

In addition, as one can see from Figure 4.3 the central volt/var control (CVVC) is feed deviation from the summation block. If the calculated stress in any of the nodes is outside the limits, then the VVC will start at new values for the control variable.

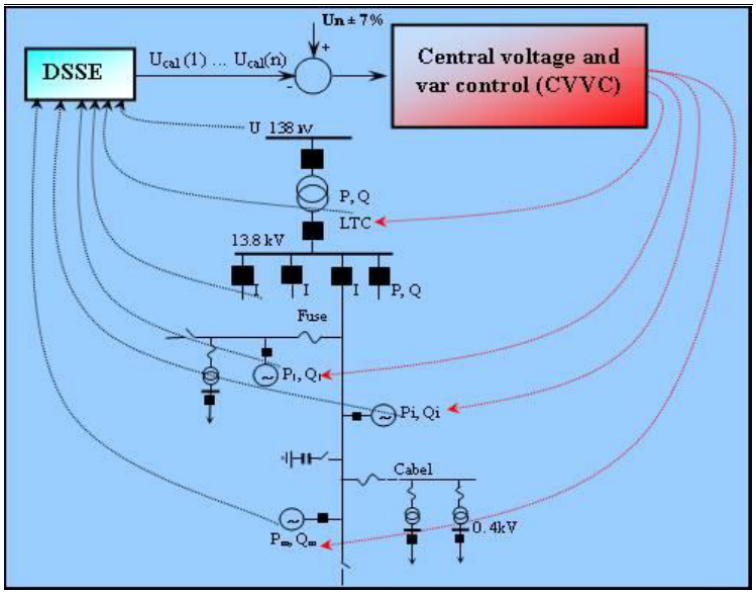

Figure 4.3: DSSE cooperation with VVC in the Salzburg grid [16]

Furthermore, as one can see from Figure 4.4 the system consist of several regulators. Where the local regulators are in charge of implementing and maintaining the setpoints. In other words, the local controller

of the transformer changes the transformer taps when the predetermined limits are reached. And the same also applies to the magnetizer of the DG units, where the excitation of the generator is controlled to match the desired value for reactive power output/input. Moreover, as one can see, the desired values (voltage or reactive power $Q_{Desired}$ $U_{Desired}$) is by closed loop control and Supervisory Control and Data Acquisition (SCADA) sent to the local regulators. This closed loop monitors the implementation of instructions, and if necessary tells the central regulator to recalculate or wait until the local regulator has reached steady state as described in [16].

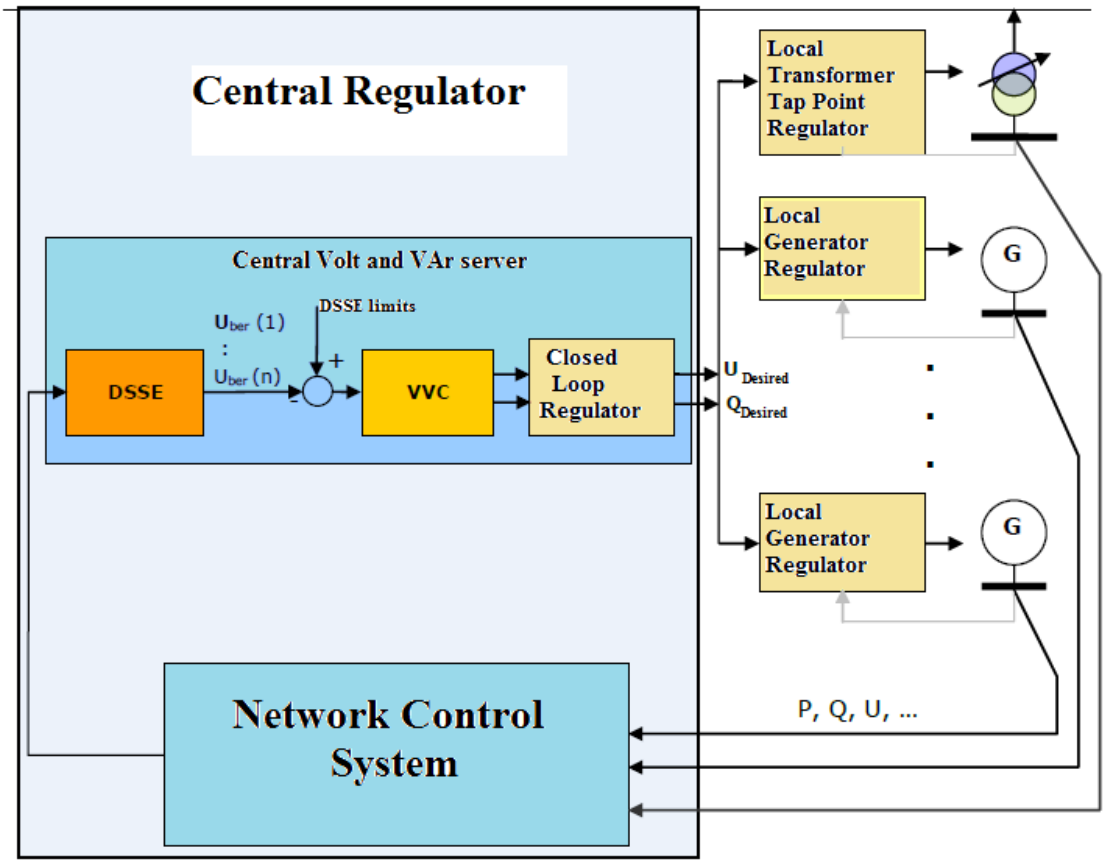

Figure 4.4: Full overview of central control [16]

The local regulators have a control loop as shown in Figure 4.5. As one can see, the electrical measurements from the machines are in a feedback loop, and then compared to the relevant set point. Furthermore, the local regulators also serve as a backup. This in case of a fallout of the central control, which may be caused by the server etc. As a result, this backup will prevent the system going outside of the operational limits.

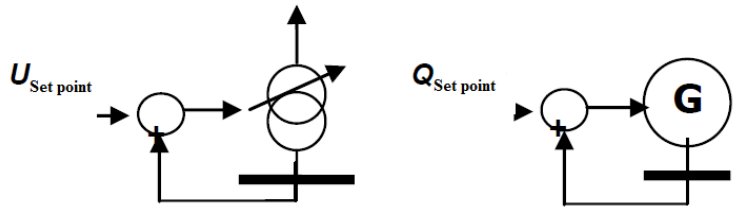

Figure 4.5: Schematic of local control loops [16]

Moreover, the local control is also important for rapid response to state changes in the grid, which are not captured by the central control due to its time resolution. The response of the local controller is in turn

according to its current- or voltage-dependent control routine. For an optimal performance of this function, one needs to tune the time resolution of the control loops, and one also need a time constant as described in [16]. Furthermore, one can summarize the task of the local control as follows:

1. Maintaining the voltage / reactive power to predetermined desired values

2. Independent backup in case of failure of the central control

3. Matching response for rapid voltage changes or system changes (maximum response time of the transformer tap changer $\approx$ 4 seconds).

The secondary outer loop of the central control (see Figure 4.6) has information from the entire network area, and the power calculations here keeps a complete overview over the grid. Furthermore, the tasks that are to be fulfilled by the central control are:

1. Optimization goals, such as

   (a) Preventing limits from being violated

   (b) Loss minimization

2. $Cos\phi$ conditions from the TSO

3. Coordination of transformer tap on the different voltage levels

4. Coordination with local regulators

5. Periodic recalculation

6. Master / slave principle with the other regulators

7. Systematically ranking the proposed action to state changes of the system, without violating the limits

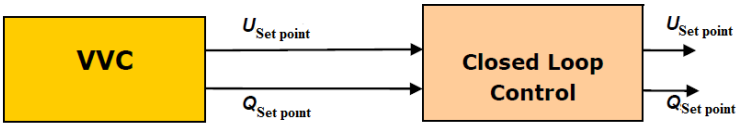

Figure 4.6: Schematic of central control [16]

4.2 The Kvinesdal radials test cases description

4.2.1 Basis for test cases

As mentioned in Section 3.6, a new production radial is needed to expand the capacity of the grid such that the new DG units can be connected. As a result, Lindland, Kvinesdal, Trælandsfoss and Rafoss DG units can not contribute to the cooperative reactive power flow in the grid. This due to the fact that they are connected to their own radial. For this reason they will all run with PF=1 in all simulations, and will therefore only contribute with active power.

Furthermore, the assumption has been made that all generators can operate within the limits given in Section 2.3.1. With the exception of the DG unit at Oksefjell (asynchronous), which is assumed to operate in such a way that it consumes reactive power from the grid in the range ≈ 0-0,1 MVAr.

The load used for the HLLP scenario is 14,0 MW / 3,0 MVAr on connected points, which in this case are the Kvinesdal and Gusedal radial. As the Gusedal radial cannot be dissconnected due to the new production radial. This load is approximately the one used in the Norconsult report, as shown in Appendix A. Low load used in LLHP scenarios is scaled to 20 % of high load, in other words 2,8 MW/ 0,6 MVAr.

As the current Kvinesdal radial uses the shunt reactor at Hisvatn to stabilize the voltage, it is assumed that having this drawing 1,3 MVAr from the grid is acceptable. The largest DG, Stakkeland, will in all cases be the governing DG. This by supplying most of the reactive power. The production /consumption of reactive power of the different DG units in each case is shown in Table 4.1 and 4.2. The production of active power is set to be fixed for all DG units in all cases simulated, and is set to be high production, in other words maximum production.

Furthermore, every case except Case I are adjusted in such a way that the DG units consumes minimal reactive power from Øye busbar. As this reactive power is supplied by other DG units.

Table 4.1: Cases 1A-1D, DG units and shunt-reactors output (MW and MVAr).

Name	P [MW]	Q Case 1A [MVAr]	Q Case 1B [MVAr]	Q Case 1C [MVAr]	Q Case 1D [MVAr]
Lindland	1,40	0,00	0,00	0,00	0,00
Kvinesdal	1,35	0,00	0,00	0,00	0,00
Trælandsfoss	10,00	0,00	0,00	0,00	0,00
Rafoss	13,60	0,00	0,00	0,00	0,00
Omland	0,40	0,00	0,00	0,00	0,00
Oksefjell	0,35	0,00	0,00	0,00	0,00
Narvestad	0,70	0,00	0,00	0,00	0,00
Åråna	0,50	0,00	0,00	0,00	0,00
Stakkeland	9,70	1,46	1,94	2,52	2,86
Kvinlog	1,20	0,00	0,00	0,00	0,00
Røynebru	1,00	0,00	0,00	0,00	-0,33
Bergsli	0,81	0,00	0,00	0,00	0,00
Røyland	0,10	0,00	0,00	0,00	0,00
Eftestøyl	0,40	0,00	0,00	0,00	0,00
Kjilen	0,35	0,00	0,00	0,00	0,00
Røylandsfoss 1	0,6	0,00	-0,09	-0,20	-0,20
Røylandsfoss 2	1,20	0,00	-0,18	-0,40	-0,40
Selandsåne	2,00	-0,20	-0,40	-0,66	-0,66
Hisvatn	3,60	0,00	0,00	0,00	0,00
Hisvatn Shunt-reactor		-1,30	-1,30	-1,30	-1,30
Summation	49,26	-0,05	-0,03	-0,03	-0,02

Table 4.2: Cases 1E-1I, DG units and shunt-reactors output (MVAr).

Name	Q Case 1E [MVAr]	Q Case 1F [MVAr]	Q Case 1G [MVAr]	Q Case 1H [MVAr]	Q Case 1I [MVAr]
Lindland	0,00	0,00	0,00	0,00	0,00
Kvinesdal	0,00	0,00	0,00	0,00	0,00
Trælandsfoss	0,00	0,00	0,00	0,00	0,00
Rafoss	0,00	0,00	0,00	0,00	0,00
Omland	0,00	0,00	0,00	0,10	0,00
Oksefjell	0,00	0,00	0,00	-0,10	0,00
Narvestad	0,00	0,00	0,00	0,17	0,00
Åråna	0,00	0,00	0,00	-0,17	0,00
Stakkeland	3,25	3,52	3,80	3,80	2,86
Kvinlog	-0,40	-0,40	-0,40	-0,40	-0,40
Røynebru	-0,33	-0,33	-0,33	-0,33	-0,33
Bergsli	0,00	-0,27	-0,27	-0,27	-0,27
Røyland	0,00	0,00	-0,03	-0,03	-0,03
Eftestøyl	0,00	0,00	-0,13	-0,13	-0,13
Kjilen	0,00	0,00	-0,12	-0,12	-0,12
Røylandsfoss 1	-0,20	-0,20	-0,20	-0,20	-0,20
Røylandsfoss 2	-0,40	-0,40	-0,40	-0,40	-0,40
Selandsåne	-0,66	0,66	-0,66	-0,66	-0,66
Hisvatn	0,00	0,00	0,00	0,00	0,00
Hisvatn Shunt-reactor	-1,30	-1,30	-1,30	-1,30	-1,30
Summation	-0,03	-0,03	-0,03	-0,02	-1,32

As one can see, all the cases are somewhat connected, as the amount of reactive power drawn from Stakkeland increases from Case A to Case B to Case C etc.

By having multiple test cases, one can identify trends related to the voltage and how the voltage and reactive power are related. Therefore 9 cases where simulated in this thesis.

4.2.2 Test case 1A

This case deals with replacing the reactive power which is supplied to Hisvatn Shunt-reactor from the grid, which is done by having Stakkeland run overexcited supplying all the necessary reactive power, and letting Selandsåne run somewhat underexited as shown in Table 4.3.

The results of this simulation is shown in Figure 4.7. Here one can see that by having an additional 1,46 MVAr draw in to Hisvatn and Selandsåne, the voltage drops almost 0,3 kV. Furthermore, under the given conditions the highest voltage is at Eftestøl, which have a voltage of 23,95 kV as shown in Appendix B. This gives a variation of 13,65 % between HLLP and LLHP at Eftesøl, which is far beond the limits mentioned in section 2.3.2. The lowest voltage in this case is 21,71 kV and is measured at node TH-83040, this represents 1,3% voltage drop, well within the limits given in section 2.3.2. In additon, the overall transmission losses are approximatly 5 MW, also shown in Appendix B.

Table 4.3: Case 1A, DG units and shunt-reactors output (MW and MVAr).

Name	Active power [MW]	Reactive power [MVAr]	Tan ϕ
Lindland	1,40	0,00	0,00
Kvinesdal	1,35	0,00	0,00
Trælandsfoss	10,00	0,00	0,00
Rafoss	13,60	0,00	0,00
Omland	0,40	0,00	0,00
Oksefjell	0,35	0,00	
Narvestad	0,70	0,00	0,00
Åråna	0,50	0,00	0,00
Stakkeland	9,70	1,46	0,15
Kvinlog	1,20	0,00	0,00
Røynebru	1,00	0,00	0,00
Bergsli	0,81	0,00	0,00
Røyland	0,10	0,00	0,00
Eftestøyl	0,40	0,00	0,00
Kjilen	0,35	0,00	0,00
Røylandsfoss 1	0,6	0,00	0,00
Røylandsfoss 2	1,20	0,00	0,00
Selandsåne	2,00	-0,20	-0,10
Hisvatn	3,60	0,00	0,00
Hisvatn Shunt-reactor		-1,30	
Summation	49,26	-0,05	

Several components are experiencing severe overload, as one can see from Figure 4.8, six components are experiencing loads that exceeds 100 % of nominal load. However, it is not surprising that the current transformer (TC) at Øye substation is experiencing the heaviest load. This due the fact that all the power generated by the DG units has to pass this component.

Furthermore, the circuit breaker (BS) at Omland and the circuit breaker (BL) at Slimestad are also heavy overloaded. The fuse (SI) at node 83033-Oksekraft experience an overload of 16,79 %, which, if continued over significant amount of time, will lead to prematurely failure of the component. The cables (KA) from Oksefjell and Eftestøl both experience an overload of 7,39 %, which is in direct violation of the requirements mentioned in section 2.3.2.

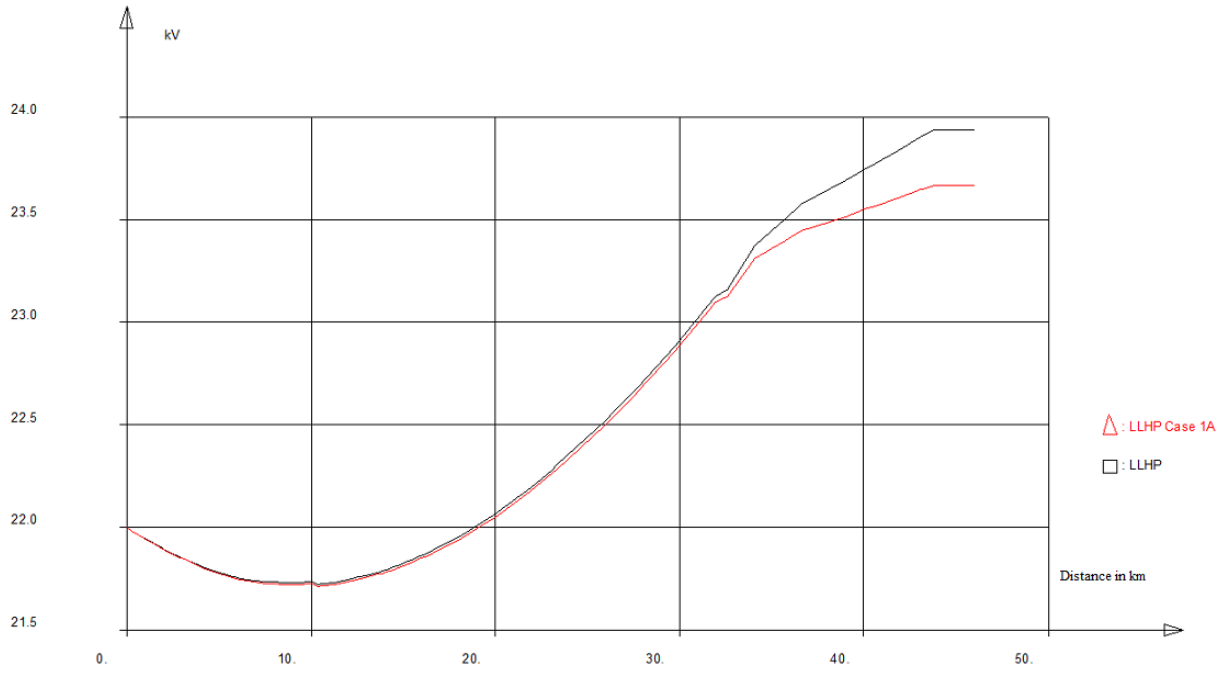

Figure 4.7: Case 1A, voltage rise from Øye substation (distance =0) to the end of the radial at Netland.

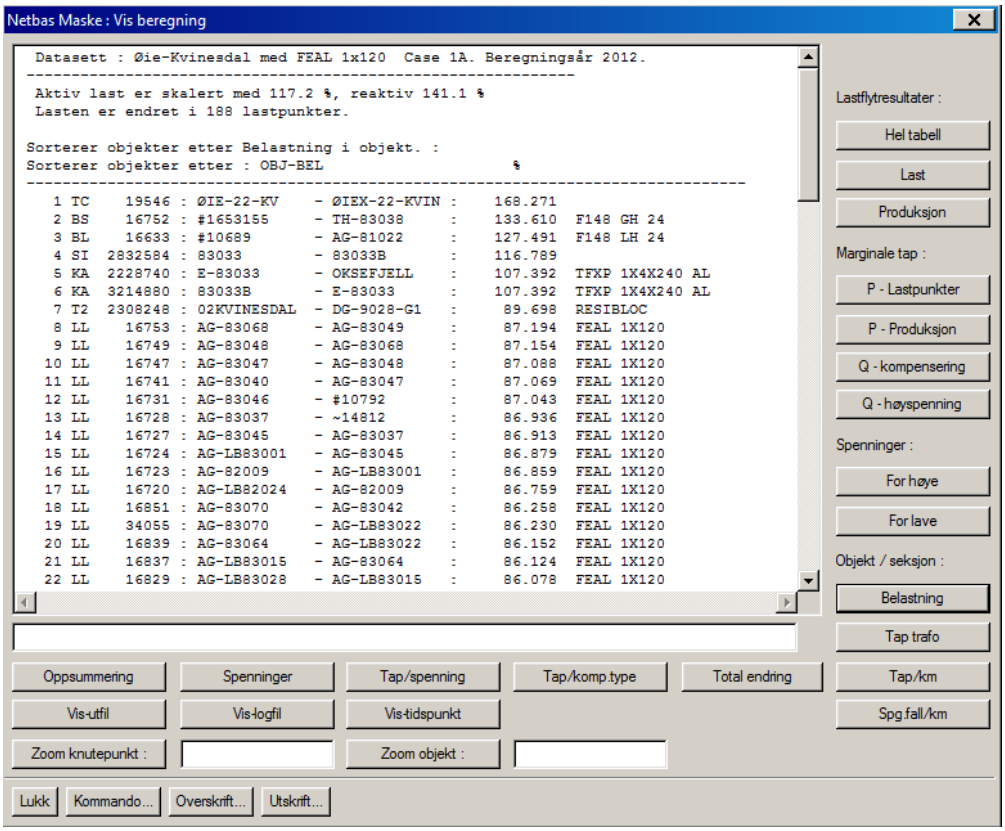

Figure 4.8: Case 1A, component load

4.2.3 Test case 1B

Stakkeland has in this case increase its production of reactive power to 1,94 MVAr, and Røylandsfoss 1 , Røylandsfoss 2 and Selandsåne are running underexited as shown in Table 4.4.

The results of this simulation is shown in Figure 4.9. Comparison of Case 1A to Case 1B shows that there is a small difference in voltage. As one can see the voltage at Netland is somewhat lower in Case 1B, than that of Case 1A. In addition, the voltage at Eftestøl is also somewhat lower than that of Case A, 23,91 kV as shown in Appendix C, which represents a variation of 13,47 % between HLLP and LLHP. This is still exceeding the limits mentioned in section 2.3.2 by far. The lowest voltage in this case is measured at TH-83040 and is 21,73 kV, which is well within the given limits. Furthermore, there is no significant increase or decrease in transmission losses, if compared to Case 1A.

Table 4.4: Case 1B, DG units and shunt-reactors output (MW and MVAr).

Name	Active power [MW]	Reactive power [MVAr]	Tan ϕ
Lindland	1,40	0,00	0,00
Kvinesdal	1,35	0,00	0,00
Trælandsfoss	10,00	0,00	0,00
Rafoss	13,60	0,00	0,00
Omland	0,40	0,00	0,00
Oksefjell	0,35	0,00	
Narvestad	0,70	0,00	0,00
Åråna	0,50	0,00	0,00
Stakkeland	9,70	1,94	0,20
Kvinlog	1,20	0,00	0,00
Røynebru	1,00	0,00	0,00
Bergsli	0,81	0,00	0,00
Røyland	0,10	0,00	0,00
Eftestøyl	0,40	0,00	0,00
Kjilen	0,35	0,00	0,00
Røylandsfoss 1	0,6	-0,09	-0,15
Røylandsfoss 2	1,20	-0,18	-0,15
Selandsåne	2,00	-0,40	-0,20
Hisvatn	3,60	0,00	0,00
Hisvatn Shunt-reactor		-1,30	
Summation	49,26	-0,03	

Furthermore, when regarding the load situation as presented in Figure 4.10, one can see that the loads have changed somewhat.

Firstly, the current transformer (TC) at Øye substation experiences a improvement of 0.03 %, which is so small that it is negligible. Secondly, the circuit breakers at Omland and Slimestad also experience changes that are of such a size that they also are negligible. Thirdly, the fuse at node 83033-Oksekraft is still heavily overloaded. The increase here is also of negligible size. Lastly, the cables at Oksefjell and Eftestøl are still overloaded to such an extent that they violated the requirements mentioned in section 2.3.2. The change for these components is as with the others, negligible.

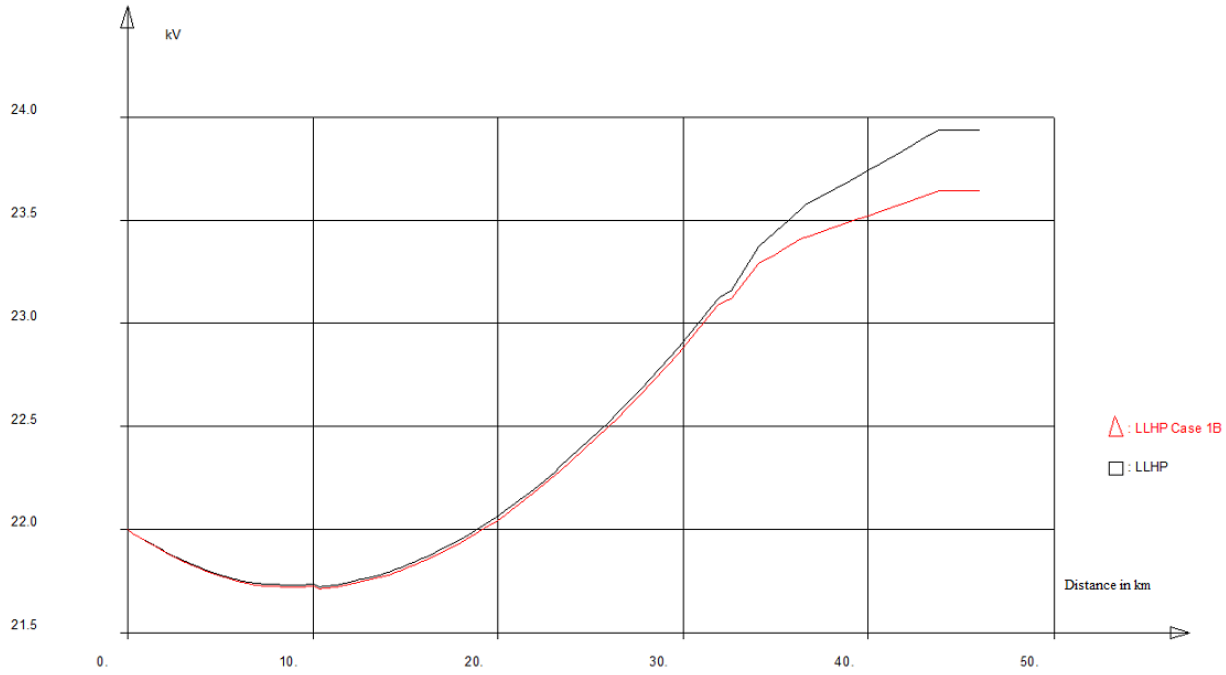

Figure 4.9: Case 1B, voltage rise from Øye substation (distance =0) to the end of the radial at Netland.

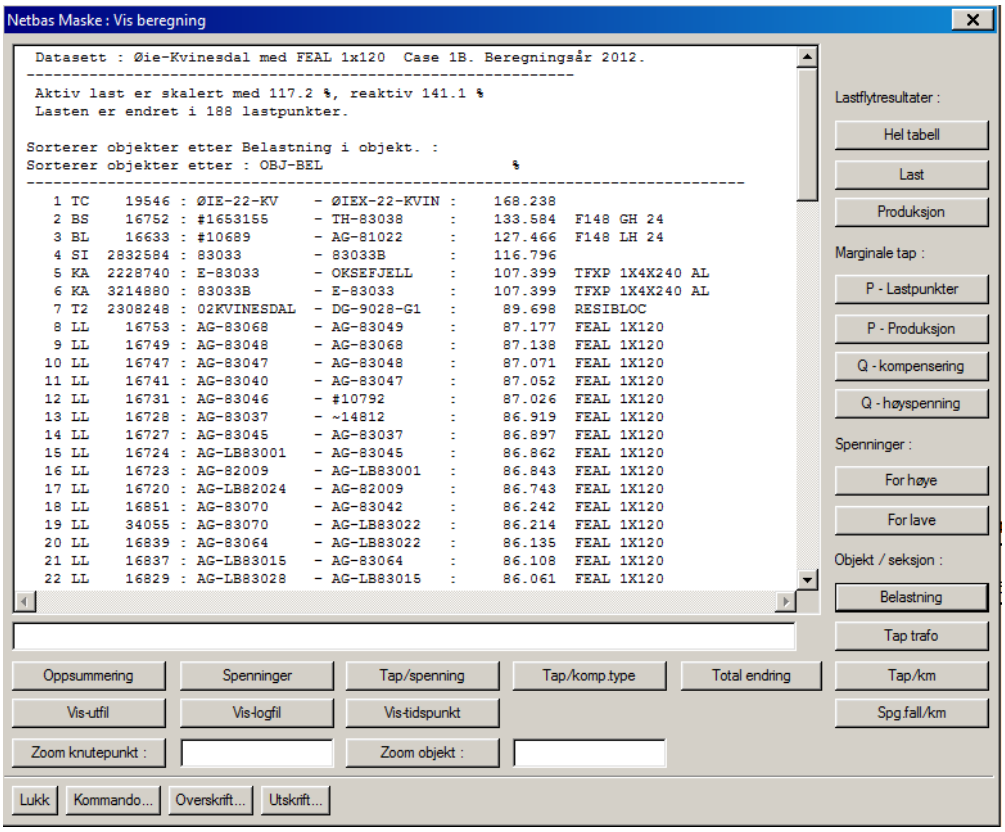

Figure 4.10: Case 1B, component load

4.2.4 Test case 1C

Going a step further, Røylandsfoss 1, Røylandsfoss 2 and Selandsåne are in this case running at their maximum under exited limit, which is given in section 2.3.1. Stakkeland is supplying almost all the reactive power, as shown in Table 4.5.

As shown in Figure 4.11, there is a significant voltage drop if one compare Case B to Case C. Furthermore, the voltage at Eftestøl has a minor drop down to 23,84 kV as shown Appendix D. This resulting in a voltage variation of 13,15 % between HLLP and LLHP, this is still exceeds the limits mentioned in section 2.3.2 by far. The lowest voltage measured in this case is at TH-83040, where the voltage is 21,70 kV. This voltage drop of 1,36 % is well within the given limits. Furthermore, the transmission losses only increase with 19 kW, which is insignificant.

Table 4.5: Case 1C, DG units and shunt-reactors output (MW and MVAr).

Name	Active power [MW]	Reactive power [MVAr]	Tan ϕ
Lindland	1,40	0,00	0,00
Kvinesdal	1,35	0,00	0,00
Trælandsfoss	10,00	0,00	0,00
Rafoss	13,60	0,00	0,00
Omland	0,40	0,00	0,00
Oksefjell	0,35	0,00	
Narvestad	0,70	0,00	0,00
Åråna	0,50	0,00	0,00
Stakkeland	9,70	2,52	0,26
Kvinlog	1,20	0,00	0,00
Røynebru	1,00	0,00	0,00
Bergsli	0,81	0,00	0,00
Røyland	0,10	0,00	0,00
Eftestøyl	0,40	0,00	0,00
Kjilen	0,35	0,00	0,00
Røylandsfoss 1	0,6	-0,20	-0,33
Røylandsfoss 2	1,20	-0,40	-0,33
Selandsåne	2,00	-0,66	-0,33
Hisvatn	3,60	0,00	0,00
Hisvatn Shunt-reactor		-1,30	
Summation	49,26	-0,03	

Furthermore, when regarding the load situation, a slight increase can be measured if compared to Case 1B, as shown in Figure 4.12.

Firstly, as one can see, the current transformer at Øye substation is now at 168,34 % of nominal load, which is an increase of 0,10 %. Secondly, the circuit breakers at Omland and Slimestad both experience an increase of 0,07 %. Thirdly, the fuse at node 83033-Oksekraft experience an increase of 0,08 %, and is now at 116,88 % of nominal load. Lastly, the cables at Oksefjell and Eftestøl also experience an increase of 0,08 % of nominal load value.

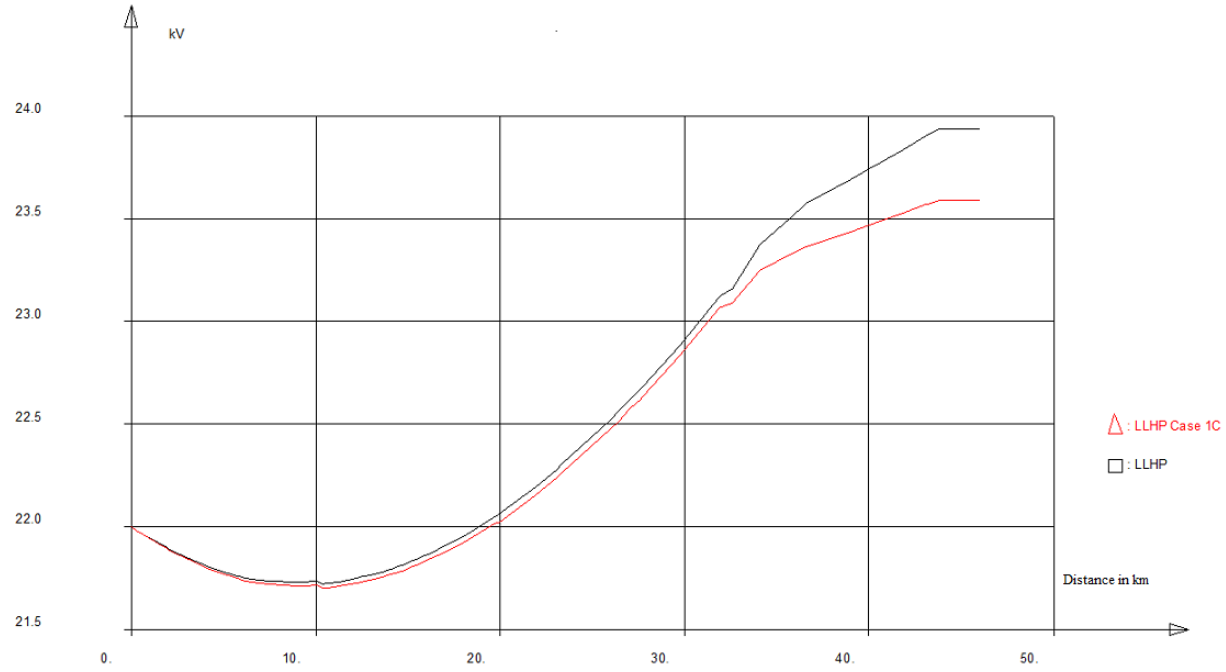

Figure 4.11: Case 1C, voltage rise from Øye substation (distance =0) to the end of the radial at Netland.

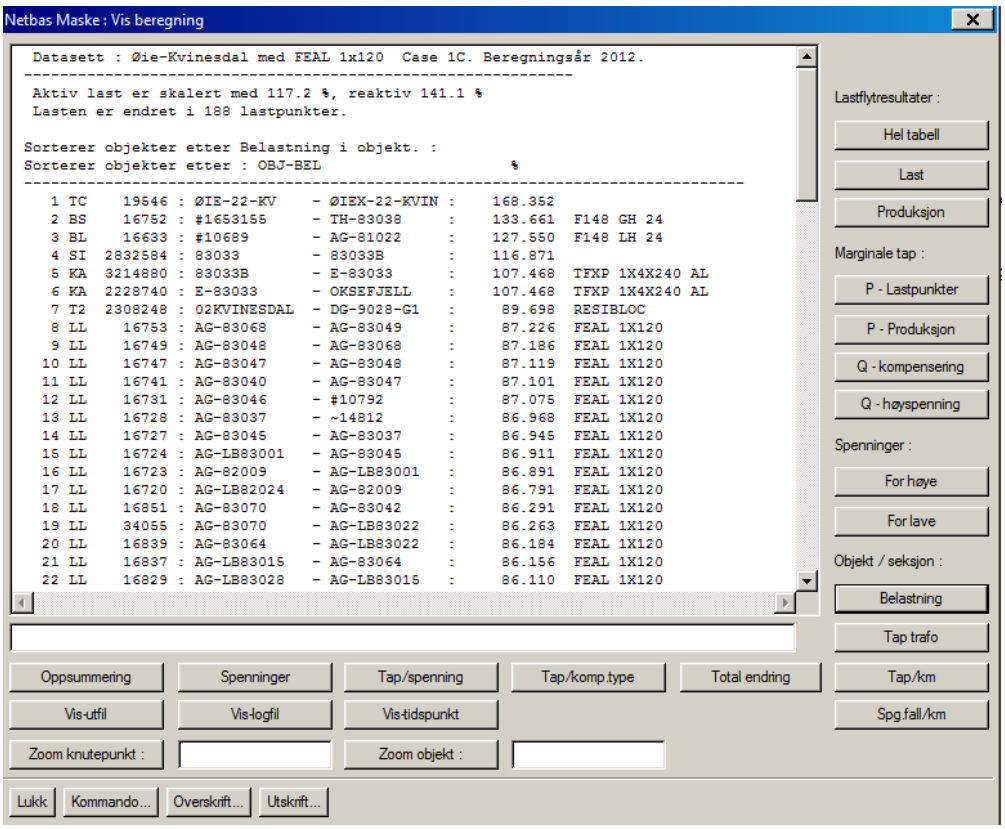

Figure 4.12: Case 1C, component load

4.2.5 Test case 1D

As one can see from Table 4.6, the difference between Case C and D is mainly Røynebu. With Røynebu runnin underexited at $Tan\phi = -0,33$ and Stakkeland increasing its production of reactive power correspondingly.

Table 4.6: Case 1D, DG units and shunt-reactors output (MW and MVAr).

Name	Active power [MW]	Reactive power [MVAr]	Tan ϕ
Lindland	1,40	0,00	0,00
Kvinesdal	1,35	0,00	0,00
Trælandsfoss	10,00	0,00	0,00
Rafoss	13,60	0,00	0,00
Omland	0,40	0,00	0,00
Oksefjell	0,35	0,00	
Narvestad	0,70	0,00	0,00
Åråna	0,50	0,00	0,00
Stakkeland	9,70	2,86	0,30
Kvinlog	1,20	0,00	0,00
Røynebru	1,00	-0,33	-0,33
Bergsli	0,81	0,00	0,00
Røyland	0,10	0,00	0,00
Eftestøyl	0,40	0,00	0,00
Kjilen	0,35	0,00	0,00
Røylandsfoss 1	0,6	-0,20	-0,33
Røylandsfoss 2	1,20	-0,40	-0,33
Selandsåne	2,00	-0,66	-0,33
Hisvatn	3,60	0,00	0,00
Hisvatn Shunt-reactor		-1,30	
Summation	49,26	-0,02	

As shown in Figure 4.13, the voltage at Netland drops somewhat if compared to Case C. In addition the voltage drop measure at Eftestøl is so small that it is negligible as shown in Appendix E, thus the variation between LLHP and HLLP is still that of 13,15 %. Furthermore, there is no significant increase in the transmission losses, which increases with only 5 kW. Furthermore, the load situation are identical to that of Case C, as shown in Figure 4.16.

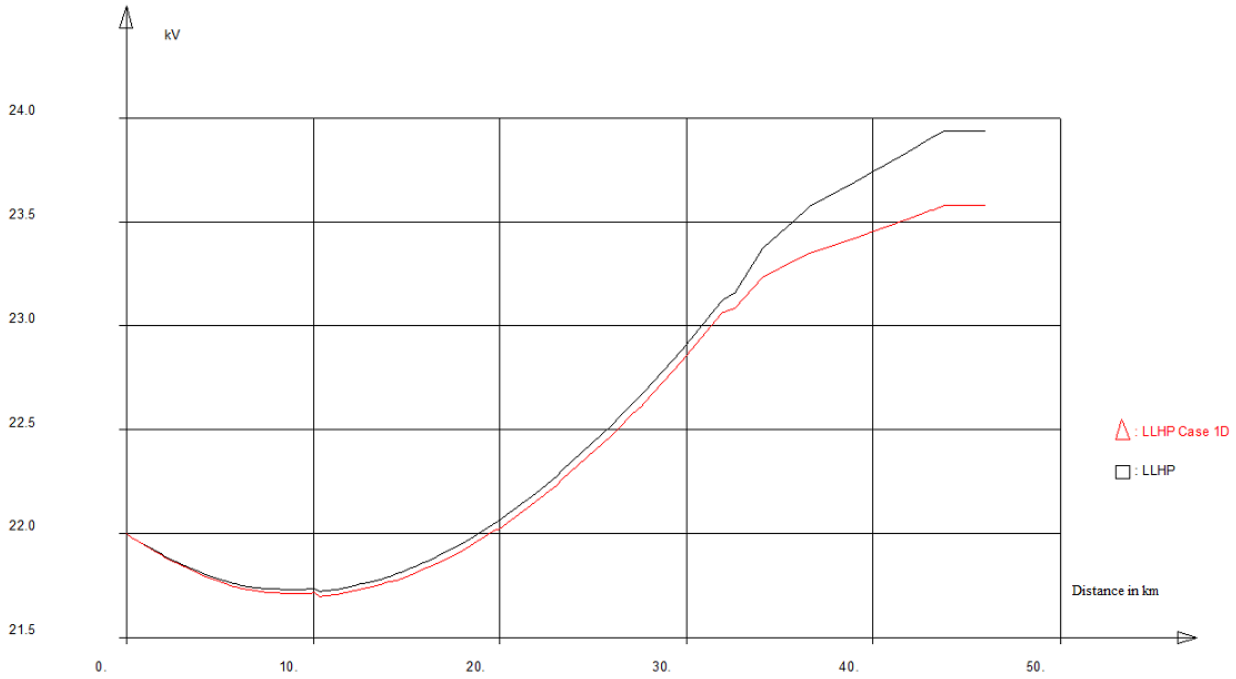

Figure 4.13: Case 1D, voltage rise from Øye substation (distance =0) to the end of the radial at Netland.

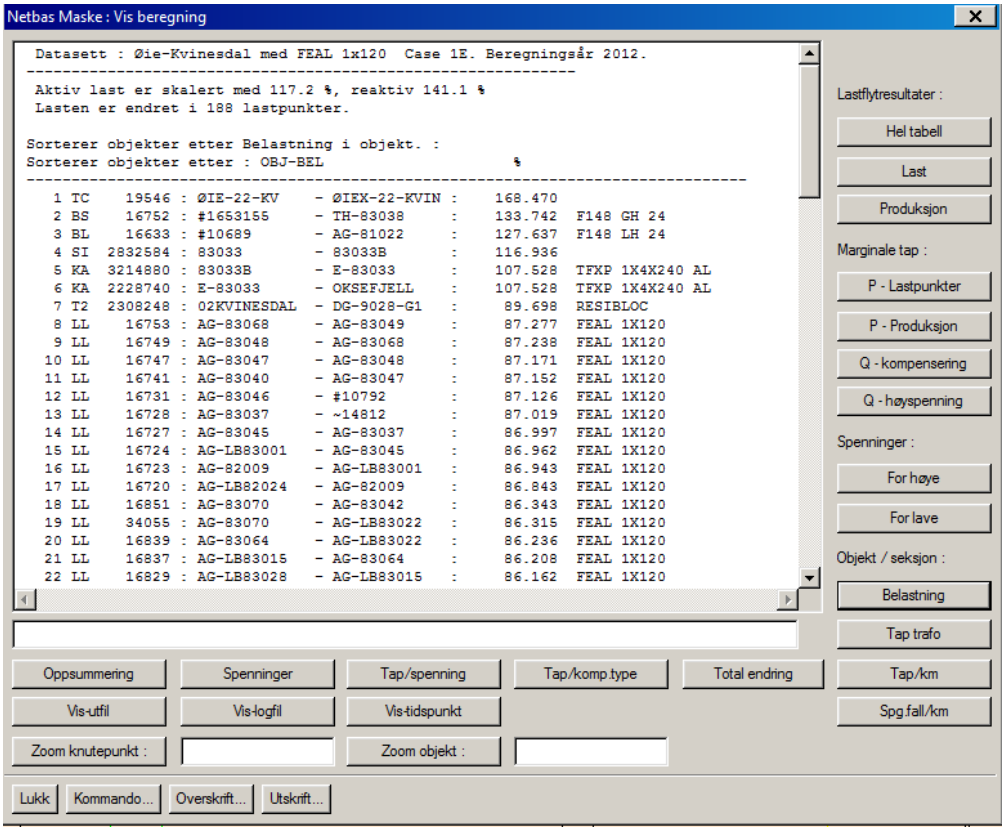

Figure 4.14: Case 1D, component load

4.2.6 Test case 1E

As one can see from Table 4.7, Kvinlog is running at $Tan\phi = -0,33$. And Stakkeland increases its production of reactive power correspondingly.

The voltage drop from Case D to Case E is minimal, but there is a somewhat improvement as one can see from Figure 4.15. The variation between LLHP and HLLP at Eftestøl is improved a bit, as the voltage drops down to 23,90 kV as shown in Appendix F the variation drops to 13,00 %. Furthermore, in this case the lowest voltage is that of node TH-83040, where the voltage has dropped to 21,69 kV. This represents a voltage drop of 1,41 %, which still is well within the given limits. The transmission losses are in this case 5,052 kW, which is an increase of 10 kW from Case D.

Table 4.7: Case 1E, DG units and shunt-reactors output (MW and MVAr).

Name	Active power [MW]	Reactive power [MVAr]	Tan ϕ
Lindland	1,40	0,00	0,00
Kvinesdal	1,35	0,00	0,00
Trælandsfoss	10,00	0,00	0,00
Rafoss	13,60	0,00	0,00
Omland	0,40	0,00	0,00
Oksefjell	0,35	0,00	
Narvestad	0,70	0,00	0,00
Åråna	0,50	0,00	0,00
Stakkeland	9,70	3,25	0,34
Kvinlog	1,20	-0,40	-0,33
Røynebru	1,00	-0,33	-0,33
Bergsli	0,81	0,00	0,00
Røyland	0,10	0,00	0,00
Eftestøyl	0,40	0,00	0,00
Kjilen	0,35	0,00	0,00
Røylandsfoss 1	0,6	-0,20	-0,33
Røylandsfoss 2	1,20	-0,40	-0,33
Selandsåne	2,00	-0,66	-0,33
Hisvatn	3,60	0,00	0,00
Hisvatn Shunt-reactor		-1,30	
Summation	49,26	-0,03	

Furthermore, as one can see from Figure 4.16, the load situation has changed somewhat if compared to Case 1D.

Firstly, the current transformer at Øye substation experiences an increase of 0,13 %. And is not at 168,47 % of nominal load. Secondly, the circuit breakers at Omland and Slimestad both experience an increase of 0,09 % . Thirdly, the fuse at node 83033-Oksekraft also experience an increase of 0,09 %. Lastly, the cables at Oksefjell and Eftestøl both experience an increase of 0,05 %, and both are now at 107,53 % of nominal load, still in violation of the requirements mentioned in section 2.3.1.

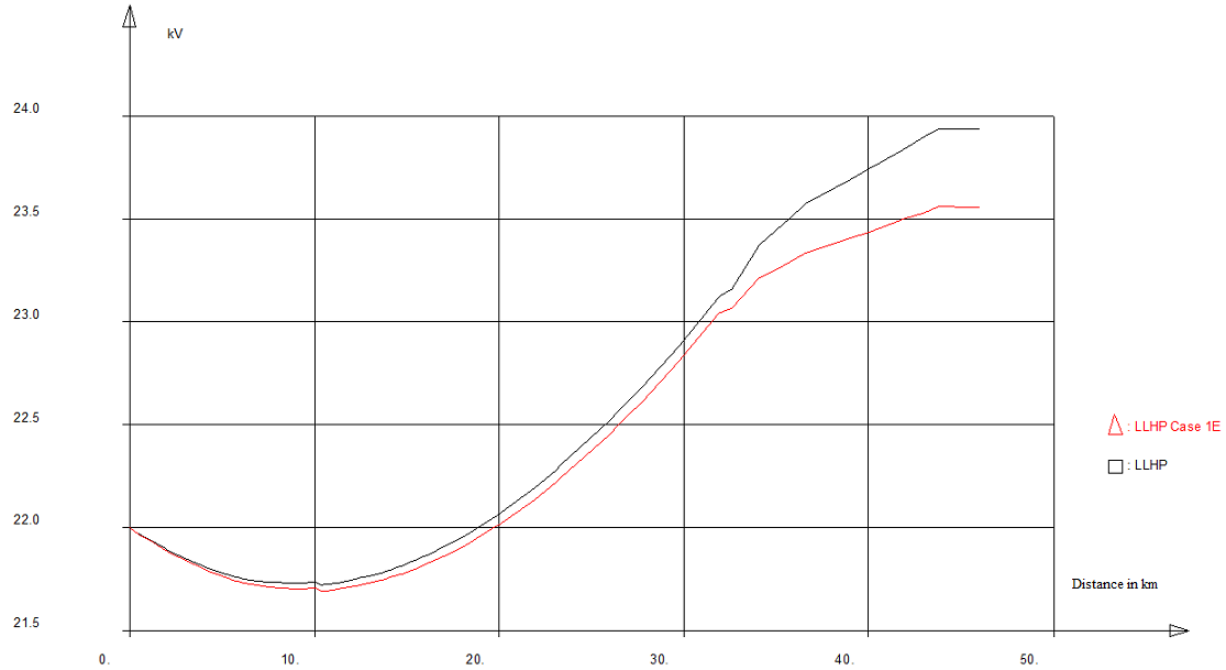

Figure 4.15: Case 1E, voltage rise from Øye substation (distance =0) to the end of the radial at Netland.

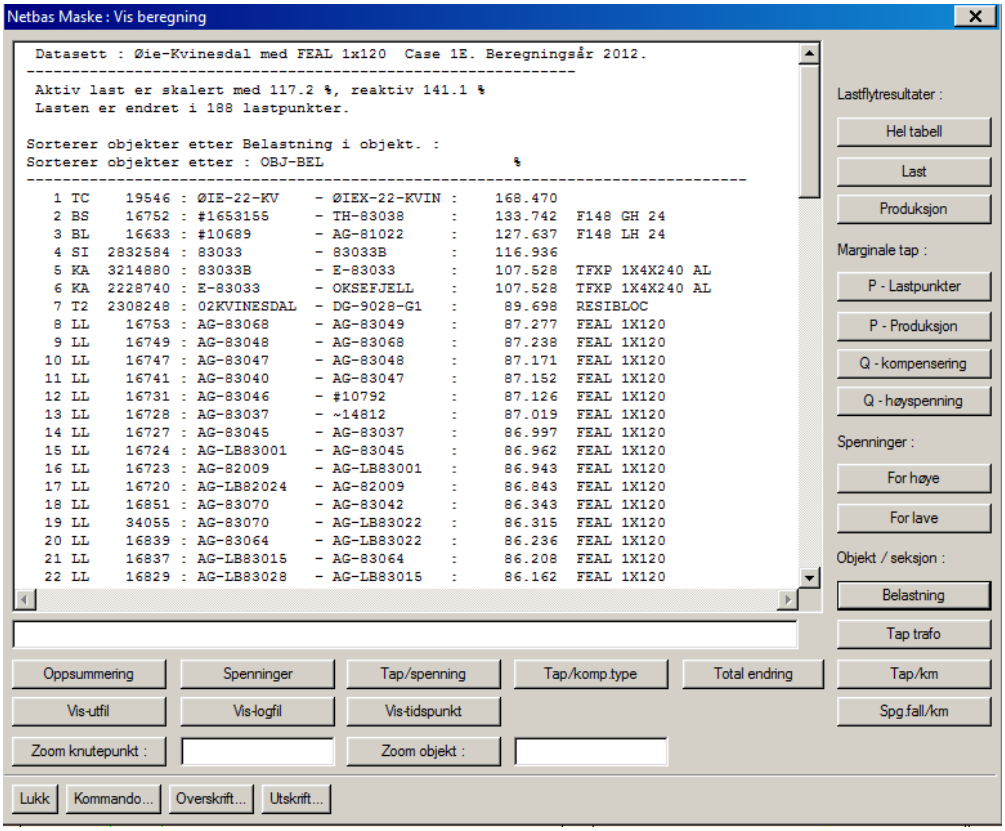

Figure 4.16: Case 1E, component load

4.2.7 Test case 1F

In this case Bergsli is added to the DGs that are running underexited, as shown in Table 4.8. And Stakkeland is supplying the reactiver power accordingly.

As one can see from Figure 4.17, the voltage drops somewhat more if compared to that of Case E. The voltage at Eftestøl has dropped to 23,78 kV as shown in Appendix G, which gives a total variation of 12,86 % between LLHP and HLLP. Total transmission losses are 5,062 MW, which is an insignificant increase of 10 kW compared to Case E. As in previous cases, the lowest voltage is at node TH-83040, and in here it is 21,69 kV. Hence the voltage drop is the same of that in Case E, 1,41 %.

Table 4.8: Case 1F, DG units and shunt-reactors output (MW and MVAr).

Name	Active power [MW]	Reactive power [MVAr]	Tan ϕ
Lindland	1,40	0,00	0,00
Kvinesdal	1,35	0,00	0,00
Trælandsfoss	10,00	0,00	0,00
Rafoss	13,60	0,00	0,00
Omland	0,40	0,00	0,00
Oksefjell	0,35	0,00	
Narvestad	0,70	0,00	0,00
Åråna	0,50	0,00	0,00
Stakkeland	9,70	3,52	0,36
Kvinlog	1,20	-0,40	-0,33
Røynebru	1,00	-0,33	-0,33
Bergsli	0,81	-0,27	-0,33
Røyland	0,10	0,00	0,00
Eftestøyl	0,40	0,00	0,00
Kjilen	0,35	0,00	0,00
Røylandsfoss 1	0,6	-0,20	-0,33
Røylandsfoss 2	1,20	-0,40	-0,33
Selandsåne	2,00	-0,66	-0,33
Hisvatn	3,60	0,00	0,00
Hisvatn Shunt-reactor		-1,30	
Summation	49,26	-0,03	

Furthermore, as one can see from Figure 4.18, the load on the components is increasing with the increasing reactive power in the grid.

Firstly, the current transformer experiences an increase of 0,04 %. And is now at 168,51 % of nominal load. Secondly, the two circuit breakers at Omland and Slimestad experience increasing loads, of 0,06% and 0,07% respectively. Thirdly, the fuse at node 83033-Oksekraft experience an increase of 0,03 %, and is now at 117 % of nominal load. Lastly, the cables at Oksefjell and Eftestøl both experience an increase of 0,07 %, and are now at 107,60 %, still in violation of requirements mentioned in section 2.3.1.

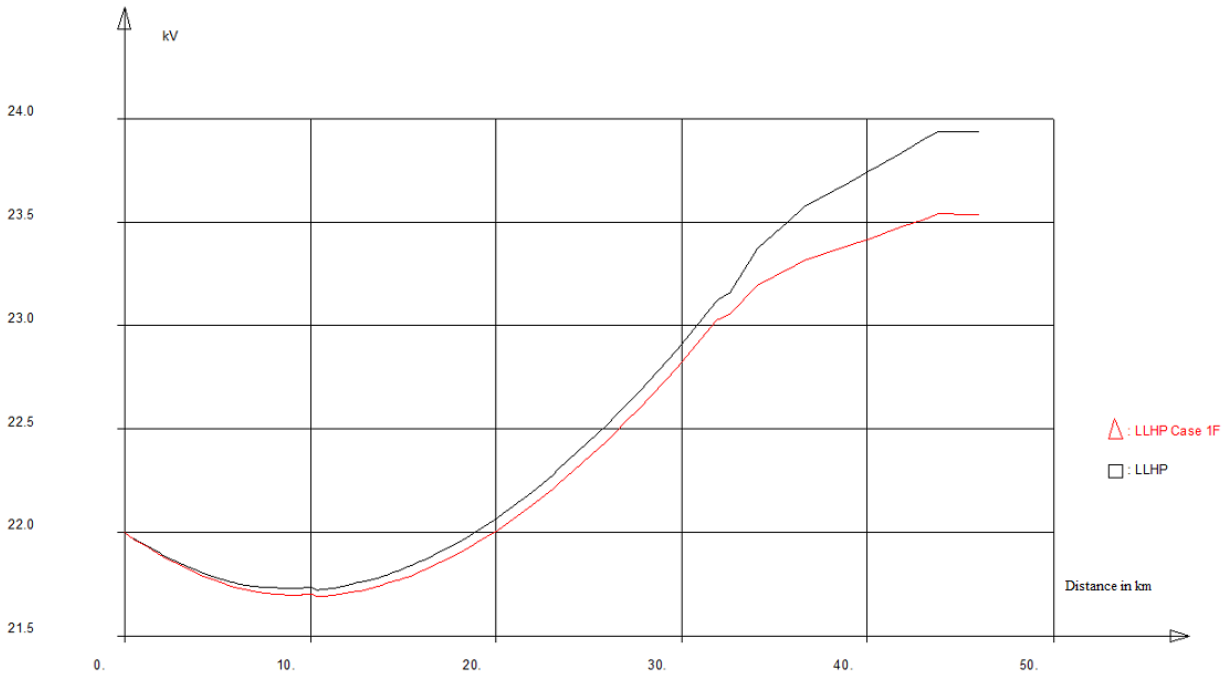

Figure 4.17: Case 1F, voltage rise from Øye substation (distance =0) to the end of the radial at Netland.

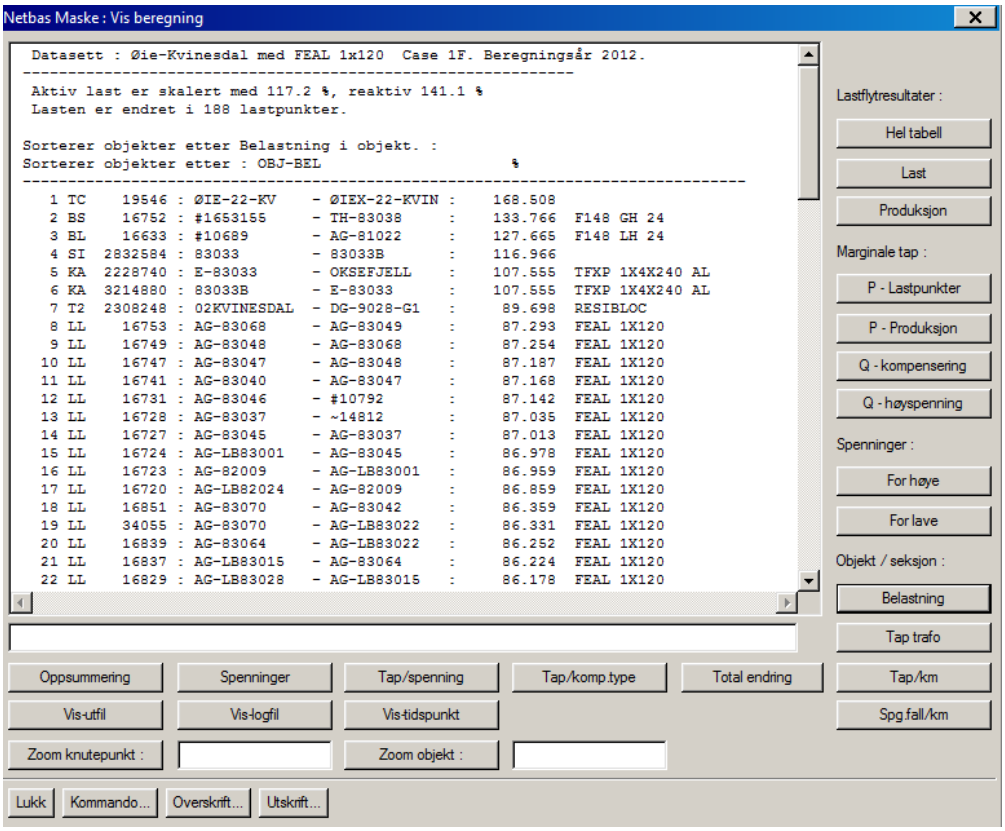

Figure 4.18: Case 1F, component load

4.2.8 Test case 1G

By letting Røyland, Eftestøl and Kjilen run underexited at $Tan\phi = -0,33$ an additional 0,28 MVAr is delivered from Stakkeland as shown in Table 4.9.

As one can see in Figure 4.19, there is a considerable improvement if compared to Case F, the voltage is now almost at 23,50 kV at Netland. As one can see in Appendix H, the voltage at Eftestøl is now at 23,72 kV, which gives a variation of 12,61 % between LLHP and HLLP. The lowest voltage is still at nodeTH-83040, where one can measure a voltage of 21,69 kV, which is the same as measure in Case F. Transmission losses increase with another 12 kW if compared to Case F, and the total losses are now 5,073 MW.

Table 4.9: Case 1G, DG units and shunt-reactors output (MW and MVAr).

Name	Active power [MW]	Reactive power [MVAr]	Tan ϕ
Lindland	1,40	0,00	0,00
Kvinesdal	1,35	0,00	0,00
Trælandsfoss	10,00	0,00	0,00
Rafoss	13,60	0,00	0,00
Omland	0,40	0,00	0,00
Oksefjell	0,35	0,00	
Narvestad	0,70	0,00	0,00
Åråna	0,50	0,00	0,00
Stakkeland	9,70	3,80	0,39
Kvinlog	1,20	-0,40	-0,33
Røynebru	1,00	-0,33	-0,33
Bergsli	0,81	-0,27	-0,33
Røyland	0,10	-0,03	-0,33
Eftestøyl	0,40	-0,13	-0,33
Kjilen	0,35	-0,12	-0,33
Røylandsfoss 1	0,6	-0,20	-0,33
Røylandsfoss 2	1,20	-0,40	-0,33
Selandsåne	2,00	-0,66	-0,33
Hisvatn	3,60	0,00	0,00
Hisvatn Shunt-reactor		-1,30	
Summation	49,26	-0,03	

Furthermore, as one can see from Figure 4.20, the only component which experiences a change in load is the current transformer at Øye substation. All other components experience no change when compared to case 1F. The change of load for the current transformer is 0,07 %, and the load for the current transformer is now at 168,58 % of nominal load.

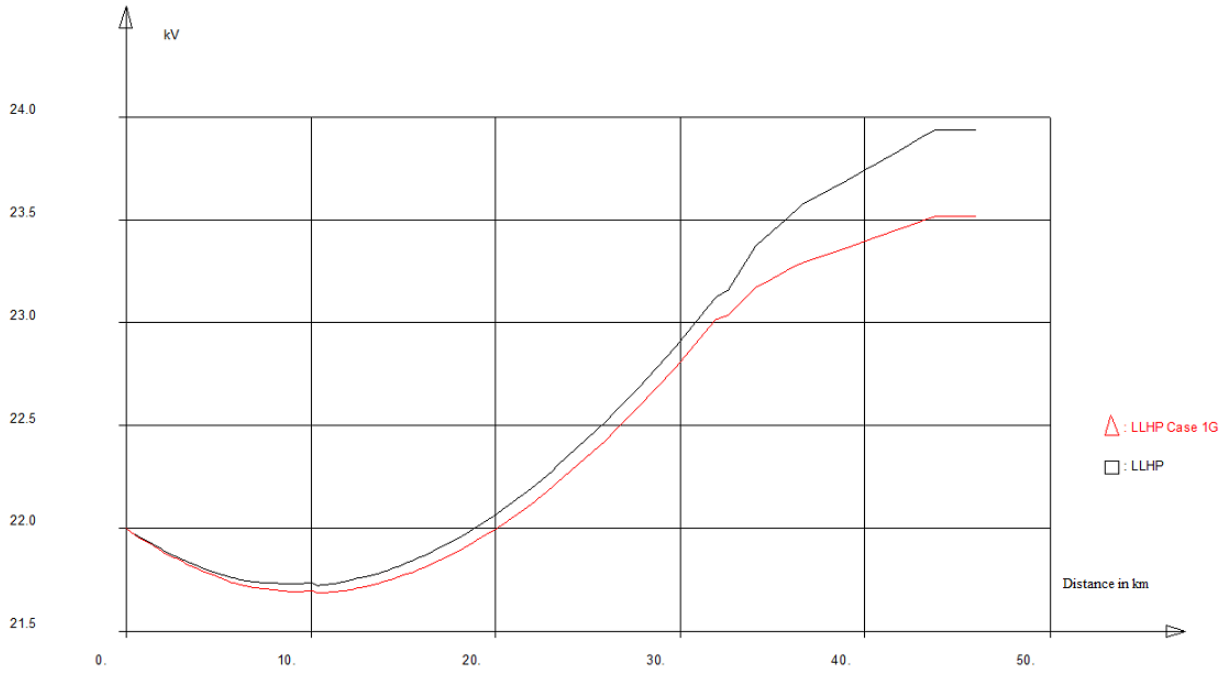

Figure 4.19: Case 1G, voltage rise from Øye substation (distance =0) to the end of the radial at Netland.

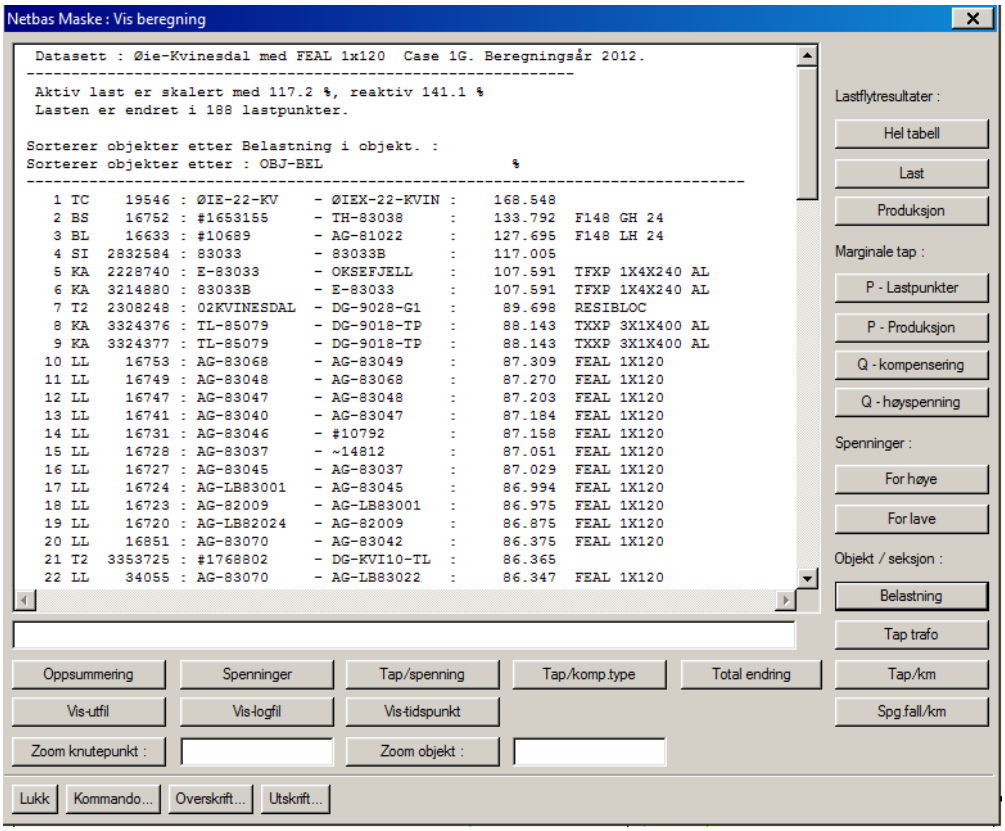

Figure 4.20: Case 1G, component load

4.2.9 Test case 1H

In this case reactive power is produced and consumed by the DG units that are south of Stakkeland. As Omland deliveres 0,10 MVAr to Oksefjell, and Narvestad deliveres 0,17 MVAr to Åråna. As a result, an aditional 0,27 MVAr is infused into the grid as shown in Table 4.11.As one can see this is also the maximum amount of reactive power one can have between the DG units in the grid.

Table 4.10: Case 1H, DG units and shunt-reactors output (MW and MVAr).

Name	Active power [MW]	Reactive power [MVAr]	Tan ϕ
Lindland	1,40	0,00	0,00
Kvinesdal	1,35	0,00	0,00
Trælandsfoss	10,00	0,00	0,00
Rafoss	13,60	0,00	0,00
Omland	0,40	0,10	0,25
Oksefjell	0,35	-0,10	
Narvestad	0,70	0,17	0,24
Åråna	0,50	-0,17	-0,33
Stakkeland	9,70	3,80	0,39
Kvinlog	1,20	-0,40	-0,33
Røynebru	1,00	-0,33	-0,33
Bergsli	0,81	-0,27	-0,33
Røyland	0,10	-0,03	-0,33
Eftestøyl	0,40	-0,13	-0,33
Kjilen	0,35	-0,12	-0,33
Røylandsfoss 1	0,6	-0,20	-0,33
Røylandsfoss 2	1,20	-0,40	-0,33
Selandsåne	2,00	-0,66	-0,33
Hisvatn	3,60	0,00	0,00
Hisvatn Shunt-reactor		-1,30	
Summation	49,26	-0,02	

As one can see from Figure 4.21 the voltage at Netland is now at 23,50 kV, which is a small improvement if compared to Case G. Furthermore, as shown in Appendix I the voltage at Eftestøyl is now at 23,70 kV, which gives a variation of 12,52 % between LLHP and HLLP. The lowest voltage is still at node TH-83040, where one can measure a voltage of 21,68 kV, which represents a voltage drop of 1,45 %. Furthermore, the transmission losses increase with another 9 kW, and the total losses are now 5,082 MW.

Furthermore, as one can see from Figure 4.22, all components except the current transformer at Øye, experiences change in load.

Firstly, the circuit breaker at Omland experiences an increase of 0,24 %, and are now at 134,04 % of nominal load. The circuit breaker at Slimestad experiences a insignificant increase of 0,02 % , and is now at 127,72 % of nominal load. Secondly, the fuse at node 83033-Oksekraft experience a significant increase of 6,70 %, and is now at 123,70 % of nominal load. Lastly, the cables at Oksefjell and Eftestøl both experience a significant increase of 6,15 %, and are now both at 113,75 % of nominal load. Still violating the requirements mentioned in section 2.3.1.

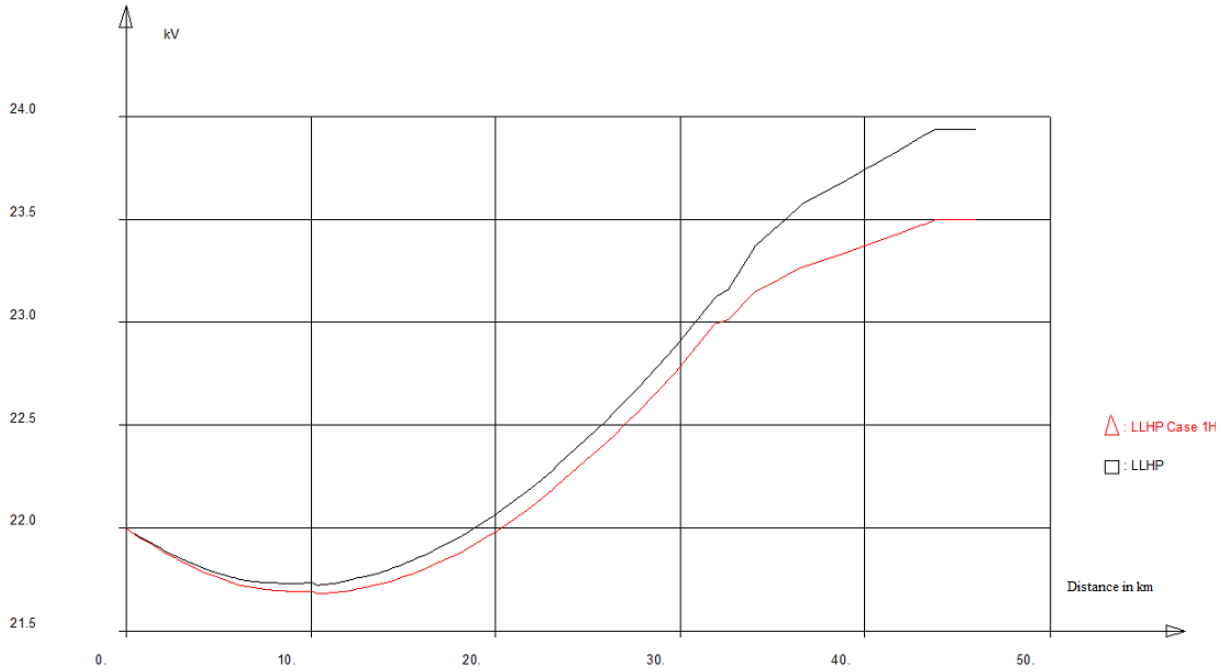

Figure 4.21: Case 1H, voltage rise from Øye substation (distance =0) to the end of the radial at Netland.

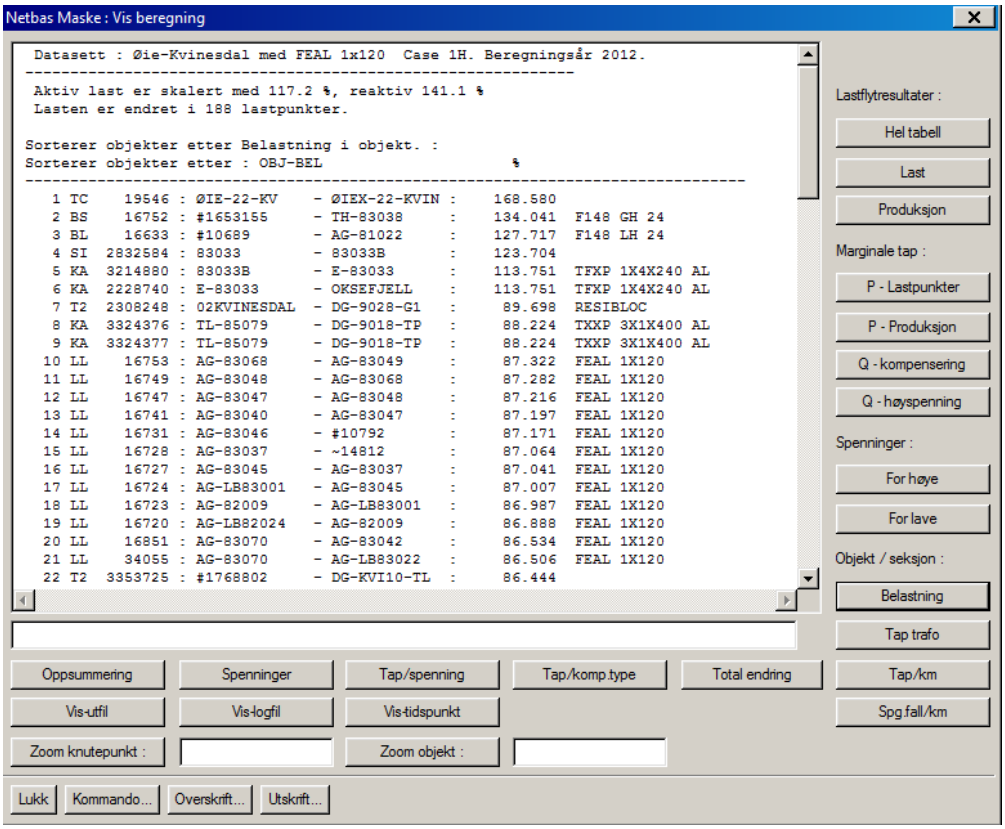

Figure 4.22: Case 1H, component load

4.2.10 Test case 1I

In this case reactive power is produced and consumed by the DG units that are south of Stakkeland. As Omland deliveres 0,10 MVAr to Oksefjell, and Narvestad deliveres 0,17 MVAr to Åråna. As a result, an aditional 0,27 MVAr is infused into the grid as shown in Table 4.11. As one can see this is also the maximum amount of reactive power one can have between the DG units in the grid.

As one can see from Figure 4.23 the voltage is considerably lower than that of Case G. By letting 1,30 MVAr flow from Øye substation to Hisvatn, the voltage at Netland is now down to 22,60 kV. Furthermore, the voltage at Eftestøl is now at 22,78 kV as shown in Appendix I, which represents a 8,34 % variation between LLHP and HLLP. This is close to the requirement of maximum 7% variation mentioned in section 2.3.2. Furthermore, the lowest voltage is now at node TH-83053, with a voltage of 21.23 kV which represents a 3,5 % voltage drop, well within the given limits. The transmission losses however, increases considereably and are now at 5,491 MW, which is an increase of 418 kW if compared to case H.

Table 4.11: Case 1I, DG units and shunt-reactors output (MW and MVAr).

Name	Active power [MW]	Reactive power [MVAr]	Tan ϕ
Lindland	1,40	0,00	0,00
Kvinesdal	1,35	0,00	0,00
Trælandsfoss	10,00	0,00	0,00
Rafoss	13,60	0,00	0,00
Omland	0,40	0,10	0,25
Oksefjell	0,35	-0,10	
Narvestad	0,70	0,17	0,24
Åråna	0,50	-0,17	-0,33
Stakkeland	9,70	2,50	0,26
Kvinlog	1,20	-0,40	-0,33
Røynebru	1,00	-0,33	-0,33
Bergsli	0,81	-0,27	-0,33
Røyland	0,10	-0,03	-0,33
Eftestøyl	0,40	-0,13	-0,33
Kjilen	0,35	-0,12	-0,33
Røylandsfoss 1	0,6	-0,20	-0,33
Røylandsfoss 2	1,20	-0,40	-0,33
Selandsåne	2,00	-0,66	-0,33
Hisvatn	3,60	0,00	0,00
Hisvatn Shunt-reactor		-1,30	
Summation	49,26	-1,32	

Furthermore, as one can see from Figure 4.24, all components experience a significant increase in load.

Firstly, the current transformer at Øye substation experience an increase of 8,64 %, and is now at 177,22 % of nominal load. Secondly, the circuit breakers at Omland and Slimestad both experience increasing loads of 6,17 % and 6,41% respectively. Thirdly, the fuse at node 83033-Oksekraft experience an increase of 3,10 %, and is now at 126,80 % of nominal load. Lastly, the cables at Oksefjellet and Eftestøl both experience an increase of 2,85 % and are now at 116,60 % of nominal load. Still in violation of the requirements mentioned in section 2.3.1.

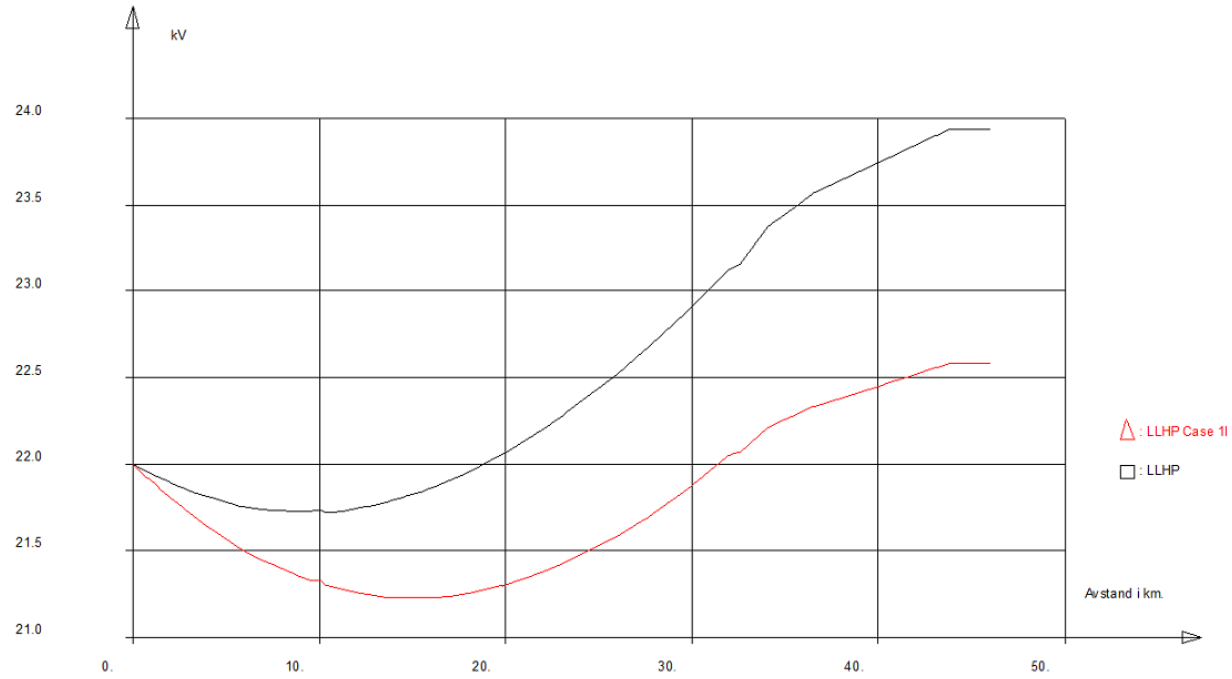

Figure 4.23: Case 1I, voltage rise from Øye substation (distance =0) to the end of the radial at Netland.

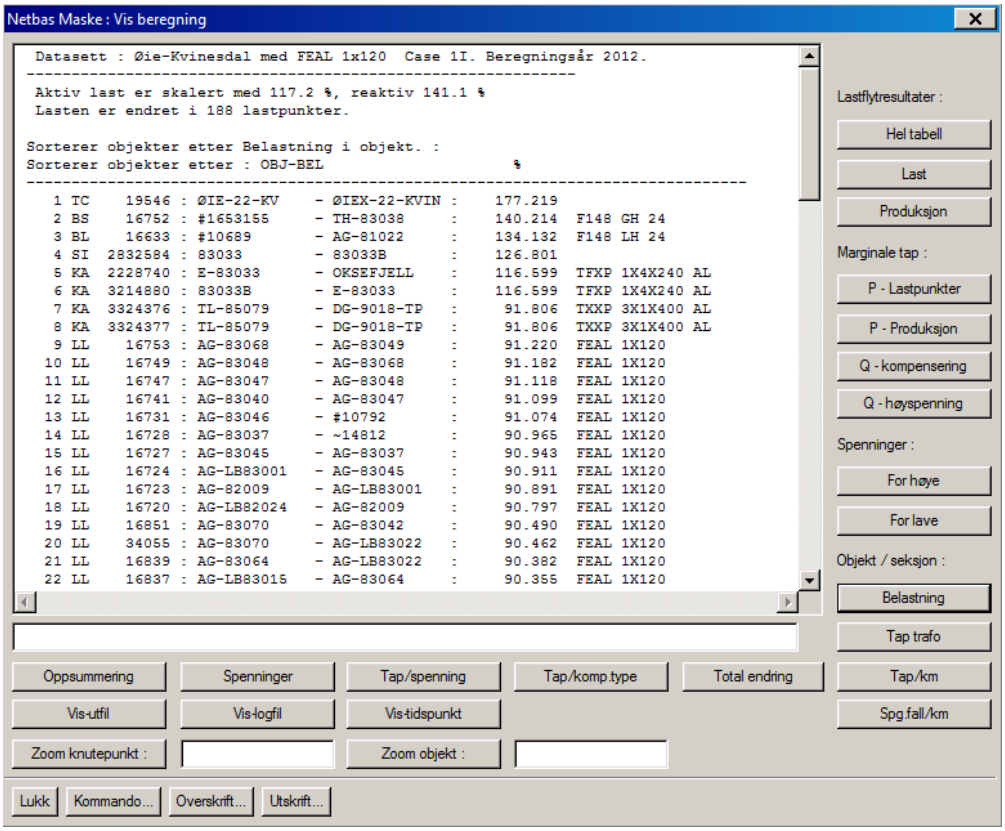

Figure 4.24: Case 1I, component load

4.2.11 Summary of simulation results

Firstly, by comparing all the previous cases, the voltage variation is reduced with the increase of reactive power in the grid. As one can see from Figure 4.25 the voltage improves considerably from Case A to Case H.

Secondly, as one can see from Figure 4.26 there is a voltage variation between HLLP and LLHP of approximately 8,5 % in Case I, measured at Netland. The voltage at Eftestøl is in Case I lowered to 22,78 kV, hence a one has a variation between HLLP and LLHP of 9,2 % at this location. As a result, the voltage variations at the most remote locations in the grid is close to fulfilling the requirement of maximum 7 % fluctuation, as mentioned in 2.3.1.

Thirdly, as one can see from Figure 4.27, the voltage at Eftestøl improves with each case. And is at Case I at 22,78 kV, which is an improvement of 5,61 % referred to the voltage at Øie busbar. The transmission losses on the other side increases, as shown in Figure 4.28. Here one can see an increase of 8,75 % referred to the initial loss during LLHP.

Lastly, as shown in Figure 4.29, the situation for overloaded components is worsened with each case. However, the overload is mostly due to the large active power component, as one can see from case 1A, where just a minimal portion of reactive power is present in the grid.

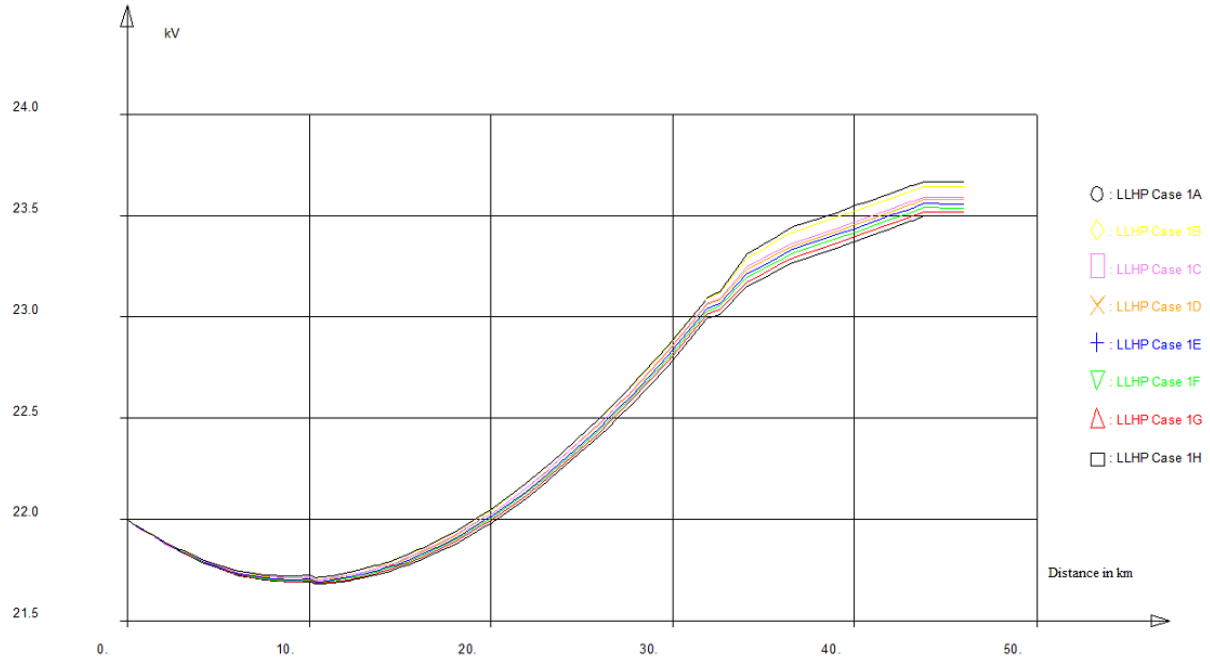

Figure 4.25: Comparing Cases, voltage rise from Øye substation (distance =0) to the end of the radial at Netland.

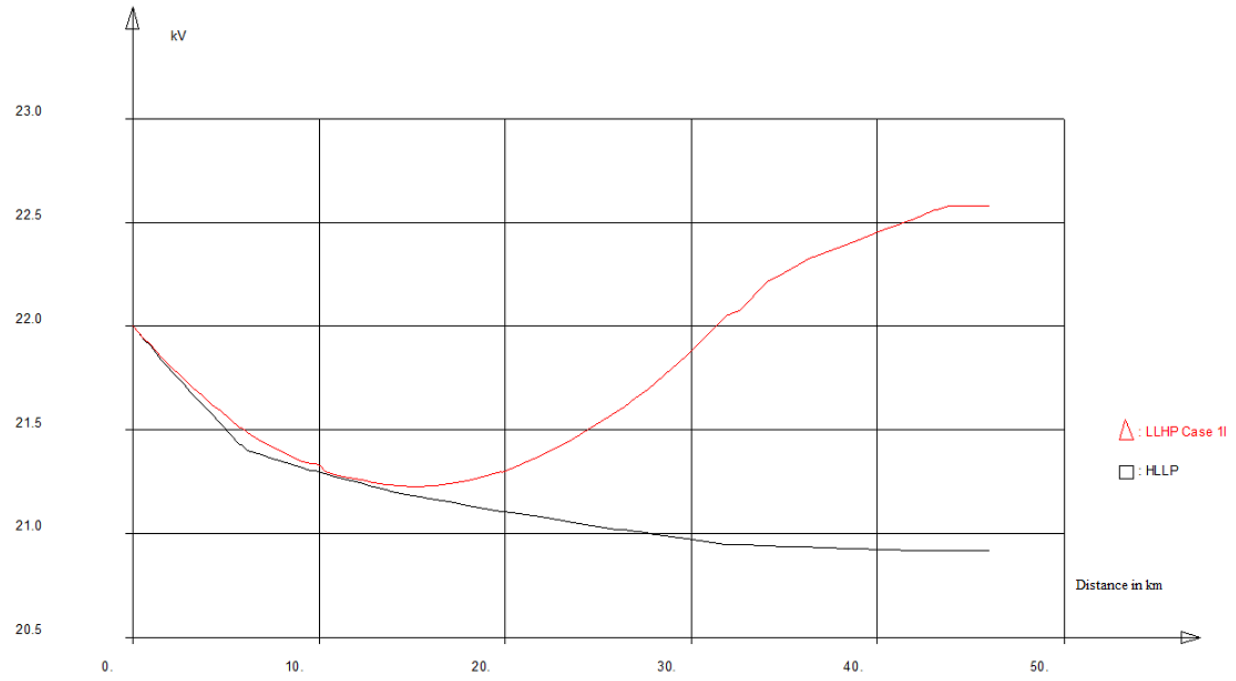

Figure 4.26: Case 1I vs HLLP, voltage rise from Øye substation (distance =0) to the end of the radial at Netland.

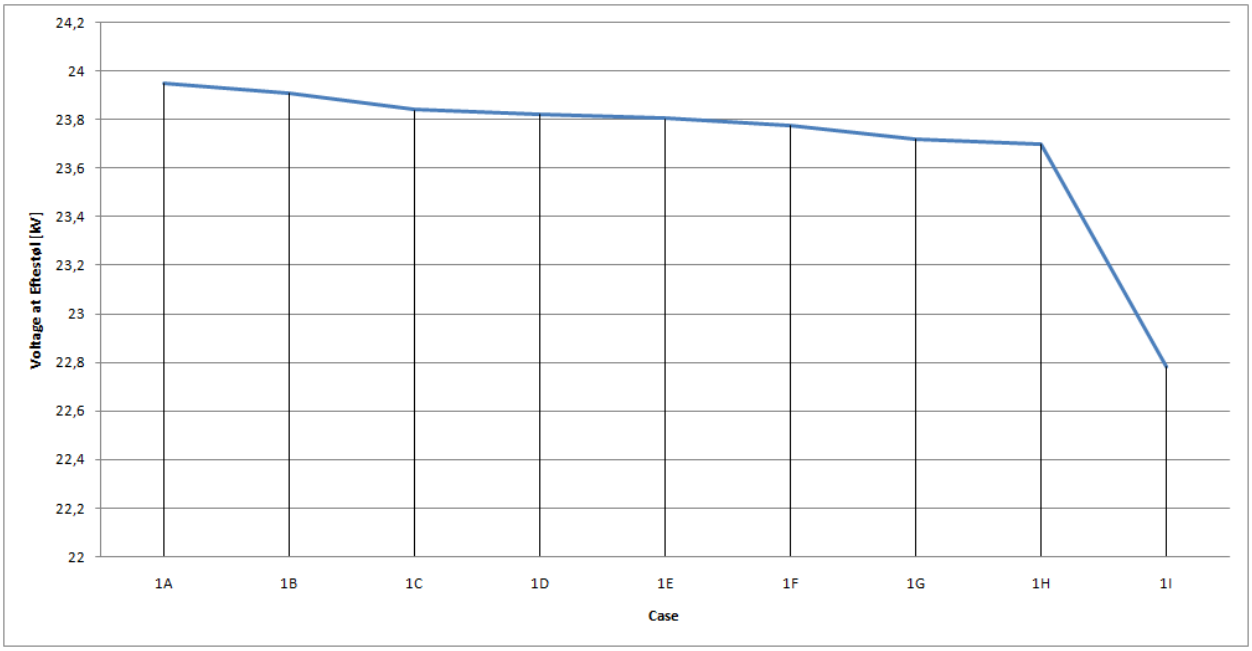

Figure 4.27: Voltage [kV] at Eftestøl, case by case

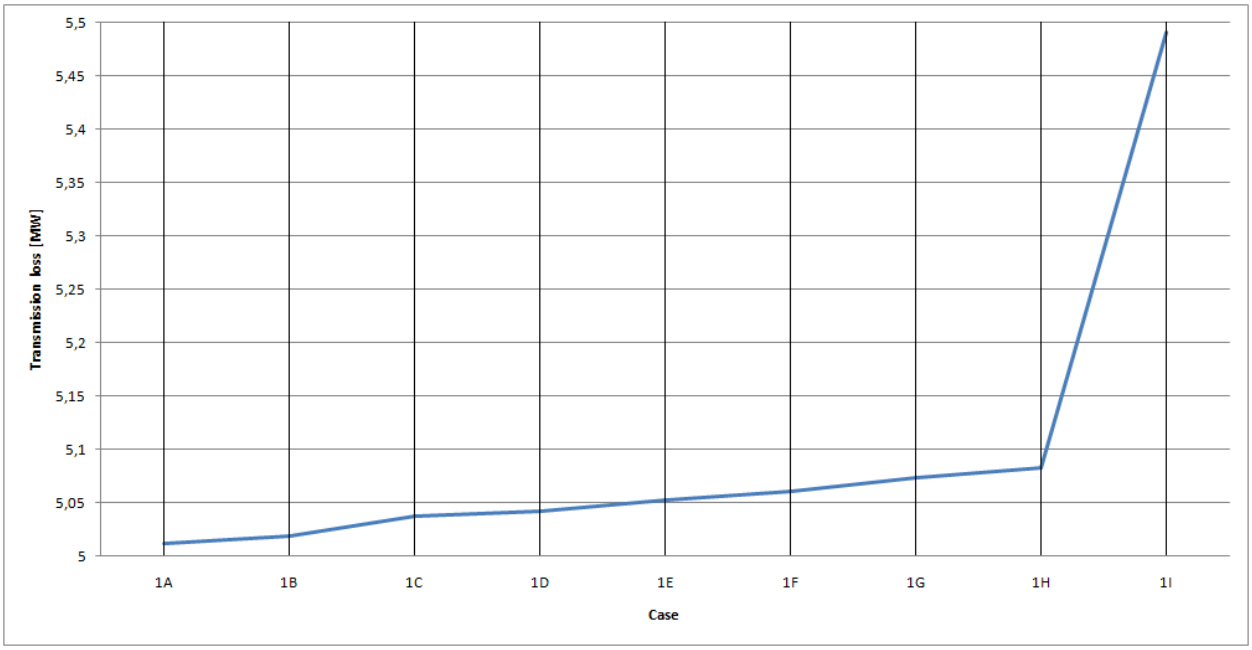

Figure 4.28: Transmission loss in the system [MW], case by case

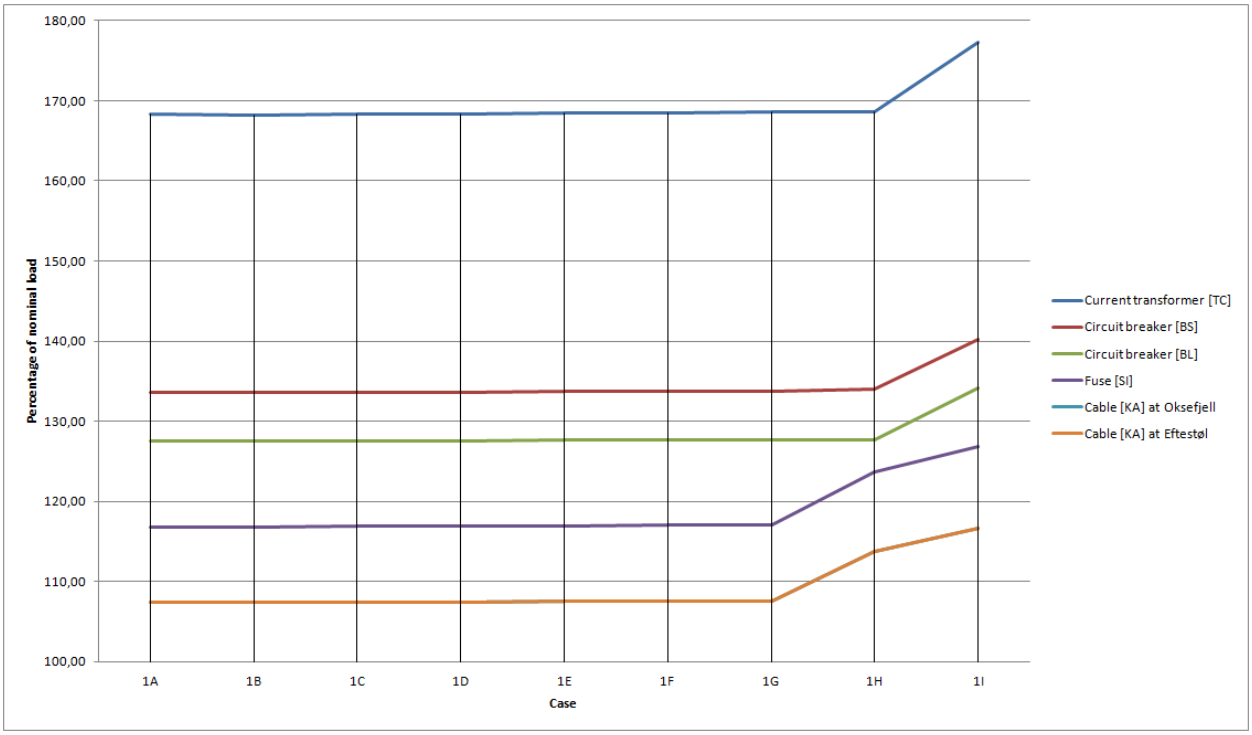

Figure 4.29: Summary of overloaded components, case by case

4.3 Costs

This section is based on the work done by Salzburg Netz in [16], and deals with the costs related to the communication related to controlling the DG units.

To fully implement reactive cooperation between the DG units one needs to invest in the integration of a new communication system. As experienced by Salzburg Netz, the cost of such an upgrade of the communication links can be expected to be as high as EUR 30 000 to EUR 50 000. In Norwegian currency this represents a cost of NOK 226 505 to NOK 377 509 [21]. To calculate a worst case, the highest value for the expenses is chosen as a foundation for further calculation. In other words, $\sim$ NOK 380 000.

Table 4.12: Cost of implementation of communication system

Name of DG unit	Cost of communication system [NOK]
Lindland	0
Kvinesdal	0
Trælandsfoss	0
Rafoss	0
Omland	380 000
Oksefjell	380 000
Narvestad	380 000
Åråna	380 000
Stakkeland	380 000
Kvinlog	380 000
Røynebru	380 000
Bergsli	380 000
Røyland	380 000
Eftestøyl	380 000
Kjilen	380 000
Røylandsfoss 1	380 000
Røylandsfoss 2	380 000
Selandsåne	380 000
Hisvatn	380 000
Summation	5 700 000

As one can see from Table 4.12 the total cost of such an implementation in the Kvinesdal distribution grid is NOK 5 700 000. As explained previously, Lindland,Kvinesdal , Rafoss and Trælandsfoss is not included here due to the fact that they will not contribute in the control of reactive power flow.

Chapter 5

Renewal of power lines in the Kvinesdal radial

As the load in the Kvinesdal radial increases with the number of installed DG units, a common measure to take is replacing the main feeder in the radial. This chapter deals with the replacement of the main feeder from Øye, step by step. The cost for such replacements will be briefly shown, to give a foundation for comparison.

5.1 Replacing existing FeAl 120 with 454-AL-59

5.1.1 Basis for test cases

As with the simulations in Chapter 4, the new production radial mentioned in Section 3.6 will be included, this to make the different cases in Chapter 4 and 5 comparable.

Furthermore, during these simulations, all DG units will run at PF=1. This to see the effect of changing feeder. The load for these cases is the same as in Chapter 4. Hence the load for the HLLP scenario is 14,0 MW /3,0 MVAr on connected points. The LLHP scenario is also here scaled to 20 % of high load, hence 2,8 MW / 0,6 MVAr. For each case, more and more of the original FeAl 120 feeder will be changed with 454-Al-59 as shown in table 5.1.

Table 5.1: Overview over feeders for simulation Case 2A, 2B and 2C

Sub radial	Case 2A Dimension	Case BA Dimension	Case 2C Dimension
Øye to Liknes	454-Al-59	454-Al-59	454-Al-59
Liknes to Sindland	FeAl 120	454-Al-59	454-Al-59
Sindland to Kvinlog	FeAl 120	FeAl 120	454-Al-59
Kvinlog to Netland	FeAl 50	FeAl 50	FeAl 50

As one can see one piece of the feeder section is changed per case, while the part going from Kvinlog to Netland is unchanged through all cases. By doing this, one will see how the 454-Al-59 influences the voltage compared to the FeAl 120.

5.1.2 Case 2A

This case deals with the replacement of the feeder from Øye to Liknes with a 454-Al-59. As mentioned in Section 3.1 this feeder has a length of 5,8 km and are currently of FeAl 120 type. As shown in table 5.2 the rest of the feeders are unchanged.

Table 5.2: Case 2A, overview over dimensions and length of power lines in the Kvinesdal radial

Sub radial	Dimension	Length
Øye substation to Liknes	454-Al-59	5,8 km
Liknes to Sindland	FeAl 120	14,1 km
Sindland to Kvinlog	FeAl 120	12,2 km
Kvinlog to Netland	FeAl 50	13,3 km

The results of this case is shown in Figure 5.1. Here one can see that by replacing 5,8 km of the excising feeder with 454-Al-59, one get a considerable drop in the voltage profile. Furthermore, during LLHP at these conditions the highest voltage is measured at Eftestøyl, which have an voltage of 23,66 kV. The lowest voltage during HLLP is measured at node TH-85077, which experience a voltage of 21,15 kV as shown in Appendix K. Hence, the variation between LLHP and HLLP is 2,51 kV, 11,41 % variation, which violates the requirements mentioned in section 2.3.2 by far. The voltage drop of 0,85 kV at HLLP represents a drop of 3,86 %, and is well within the given limits mentioned in section 2.3.2. The overall transmission losses are approximately 4,70 MW, which is also shown in Appendix K.

As one can see from Figure 5.2, six components are experiencing loads that exceed 100 % of nominal load. The current transformer (TC) at Øye is experiencing a load of 171,03 % of nominal load. This however is not surprising, due to the fact that all the power needs to pass this point as mentioned in section 4.2.2. Furthermore, the circuit breaker (BS) at Omland and the circuit breaker (BL) at Slimestad are also heavy overloaded. The fuse (SI) at node 83033-Oksekraft is experiencing an overload of 18,36 %, and as mentioned in section 4.2.2, this can influence the lifetime of the fuse. The cables (KA) from Oksefjell and Eftestøl both experience an overload of 8,84 %, which is in direct violation with the requirements mentioned in section 2.3.2.

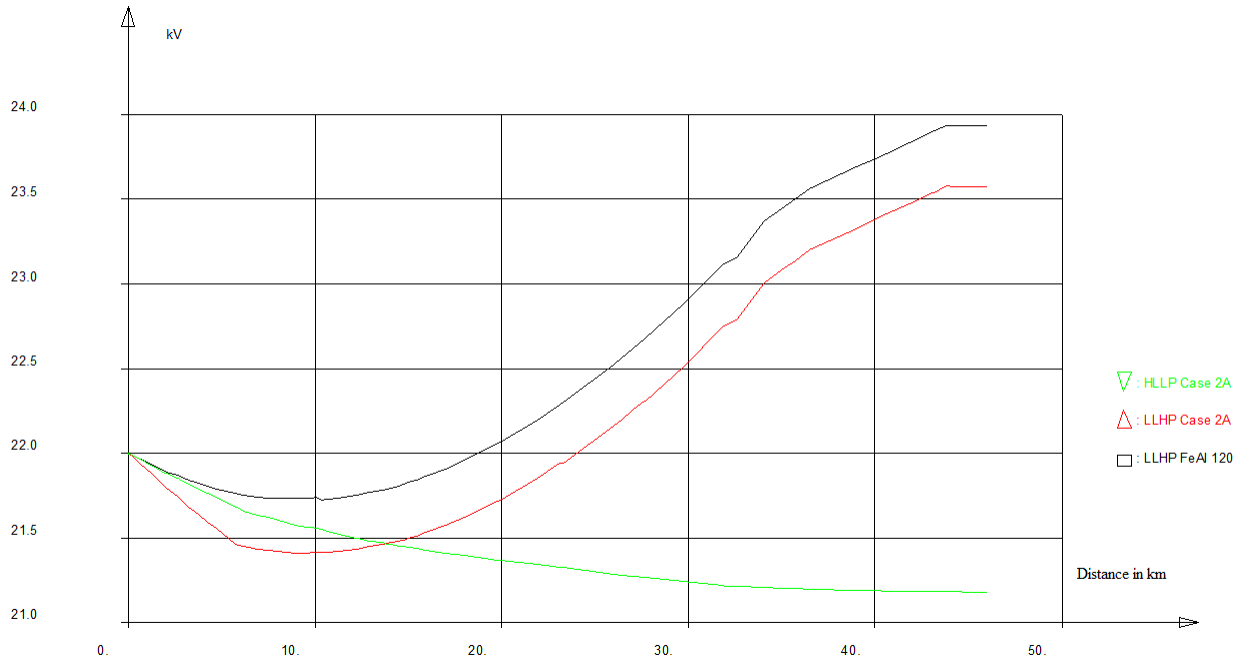

Figure 5.1: Case 2A, voltage rise from Øye substation (distance =0) to the end of the radial at Netland.

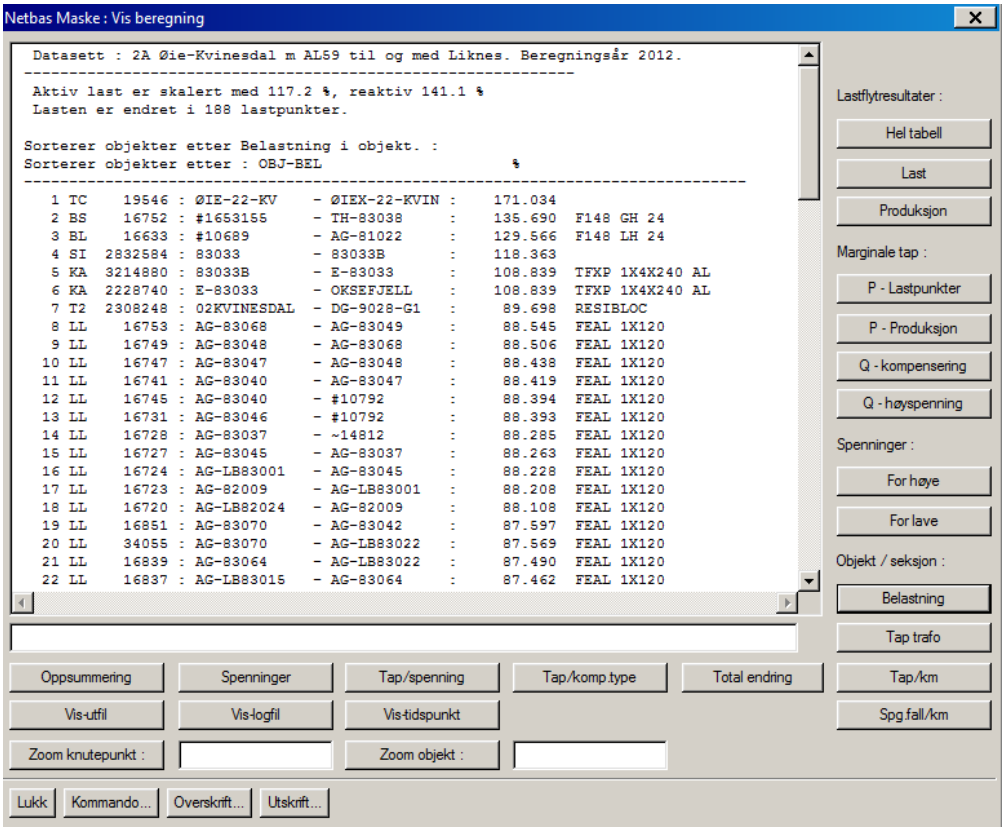

Figure 5.2: Case 2A, component load LLHP

5.1.3 Case 2B

In this case the feeder from Øye to Sindland has been exchanged with a 454-Al-59. As one can see from table 5.3 the total length of the exchanged feeder is 19,9 km, and is currently of FeAl 120 type. One can also see that the rest of the feeders remain unchanged.

Table 5.3: Case 2B, overview over dimensions and length of power lines in the Kvinesdal radial

Sub radial	Dimension	Length
Øye substation to Liknes	454-Al-59	5,8 km
Liknes to Sindland	454-Al-59	14,1 km
Sindland to Kvinlog	FeAl 120	12,2 km
Kvinlog to Netland	FeAl 50	13,3 km

By changing the first 19,9 km of the feeder from FeAl 120 to 454-Al-59, one gets a significant drop in voltage as shown in Figure 5.3. During LLHP at these conditions the highest voltage is at Eftestøl, which experience a voltage of 22,70 kV. The lowest voltage is measured at node TH-83014, which experience a voltage of 20,75 kV as shown in Appendix L. The lowest voltage at HLLP is never lower than that of LLHP as one can see from Appendix L, hence the voltage variation is that of 8,86 %. Which is close to fulfilling the requirements mentioned in section 2.3.2. The voltage drop is that of 1,25 kV, which represents a voltage drop of 5,68 %, which is within the requirements mentioned in section 2.3.2. As shown in Appendix L, the overall transmission losses are 3,93 MW, an improvement of 0,77 MW if compared to Case 2A.

As one can see from Figure 5.4 there is a 8,0 % increase in load for the current transformer (TC) at Øie if compared to Case 2A. Furhermore, the circuit breaker (BS) at Omland and the circuit breaker (BL) at Slimestad experiences an increase of $\sim 6\%$. The fuse (SI) at node 83033-Oksekraft experience an increase of $\sim 3\%$, and the cables (KA) from Oksefjell and Eftestøl both experience an increase of $\sim 3{,}2\%$, hence, they are now experiencing an overload of 12 %, violating the requirements mentioned in section 2.3.2.

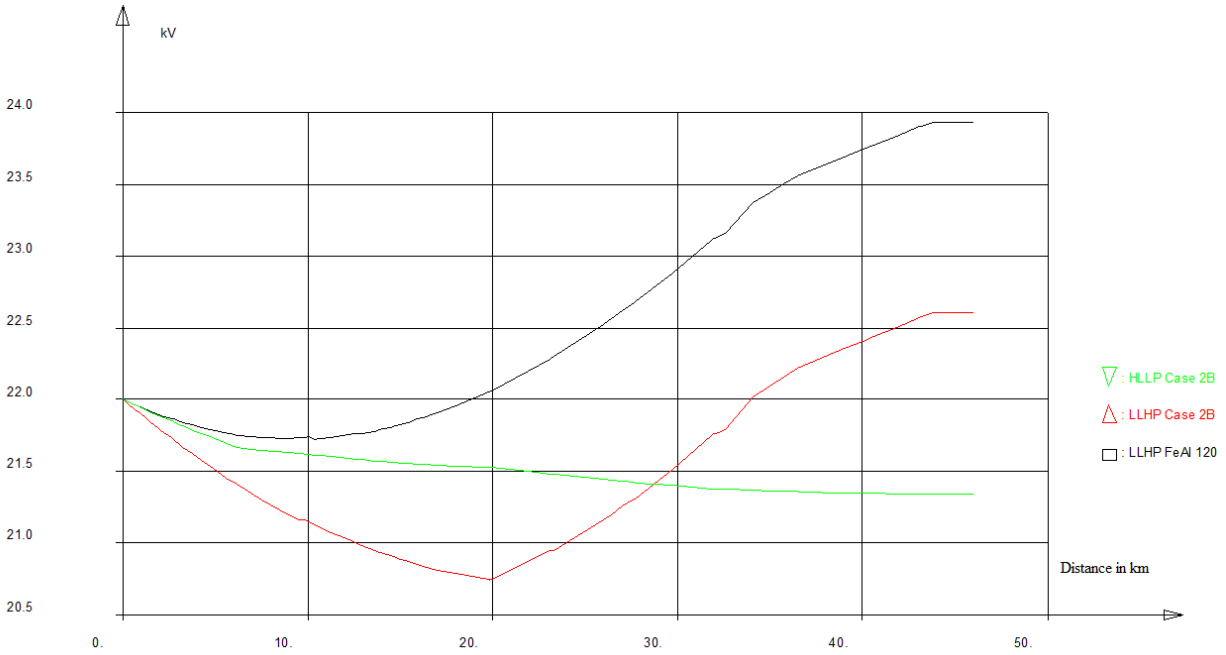

Figure 5.3: Case 2B, voltage rise from Øye substation (distance =0) to the end of the radial at Netland.

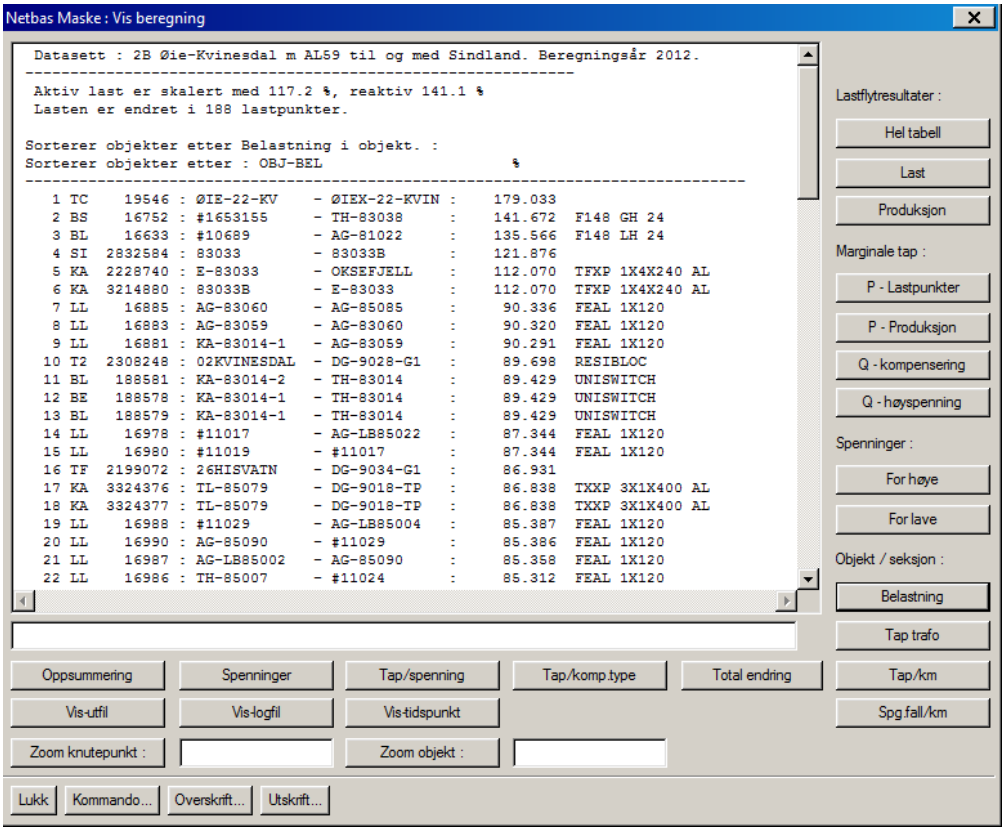

Figure 5.4: Case 2B, component load LLHP

5.1.4 Case 2C

This case deals with the replacement of the feeder from Øye to Kvinlog with a 454-Al-59. As shown in table 5.4 the total length of the substituted feeder is 32,1 km, and is currently of FeAl 120 type. One can also see that the feeder from Kvinlog to Netland is unchanged in this case.

Table 5.4: Case 2C, overview over dimensions and length of power lines in the Kvinesdal radial

Sub radial	Dimension	Length
Øye substation to Liknes	454-Al-59	5,8 km
Liknes to Sindland	454-Al-59	14,1 km
Sindland to Kvinlog	454-Al-59	12,2 km
Kvinlog to Netland	FeAl 50	13,3 km

The result of this case is shown in Figure 5.5. As one can see, changing 32,1 km of the feeder with 454-Al-59 gives a considerable voltage drop. As one can see from Appendix M, the lowest and highest voltage occurs during LLHP, hence the voltage variation is decided purely by the LLHP situation. During LLHP at these conditions the highest voltage is measured at node#1768568, which experience a voltage of 22,21 kV. The lowest voltage during LLHP is measured at node#11019, which experience a voltage of 20,69 kV. This gives a variation of 7,60 % , which is close to fulfilling the requirements mentioned in section 2.3.2. The voltage drop of 1,31 kV is also within the given limits, as this represents a 5,95 % voltage drop. As shown in Appendix M, the overall transmission losses are 3,23 MW, an improvement of 0,70 MW if compared to Case 2B.

As shown in Figure 5.6 there is a 7,5 % increase in load for the current transformer (TC) at Øie, if compared to Case 2B. The circuit breakers (BS and BL) at Omland and Slimestad both experience an increase of 5,61 %. In addition the fuse (SI) at node 83033-Oksekraft experience a small increase of 0,2 %. The cables (KA) at Oksefjell and Eftestøl both experience an increase of 0,18 %, hence they are now at 12,25 % overload, still violating the requirements mentioned in section 2.3.2.

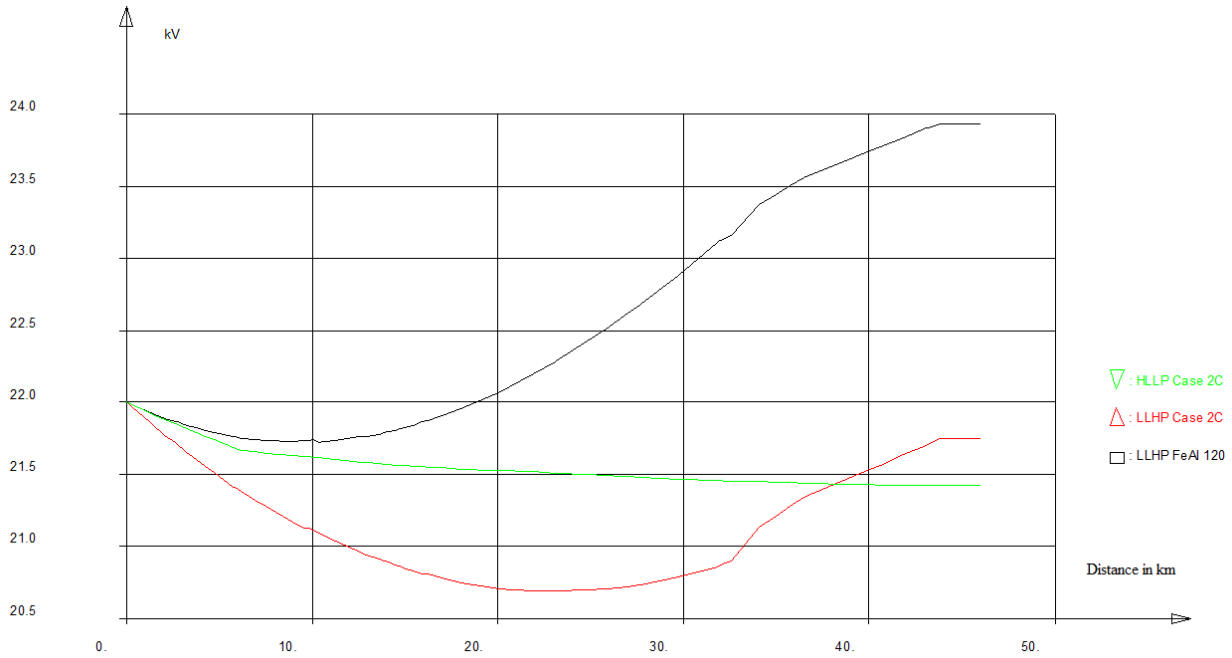

Figure 5.5: Case 2C, voltage rise from Øye substation (distance =0) to the end of the radial at Netland.

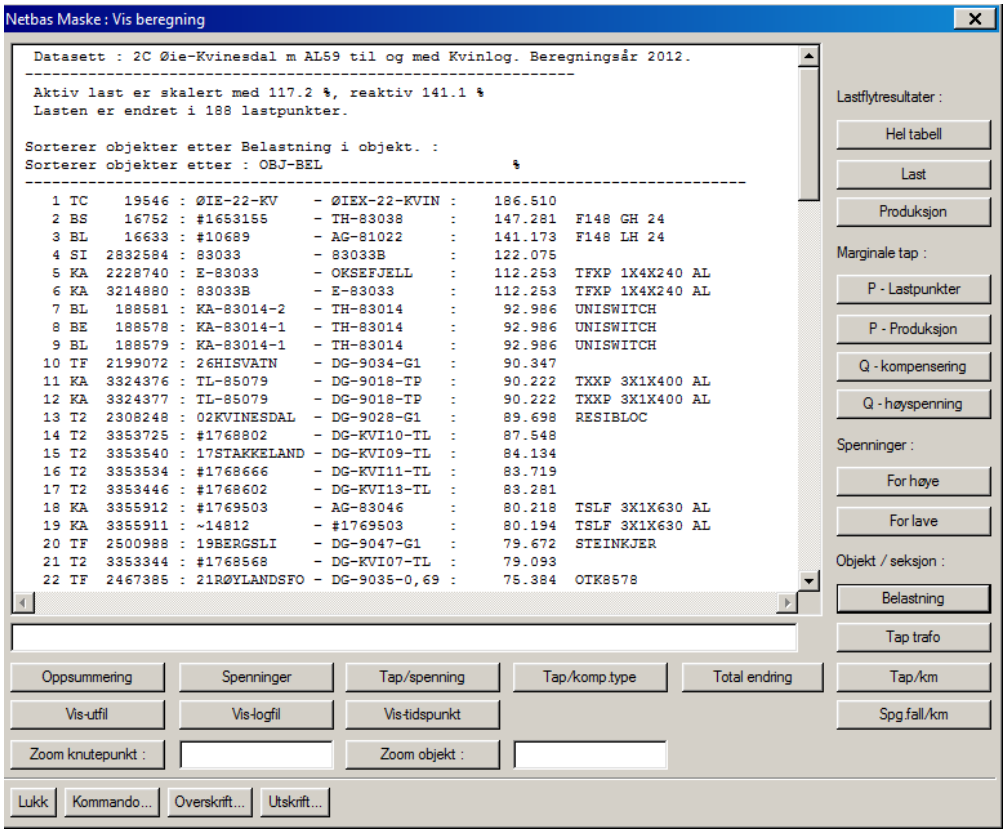

Figure 5.6: Case 2C, component load LLHP

5.1.5 Summary of simulation results

Firstly, as one can see by comparing Case 2A, 2B and 2C is that the voltage variation is improved from case to case. From an 11,41 % voltage variation in Case 2 A to a voltage variation of 7,60 % in case 2C.

Secondly, as shown in Figure 5.7 and Figure 5.8, the replacement of the feeder in the radial has a huge impact, when compared to the original FeAl 120 feeder. As one can see from Figure 5.7, the voltage is lowered with 2,5 kV in some areas if one compare Case 2C with the original grid with FeAl 120. This comes as a direct result of the X/r ratio of the 454-Al-59, which is almost two times as large as the X/r ratio of the FeAl 120. As a result, the reactive power component has a greater influence on the voltage in a power system when 454-Al-59 is used. As one can see from Appendix K,L and M, there is a great amount of reactive power in the grid due to the inductance of the feeders. Which gives a great voltage drop over the 454-Al-59 feeder, as shown in Figure 5.7. As one can see from Figure 5.8, the voltage drop improves. However, this is due to the low current at HLLP. As the load during HLLP is $\frac{1}{3}$ of that of LLHP.

Thirdly, as shown in Figure 5.9, several components are severely overloaded. And the situation is worsened with the replacement of the feeder, case by case. However, as discussed in section 4.2.11.

Lastly, as one can see from Figure 5.10, the overall transmission loss decreases in the radial, as more and more of the FeAl 120 feeder is replaced by 454-Al-59. This is due to the fact that the ohmic resistance in the 454-Al-59 is half of that of FeAl 120. Hence, the transmission loss is lower.

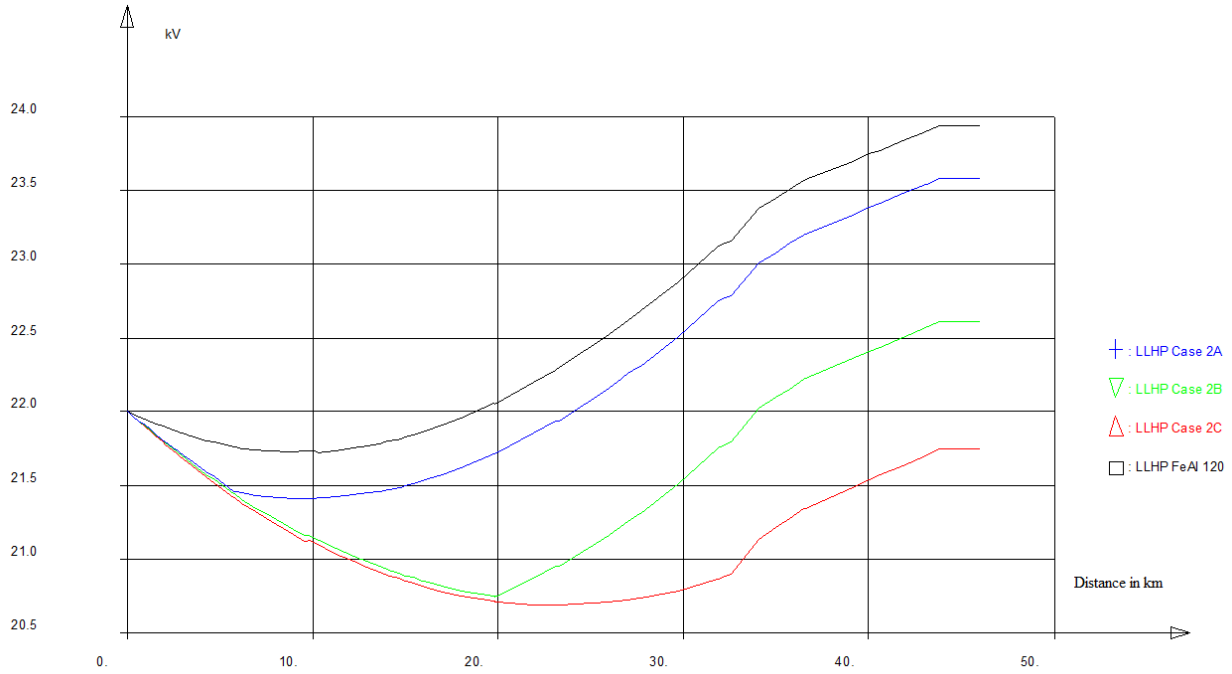

Figure 5.7: Summary of Case 2, LLHP.

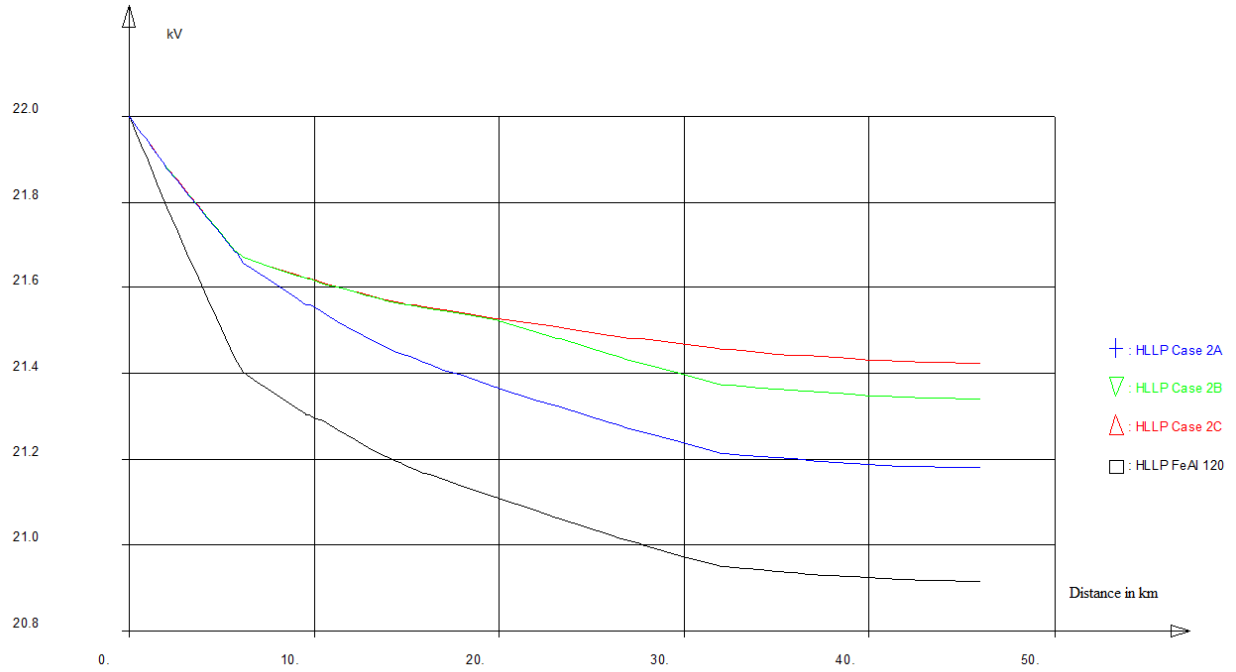

Figure 5.8: Summary of Case 2, HLLP.

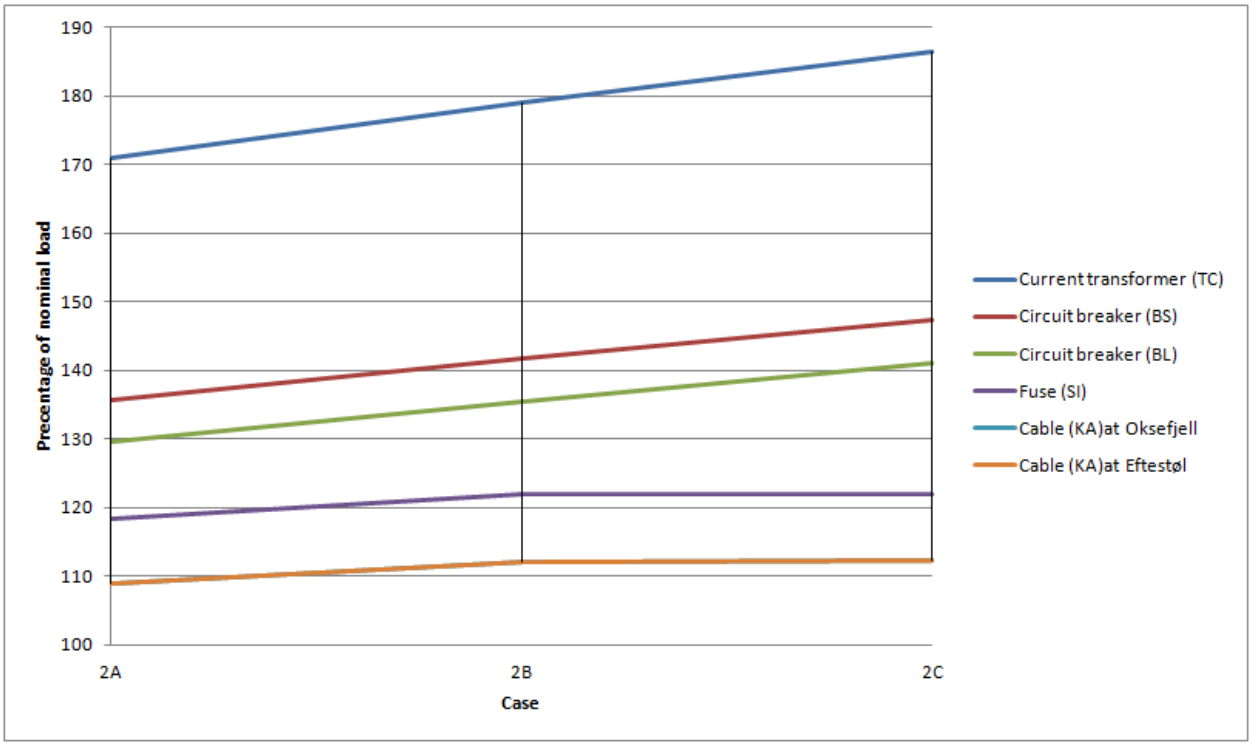

Figure 5.9: Summary of Case 2, component load, case by case.

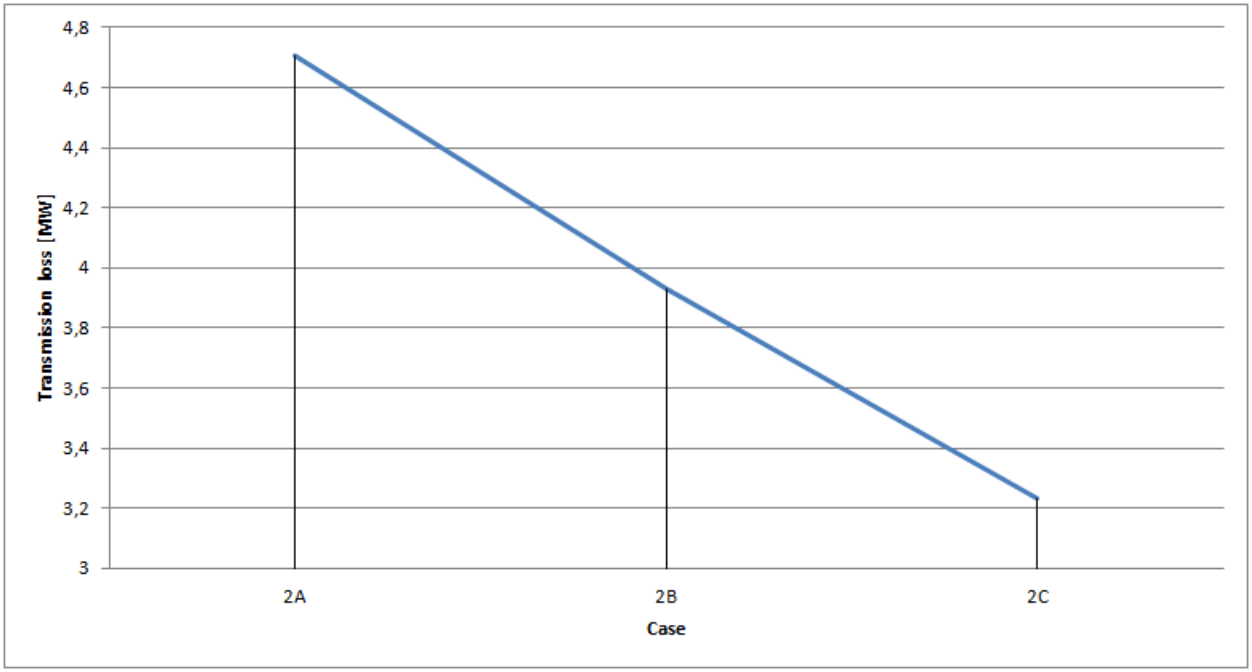

Figure 5.10: Summary of Case 2, transmission loss, case by case.

5.2 Costs

The costs in question will only be present costs, depreciation and such will not be included. When changing the feeder from FeAl 120 to 454-Al-59, one must calculate with the demolition cost for the old power lines. These cost are estimated to be approximately 100 000 ,- NOK per kilometer of old transmission lines [22]. Building the new 454-Al-59 transmission line is estimated to 1 400 000 ,- NOK per kilometer. Hence, the total expenses per kilometer of 454-Al-59 will be 1 500 000,- NOK [22]. Hence the function for the total cost is as shown in Equation 5.1.

$$C(x) = 1500000x \tag{5.1}$$

C= Total cost
x = Number of km of feeder which are to be replaced

Table 5.5: Cost of renewal of power lines in the Kvinesdal radial

Case	Number of km with 454-Al-59	Cost [NOK]
2A	5,8	8 700 000
2B	19,9	29 850 000
2C	32,1	48 150 000

As one can see from table 5.5, there are considerable costs involved in renewal of the main feeder in Øye.

Chapter 6

Discussion

In the prior study of the network radial, it is shown that the current voltage variation is in clear violation with the requirements stated in section 2.3.2. To allow more DG units to be connected, measures have to be taken. Therefore a new production radial is suggested for making the connection of the new DG units possible as shown in section 3.6. However, with all DG units connected, the voltage variation is still too high, even with the new production in place.

Case 1 shows the advantage of having generators running in co-operative reactive mode. As shown in Figure 4.25, the voltage at LLHP is clearly decreased in each case. Hence, increasing the reactive component in the grid, contributes to lowering the voltage within the geographical area. As shown in Case 1I, it is possible to reduce the voltage variation down to 8,34 %, which is close to fulfilling the requirement stated in section 2.3.2. However, by doing so, several generators have to run at their maximum level of under-excitement. As a result, one can expect a significant temperature increase in the generator due to the resulting reactive power. In addition, the losses increase with the increasing reactive component in the feeder as shown in Figure 4.28.

Case 2 gives a clear indication on how 454-Al-59 reacts to reactive power, when compared to FeAl 120. As shown in Case 2A, 2B and 2C, 454-Al-59 gives a higher voltage drop due to the reactive component in the feeder. This is directly related to the X/r relationship, which is approximately 5,0 for the 454-Al-59, while it is approximately 2,5 for FeAl 120. The interesting part in these cases is that the voltage drop is caused mostly by the feeders self inductance. As one can see from Appendix K, L and M the reactive power drawn by the feeder amounts to approximately 80 % of the total reactive power in the grid. Hence, the voltage drop is caused by the reactive power drawn by the feeder itself. This due to the high X/r ratio of the feeder. The ohmic loss for 454-Al-59 which is caused by the DG units production, is not large enough to counter the reactive power drawn by the feeder itself. As a result, the voltage in the grid drops when the FeAl 120 feeder is replaced with a 454-Al-59 feeder. However, as one can see, the 454-Al-59 gives a smaller $\triangle$U, hence the total impedance is smaller and one gets a more robust grid.

As shown in Chapter 5, the voltage variation in Case 2C is close to fulfilling the requirements mentioned in section 2.3.2, as the voltage variation in this case is 7,60 %. In addition, the losses are down to 3,23 MW in Case 2C. Hence, one can see that 454-Al-59 is considerable better in terms of voltage variation and loss, when compared to FeAl 120.

Furthermore, when the voltage reaches certain predetermined min/max values, the AVR in the DG units will start to run under or overexcited to stabilize the voltage to the preferred predetermined value. Hence, as all simulations are performed at what is called PQ (predetermined active and reactive power values, with no voltage control) mode in NetBas, they are not reacting to the voltage variation. In practice the AVR in the DG units would run at PQ mode until the voltage limit is reached, then switch over to some sort of quasi PE (predetermined voltage) mode. In other words, voltage regulation is not considered in the simulations done in Case 2. As a result, the simulations done in Case 2, are not completely realistic. However, they give a clear indication of a decidedly worst case imaginable, and in addition given an insight in the difference in properties for the FeAl 120 and 454-Al-59.

Regarding the cost of the different cases, one can clearly see that Case 1 is less expensive than that of Case 2A, 2B and 2C. However, as shown in Chapter 5, the improvement regarding voltage variation and loss are considerably better than that of Case 1I shown in Chapter 4.

The optional Case 3 was not carried out due to the lack of time.

Chapter 7

Conclusion

The purpose of the work was to get a better insight in how much different measures can reduce voltage variations in the Kvinesdal radial. As the current voltage variations in the Kvinesdal radial considerably exceeds given limits, Agder Energy wanted to know how much it was possible to reduce these variations with co-ordinated VAr control, and compare this to the common measure of changing the feeder itself.

To simulate the co-ordinated VAr control and changing of feeder, several simulation models were established in the simulation program NetBas. To fully see the trend for co-operative VAr control, a total of 9 cases were simulated, because the change in the voltage profiles is small, due to the small size of several of the DG units. For feeder change, only 3 cases were simulated, as the change of feeder gives a significant change in the voltage profile.

Case 1 deals with the co-ordinated VAr control, and the findings here show several interesting points. Firstly, running generators underexited helps to reduce the voltage at the DGs location. Secondly, by having a large generator in the grid running overexcited and supplying the smaller ones with reactive power, one avoids reactive power being drawn for the Regional grid. Lastly, in the Kvinesdal radial one can at best reduce the voltage variation with approximately 0,40 kV with co-operative VAr control alone. However, by letting the shunt-reactor at Hisvatn run at full capacity, one can reduce the voltage variation with approximately 1,20 kV. As a result, it is shown that it is possible to reduce the voltage variation in the Kvinesdal radial down to approximately 8,3 %.

Case 2 deals with the change of feeder from FeAl 120 to 454-Al-59. Here the findings clearly show that changing the feeder itself gives a significant voltage variation drop. As shown in Case 2C, one can see that a complete change from FeAl 120 to 454-Al-59 results in a voltage variation in the grid of only 7,6 %. However, one should notice that the voltage drop for 454-Al-59 is mostly caused by the reactive power consumed by the feeder itself. And that the simulation results of all generators running at power factor = 1 is not realistic, as the generators automatic voltage regulator would react to these high voltages and force the generators to run at an alternative power factor, hence stabilizing the voltage. Netbas on the other hand does not cover this fact, and in the simulations done, all generators are locked in PQ mode, where the power factor of the generators is locked.

A cost analysis clearly shows that changing the feeder is considerable more expensive than the co-ordinated VAr control. However, as the co-ordinated VAr control puts a lot of strain on the generators (running at tan ϕ = -0,33), increasing the transmission losses and only lowering the voltage by a small amount, one should consider this as an option of maximizing the number of DG units in the grid. Nevertheless, when the grid already is experiencing heavy loads, one should rather consider changing the feeder. As shown, by changing the feeder in the Kvinesdal radial, one will get a more robust grid, and lower transmission losses.

It is recommended that further work is done on the co-ordinated VAr control, as this type of control can be helpful in radials where one only needs a slight reduction in voltage to enable the connection of more DG units. In addition, a study of the 454-Al-59 and its reaction to extensive reactive power flow should be done, to see how the 454-Al-59 behaves in different situations when compared to FeAl 120.

Bibliography

[1] T. Tran-Quoc, L. Le Thanh, N. Hadjsaid, C. Kieny, O. Devaux , O. Chilard, *Stability analysis for distribution network with distributed generation*, Transmission and Distribution Conference and Exhibition, 2005/2006 IEEE PES

[2] SINTEF, "Småkraft", *http://www.sintef.no/Miljo/Fornybar-energi/Vannkraft/Smakraft, 07.12.2012.*

[3] T.Ackermann, G.Andersson, L. Søder, "Distributed generation: a definition", *http://www.sciencedirect.com/science/article/pii/S0378779601001018, 07.12.2012.*

[4] N. Jenkins, R. Allan, P. Crossley, D. Kirschen, G. Strbac, *Embedded Generation*, IEE Power and Energy Series 31, London, 2000.

[5] Stephen J. Chapman, *Electric Machinery and Power System Fu-ndamentals*, McGraw-Hill Higher Education, New York, 2002.

[6] J. D. Hurley, L. N. Bize, and C. R. Mummert, *"The adverse effects of excitation system VAr and power factor controllers,"*, Energy Conversion, IEEE Transactions on, vol. 14, no. 4, pp. 1636-1645, Dec.1999.

[7] IEEE Std 421.1-2007, *IEEE Standard Definitions for Excitation Systems for Synchronous Machines* , 2007

[8] R. Singh, B.C. Pal and R.A. Jabr, *" Choice of estimator of distributed system state estimator"*, IET Generation, Transmission & Distribution, IEEE Transactions on, vol. 3, no. 7, pp. 666-678, July 2009.

[9] Rasjonell Elektrisk Nettvirksomhet, *" Rammeavtale Tilknytnings- og nettleieavtale for innmatingskunder"*, *http://www.ren.no/web/guest/smaakraft*, 17.02.2013.

[10] Norconsult, *"Nettilknutning av småkraftverk i Kvinesdal"*, Confidensial study made for AEN, February 2013.

[11] Lovdata, "Forskrift om leveringskvalitet i kraftsystemet", *http://www.lovdata.no/for/sf/oe/oe-20041130-1557.html, 13.02.2013.*

[12] Agder Energy, "Technical challenges due to voltage and frequency fluctuations.",2012, University of Agder.

[13] Agder Energy , "Tilknytning av DG",03.05.2010, University of Agder.

[14] C.Gao and M.A. Redfern, *"A review of voltage control techniques of networks with distributed generations using On-Load Tap Changer transformers "*, IEEE Transactions on, Universities Power Engineering Conference (UPEC), 2010 45th International, Aug. 31 2012 - Sept. 3 2012.

[15] A. G. Endegnanew, *"Integration of Distributed Generation in the Future Distribution System"*, NTNU, Trondheim,Dec.2009.

[16] Salzburg Netz and Simens AG Österreich , *"Smart Grids Modellregion Salzburg:Zentrale Spannungs-(U) und Blindleistungsregelung (Q) mit dezentralen Einspeisungen in der Demoregion Salzburg"*, Neue Energien 2020, Österreich ,30.04.2012.

[17] A. Maknouninejad, Z. Qu, J. Enslin and N. Kutkut, *"Clustering and cooperative control of distributed generators for maintaining microgrid unified voltage profile and complex power control"*, IEEE Power Engineering Society Transmission and Distribution Confrence, 2012.

[18] WIKIPEDIA, "World energy consumption", *http://en.wikipedia.org/wiki/World_energy_consumption, 02.03.2013*

[19] WIKIPEDIA, "Renewable energy in the European Union", *http://en.wikipedia.org/wiki/Renewable_energy_in_the_ 02.03.2013*

[20] WIKIPEDIA, "Renewable energy in Norway", *http://en.wikipedia.org/wiki/Renewable_energy_in_Norway, 02.03.2013*

[21] Norges Bank, "Valutakurs for euro (EUR)", *http://www.norges-bank.no/no/prisstabilitet/valutakurser/eur/, 02.04.2013*

[22] Correspondanse with Rolf Håkan Josefsen, engineer at Agder Energy, 23.04.2013

Appendices

Appendix A

Calculation of base load and voltages in the Kvinesdal radial

To find the correct load used in the Norconsult rapport, trial and error were used. By this method the voltage profile shown in Figure A.1 was found when the load was 14,0MW / 3,0 MVAr. By comparison, one can see that this figure has a sticking similarity to that of the Norconsult report shown in Figure A.2. During these simulations the shunt reactor at Hisvatn was disabled, and the grid which was used was the original grid without modifications. The production which the DGs had during LLHP simulation is shown in Table A.1.

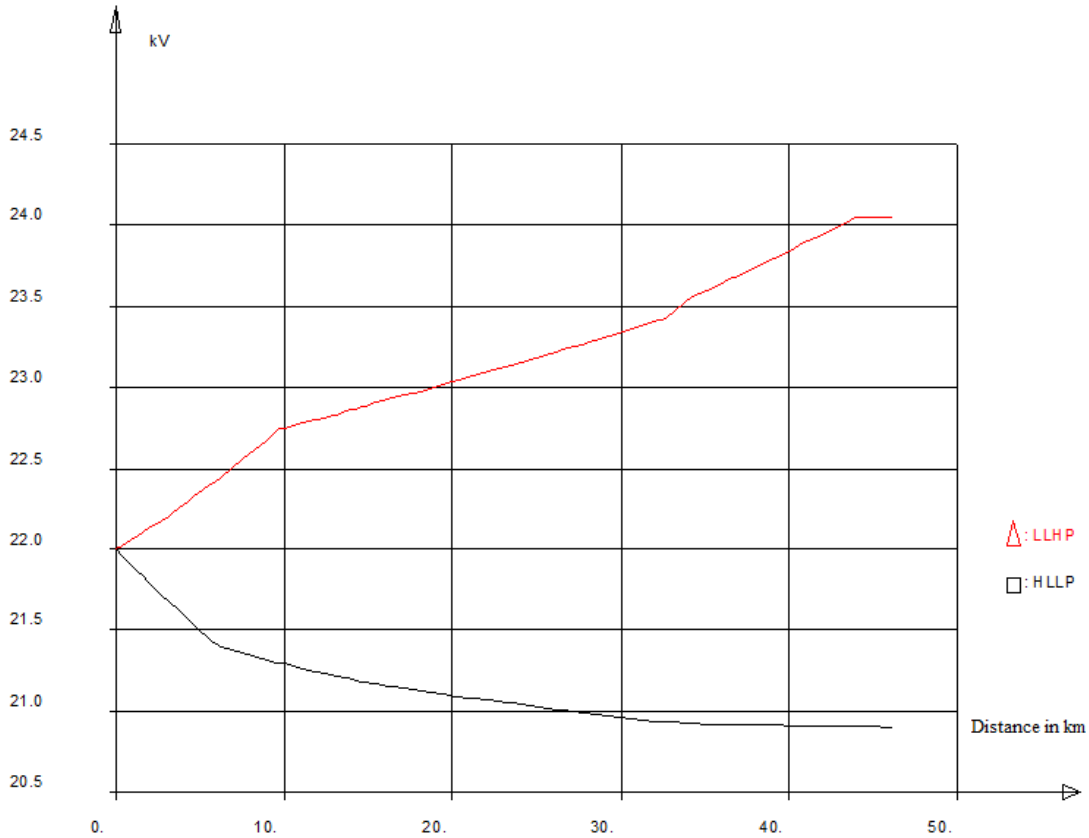

Figure A.1: Appendix A, Voltage rise from Øye substation (distance =0) to the end of the radial at Netland.

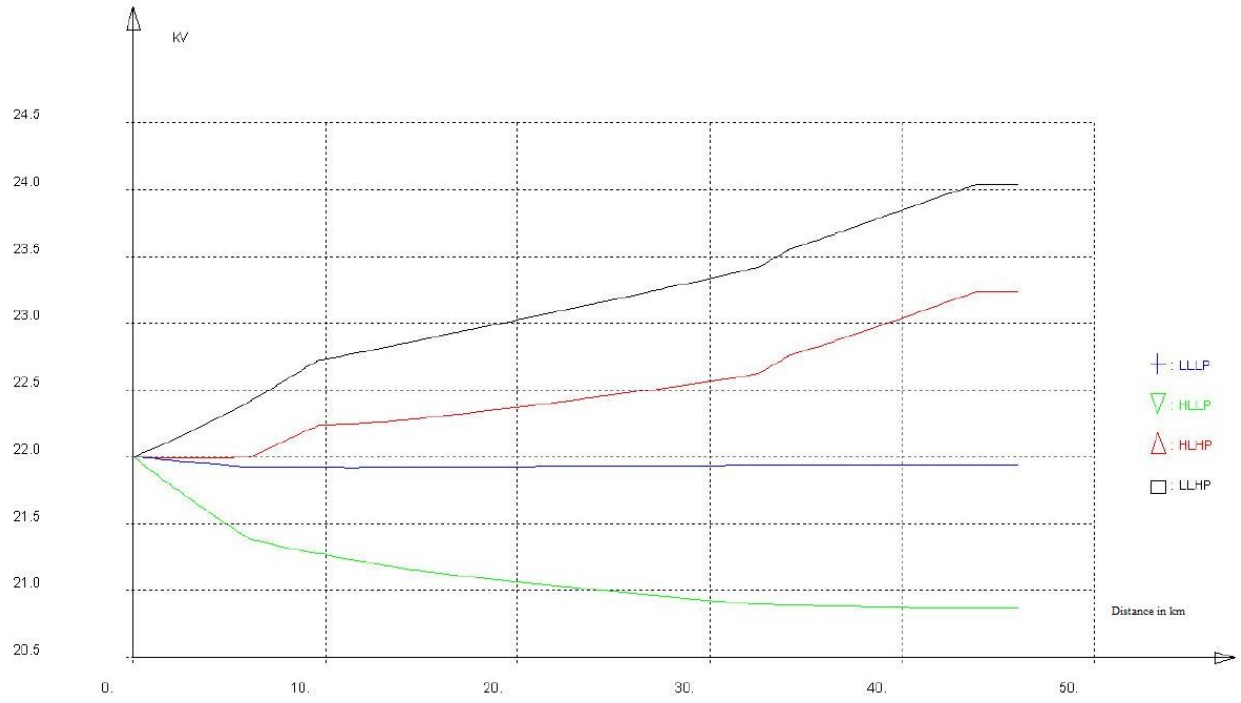

Figure A.2: Voltage rise from Øye substation (distance =0) to the end of the radial at Netland. [10]

Table A.1: DG units and shunt-reactors output (MW and MVAr) during LLHP basis.

Name	Active power [MW]	Reactive power [MVAr]	Tan ϕ
Kvinesdal	1,35	0,00	0,00
Trælandsfoss	10,00	0,00	0,00
Oksefjell	0,35	0,00	
Bergsli	0,81	0,00	0,00
Eftestøyl	0,40	0,00	0,00
Røylandsfoss 2	1,20	0,00	0,00
Hisvatn	3,60	0,00	0,00
Hisvatn Shunt-reactor		0,00	
Summation	17,71	0,00	

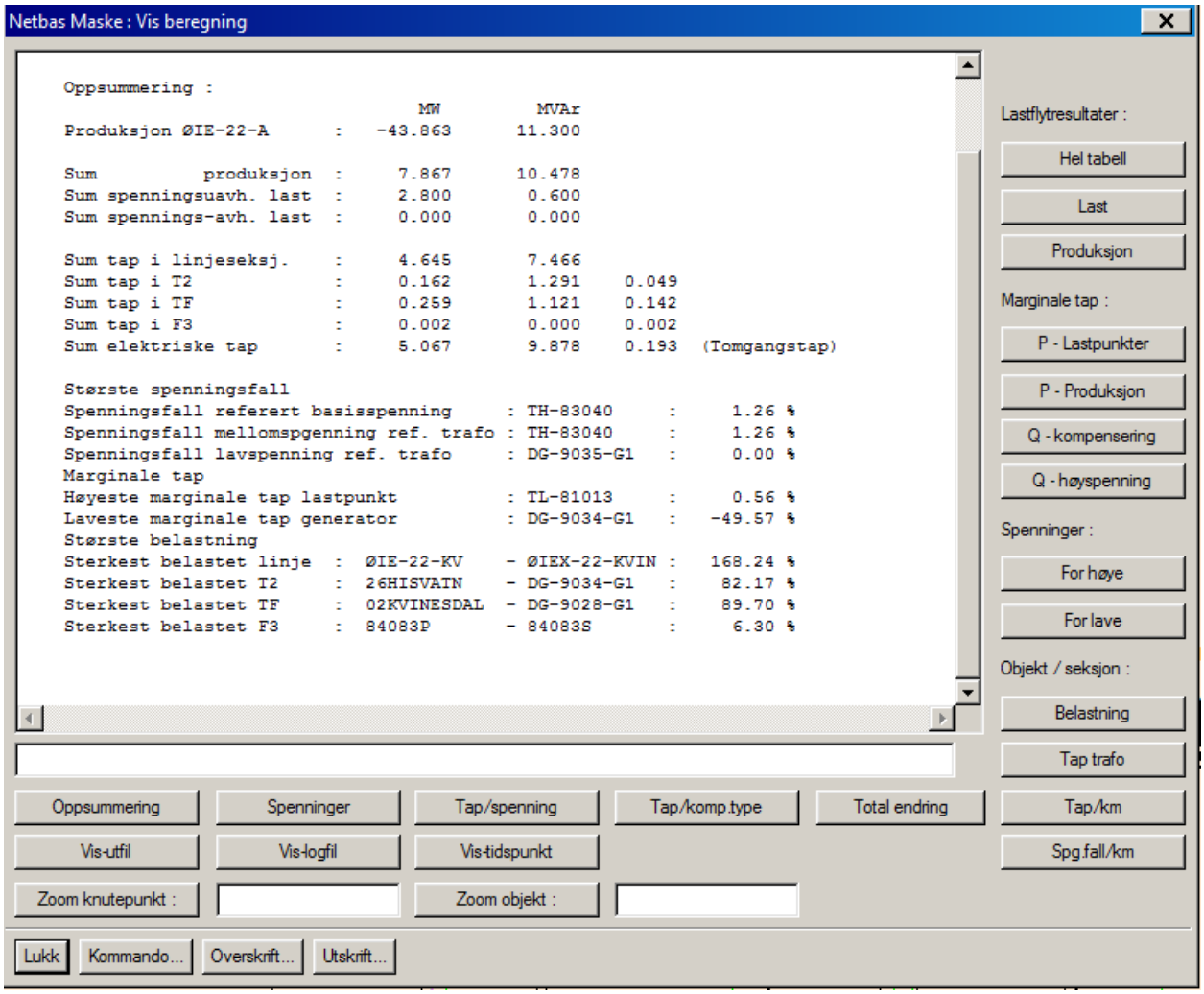

Figure A.3: Summary LLHP

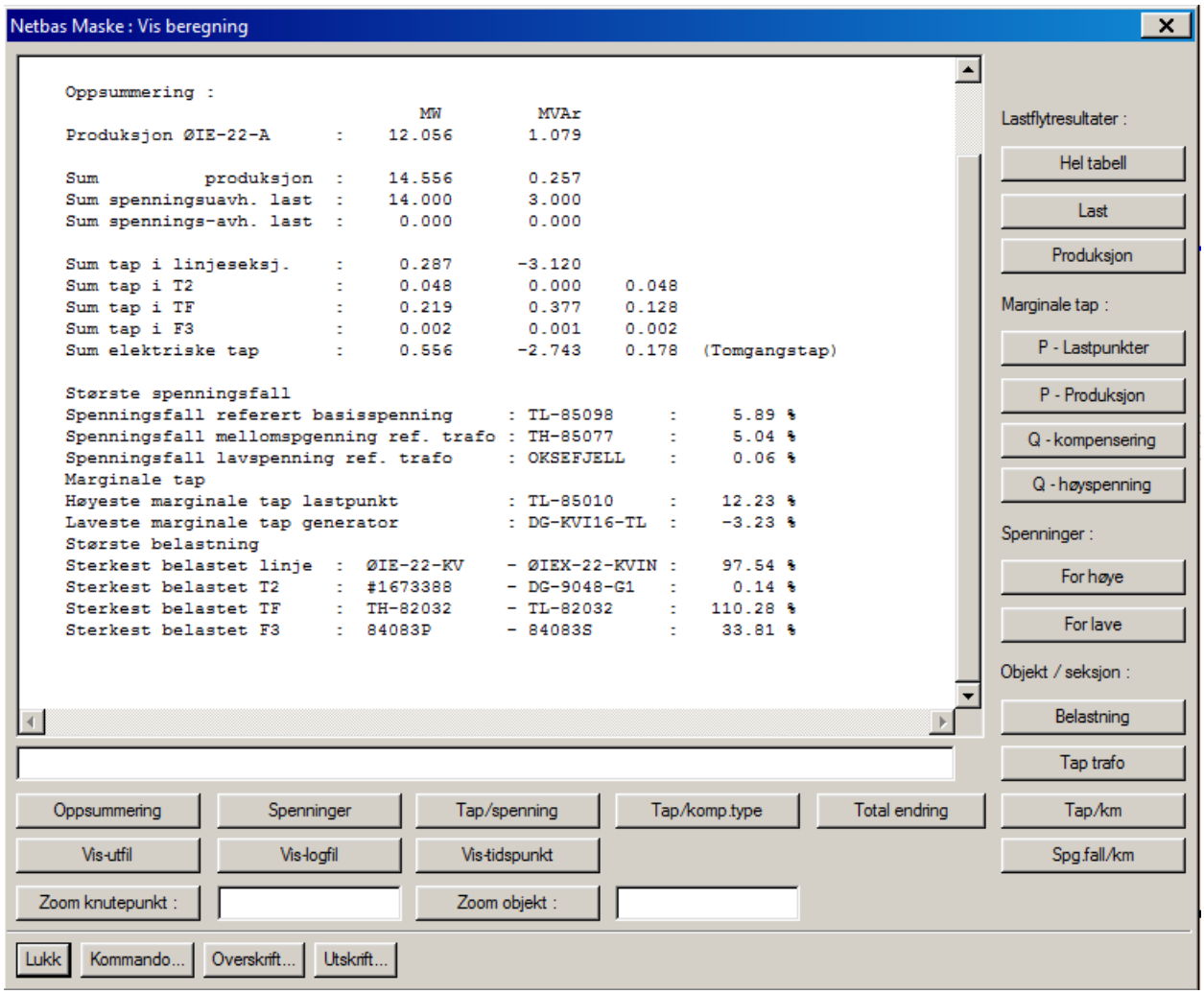

Figure A.4: Summary HLLP

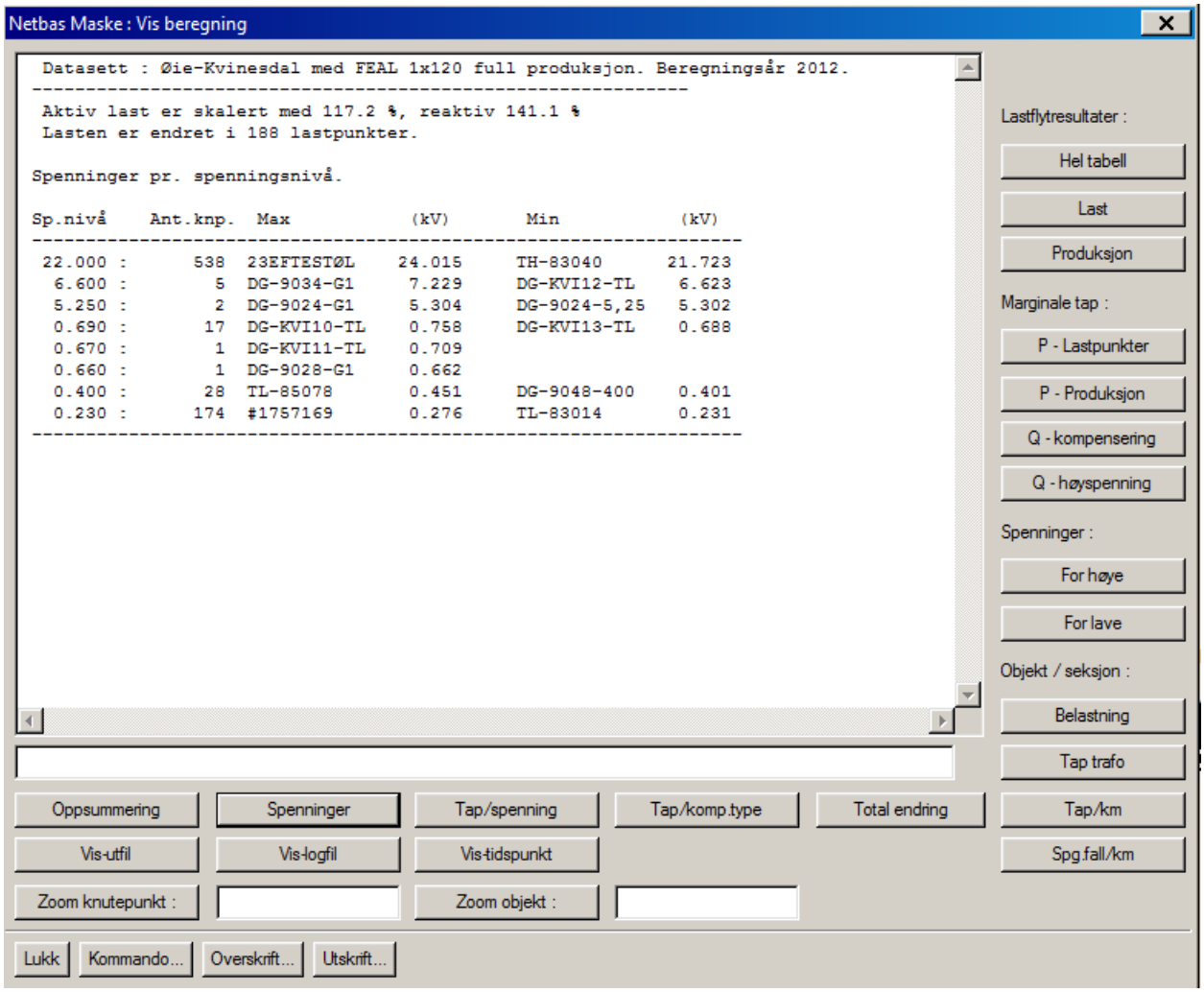

Figure A.5: Voltages LLHP

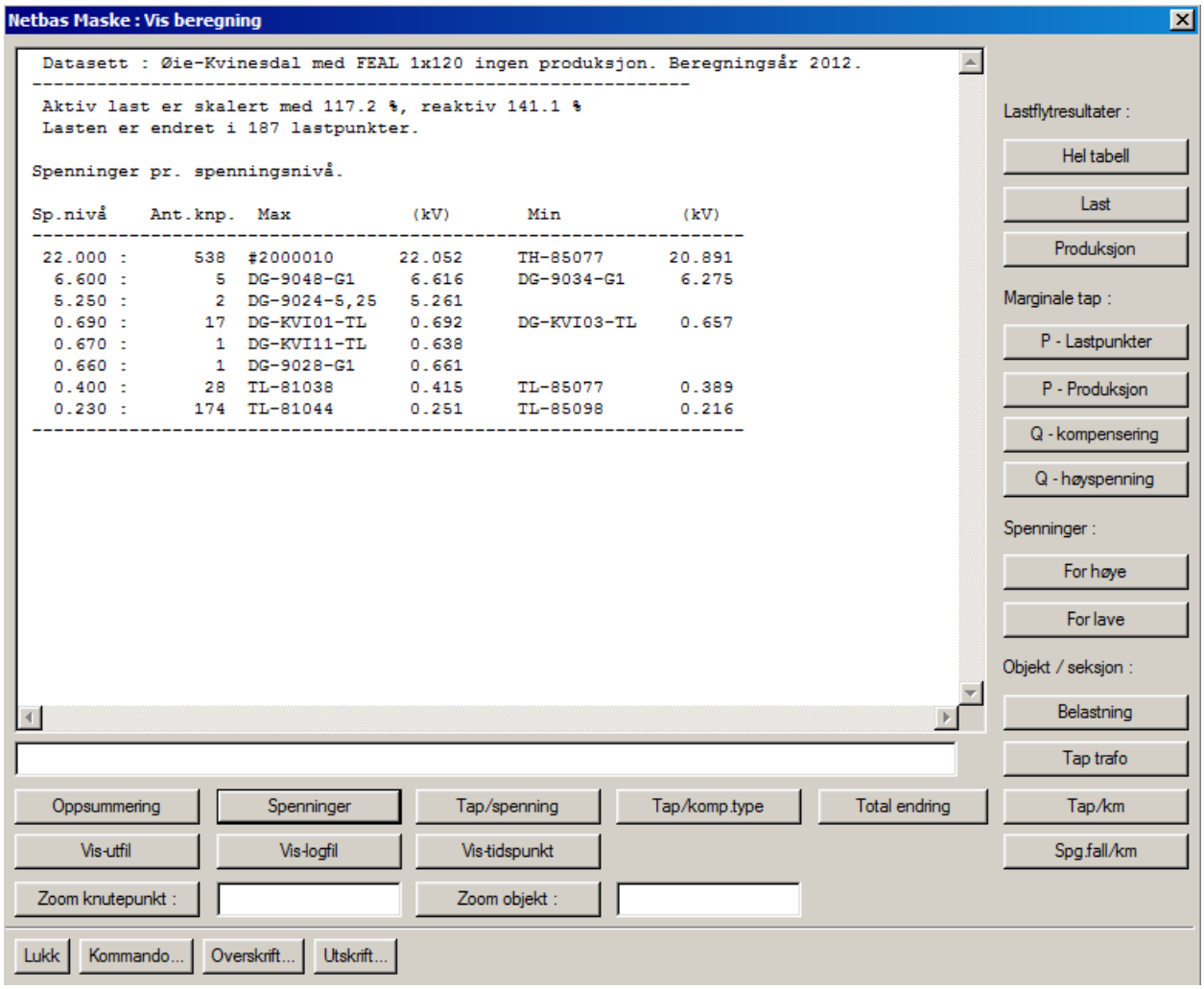

Figure A.6: Voltages HLLP

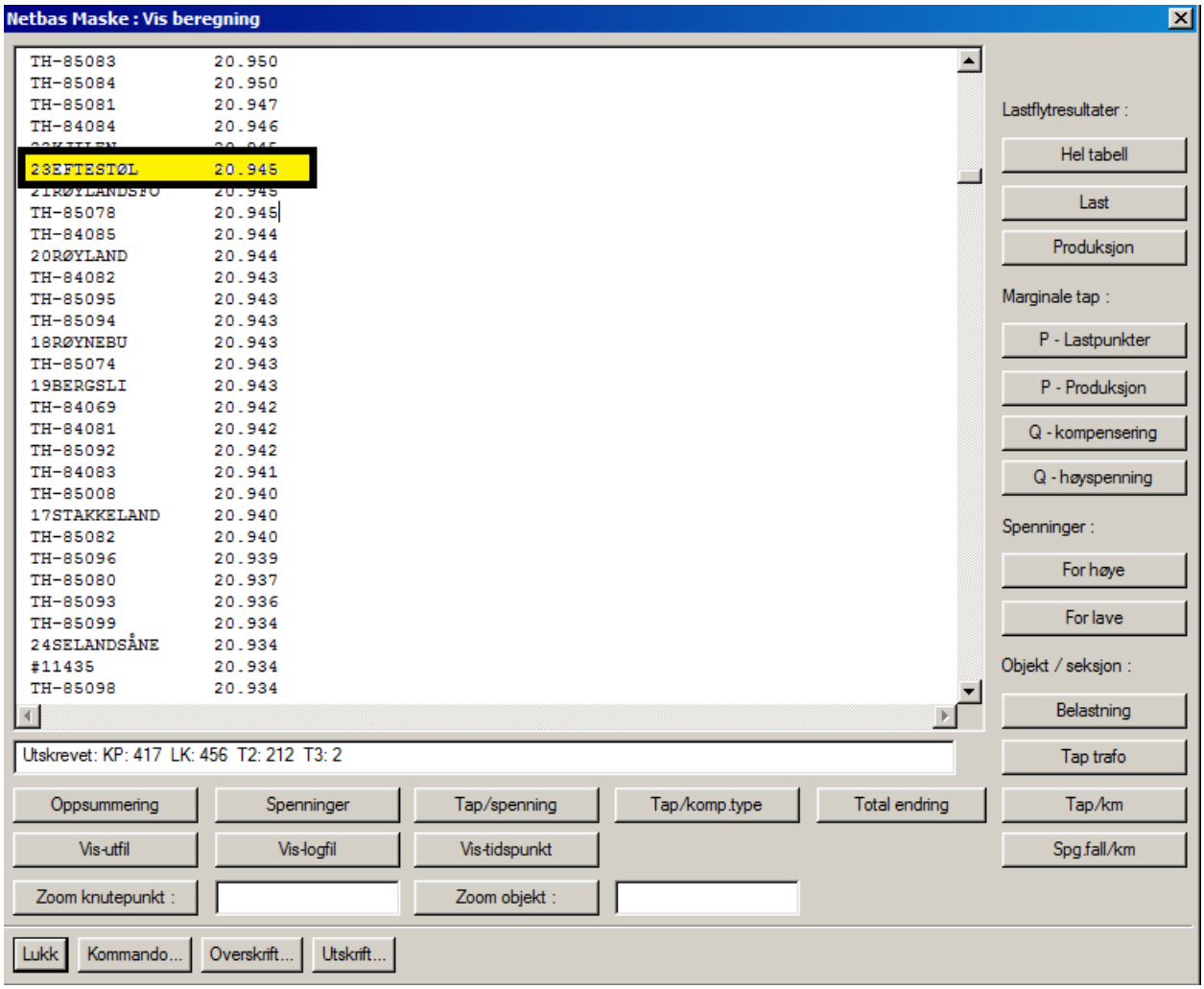

Figure A.7: Voltages at Eftestøl, HLLP

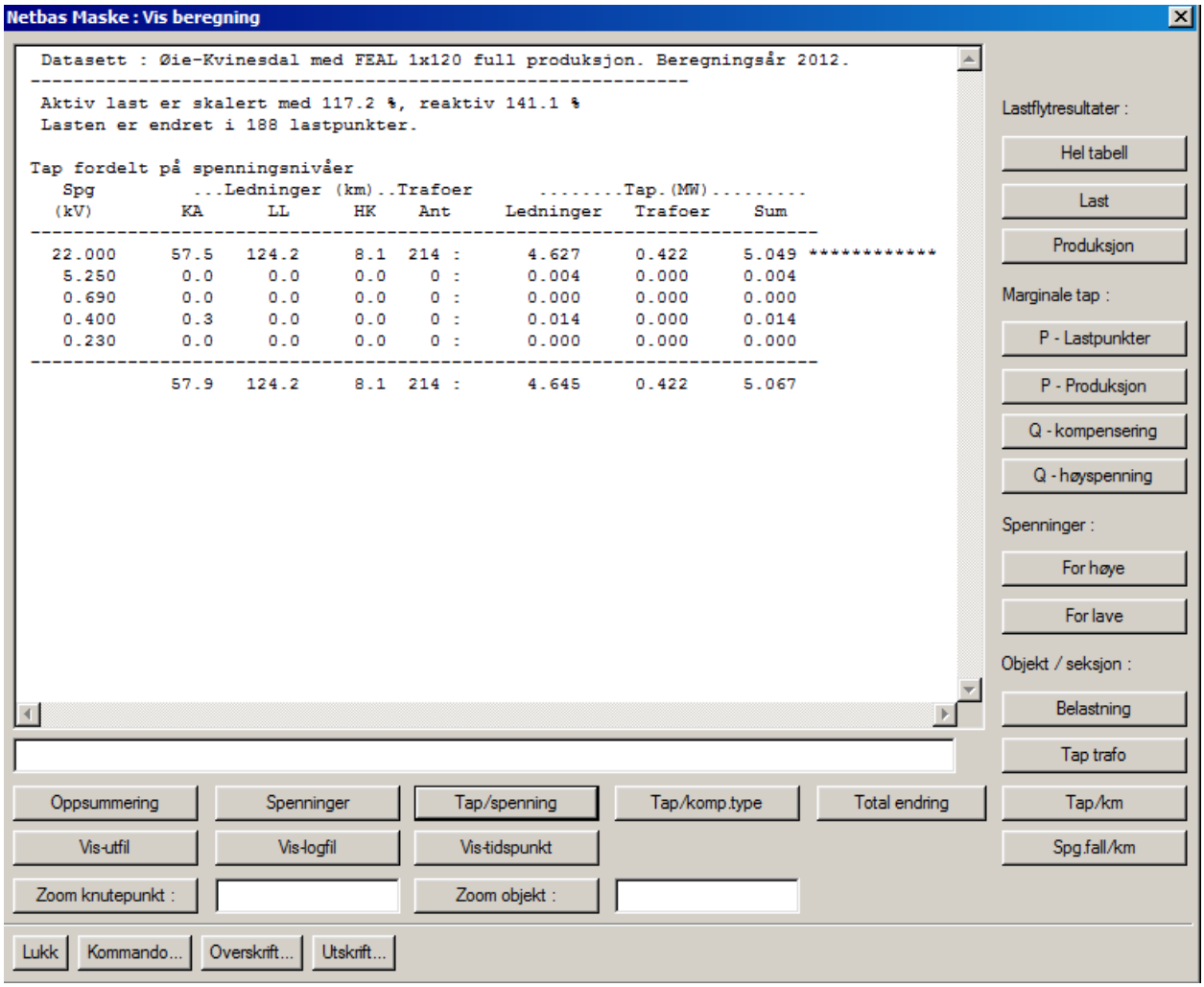

Figure A.8: Transmission losses LLHP

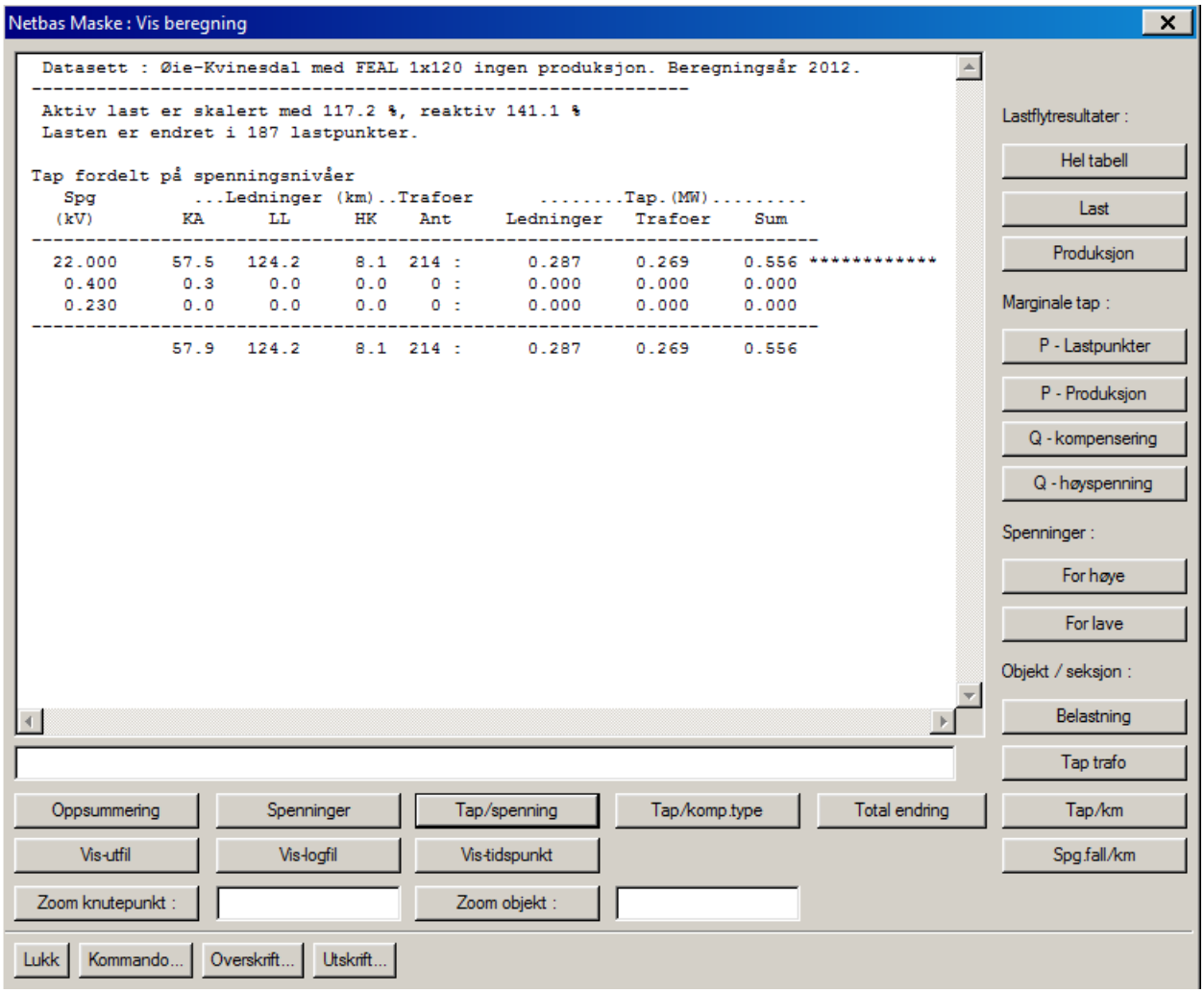

Figure A.9: Transmission losses HLLP

Appendix B

Case 1A simulation results

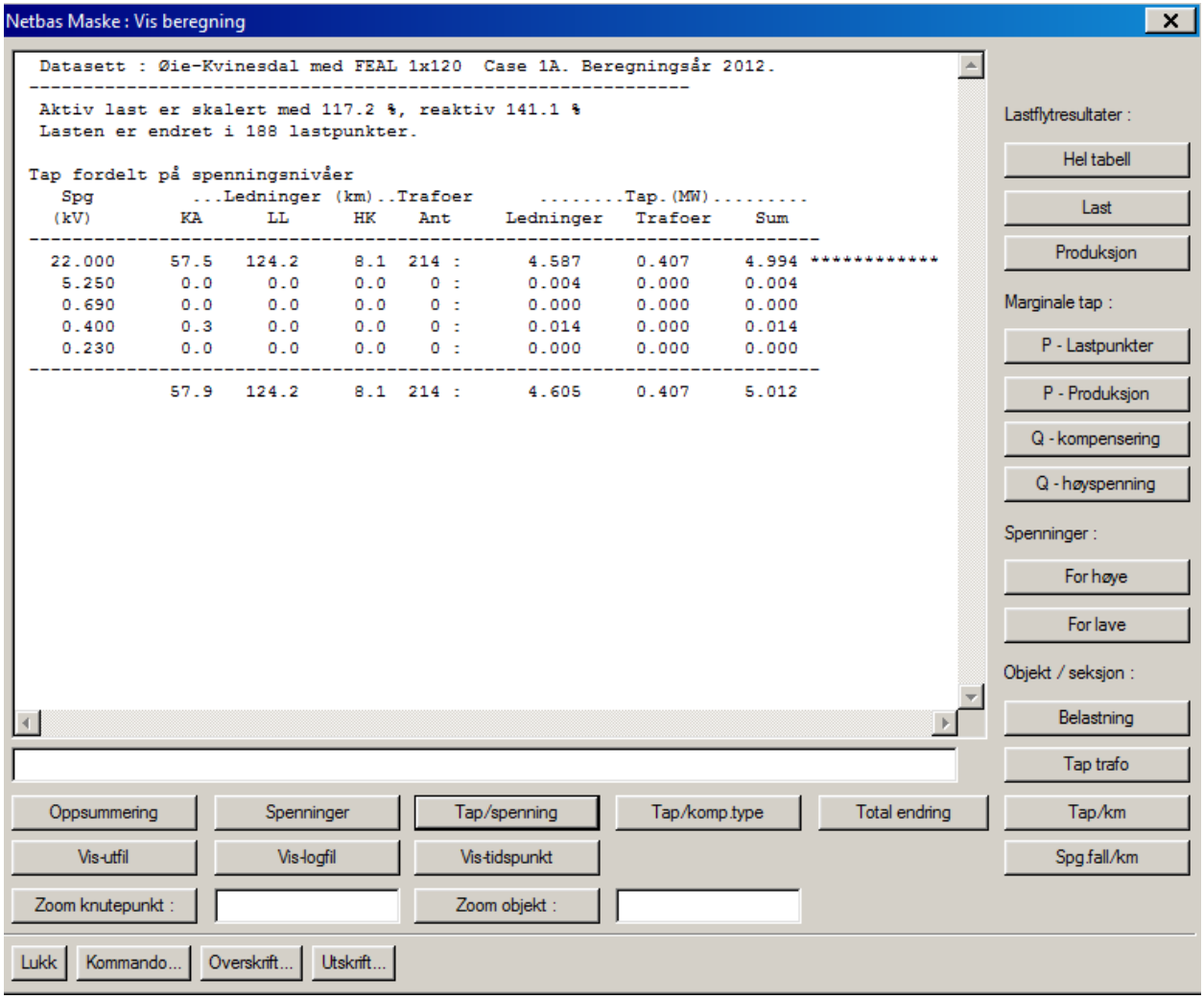

Figure B.1: Case 1A, transmission losses

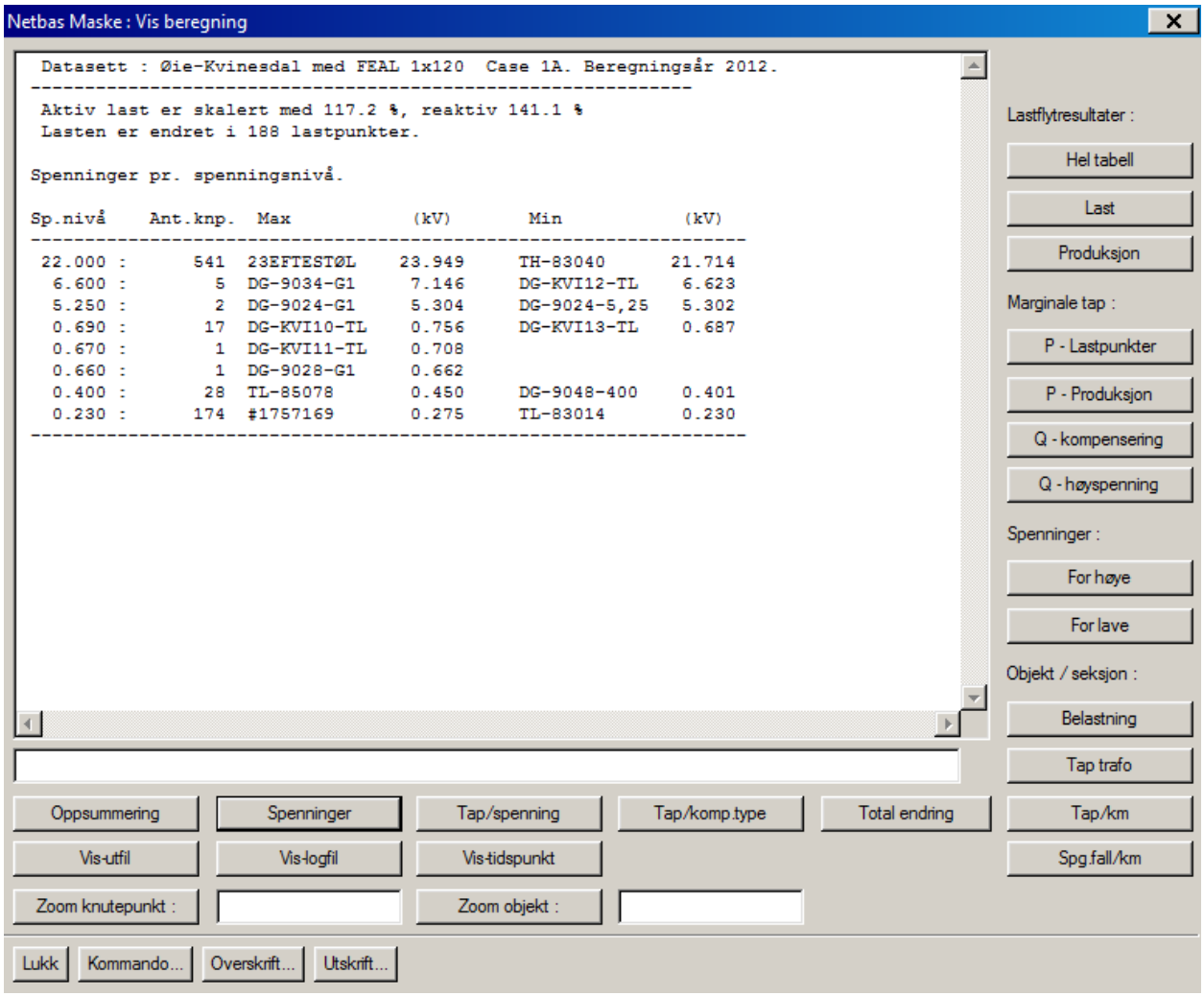

Figure B.2: Case 1A, Max/Min voltage levels

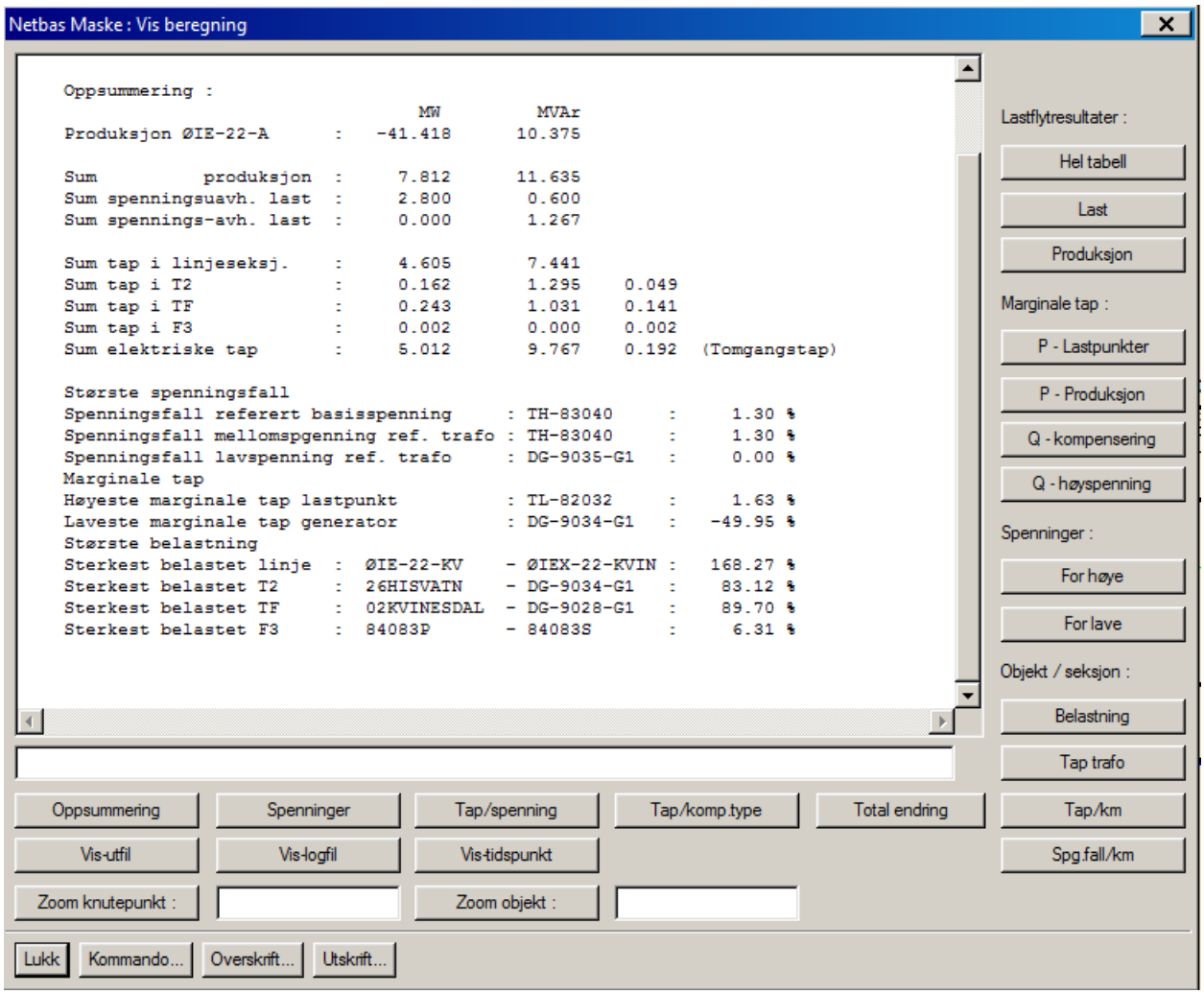

Figure B.3: Case 1A, summary

Appendix C

Case 1B simulation results

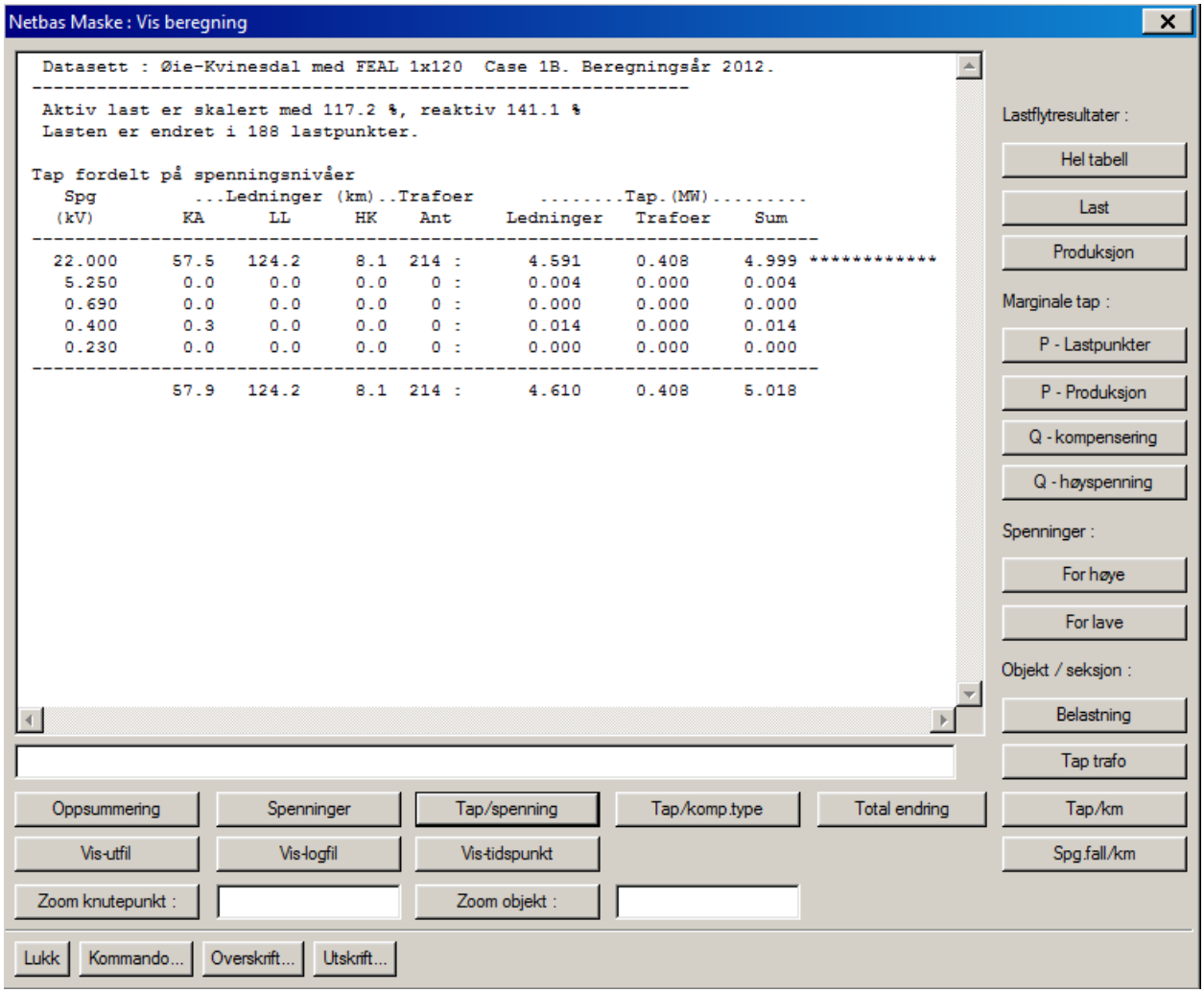

Figure C.1: Case 1B, transmission losses

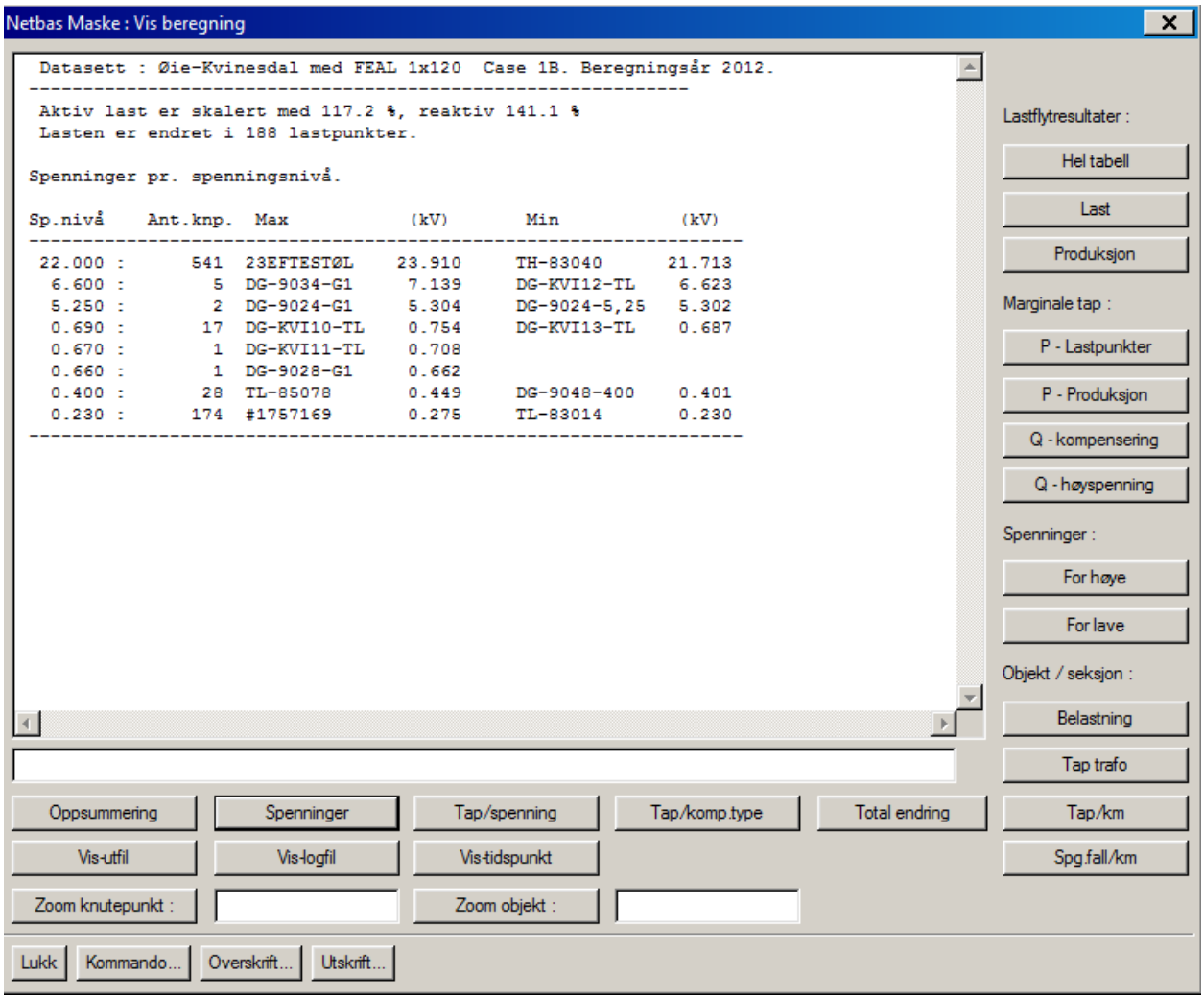

Figure C.2: Case 1B, Max/Min voltage levels

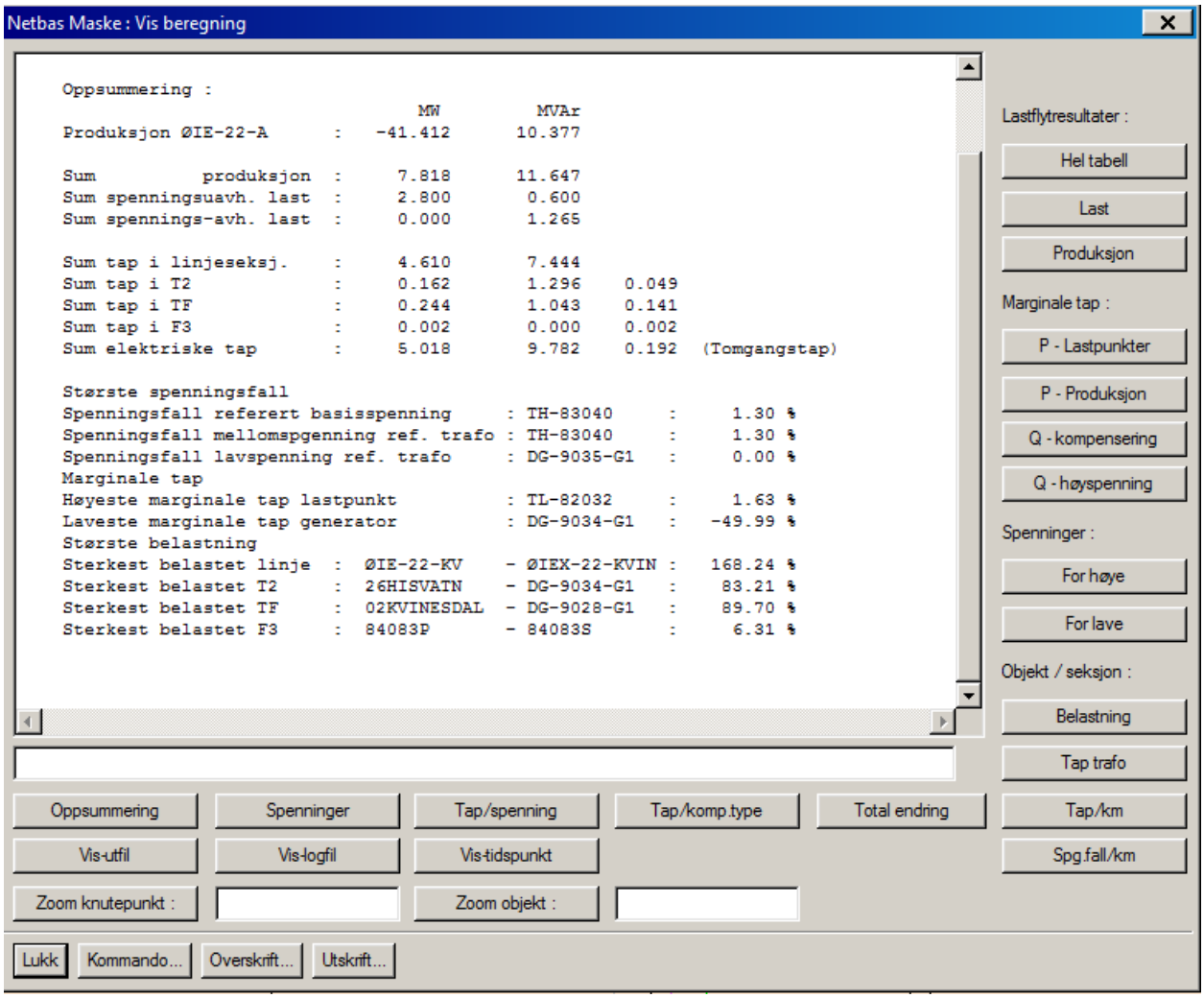

Figure C.3: Case 1B, summary

Appendix D

Case 1C simulation results

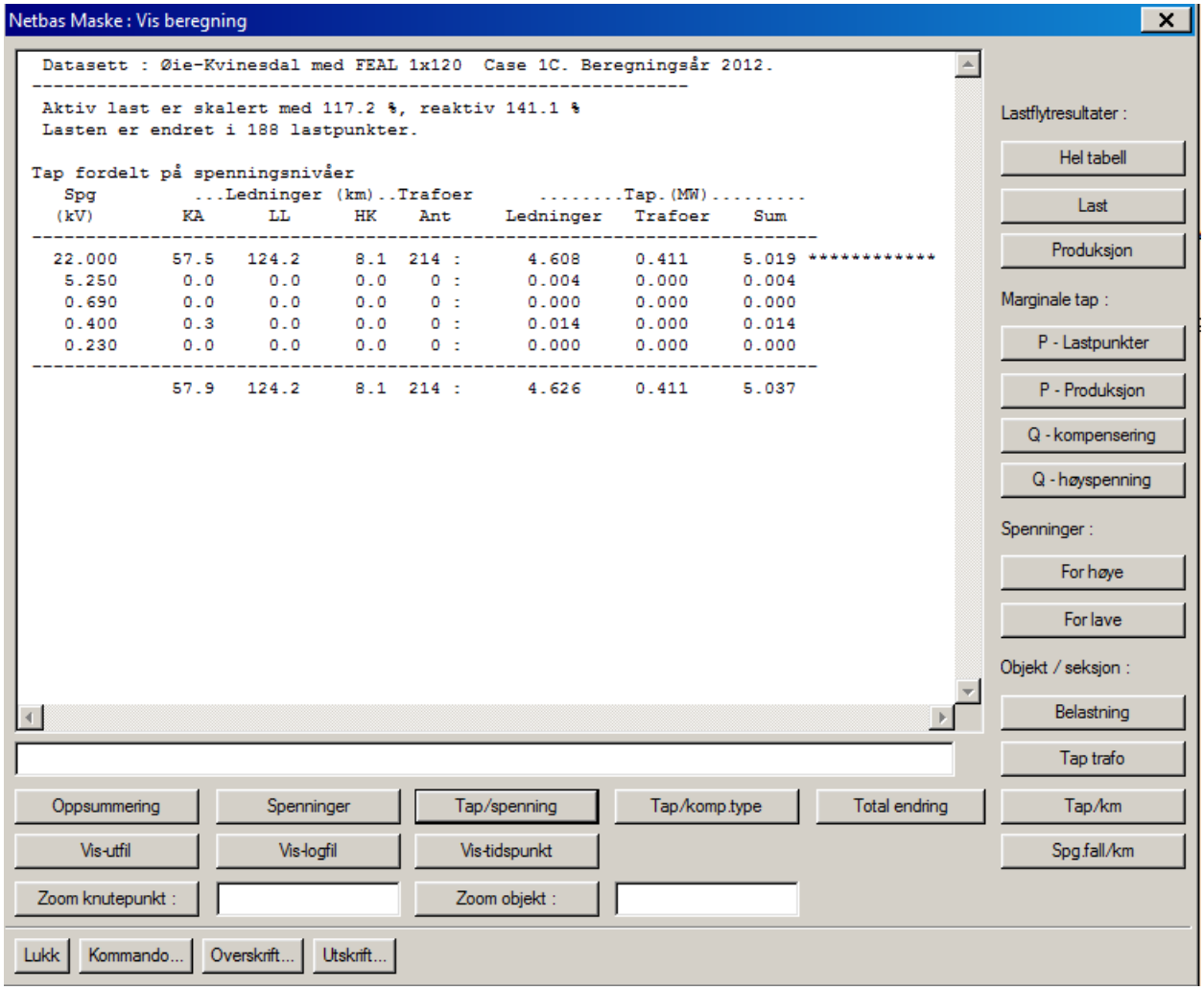

Figure D.1: Case 1C, transmission losses

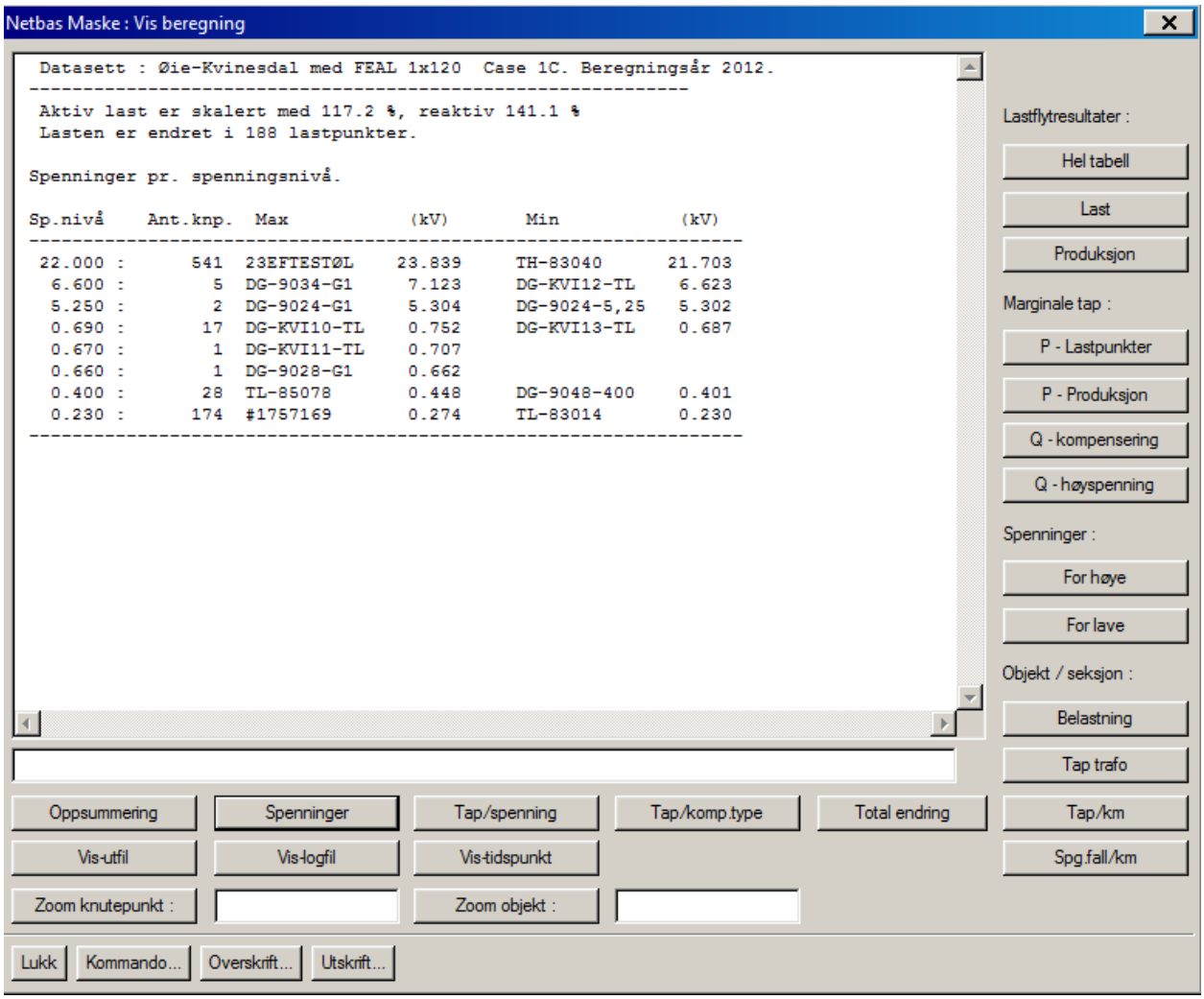

Figure D.2: Case 1C, Max/Min voltage levels

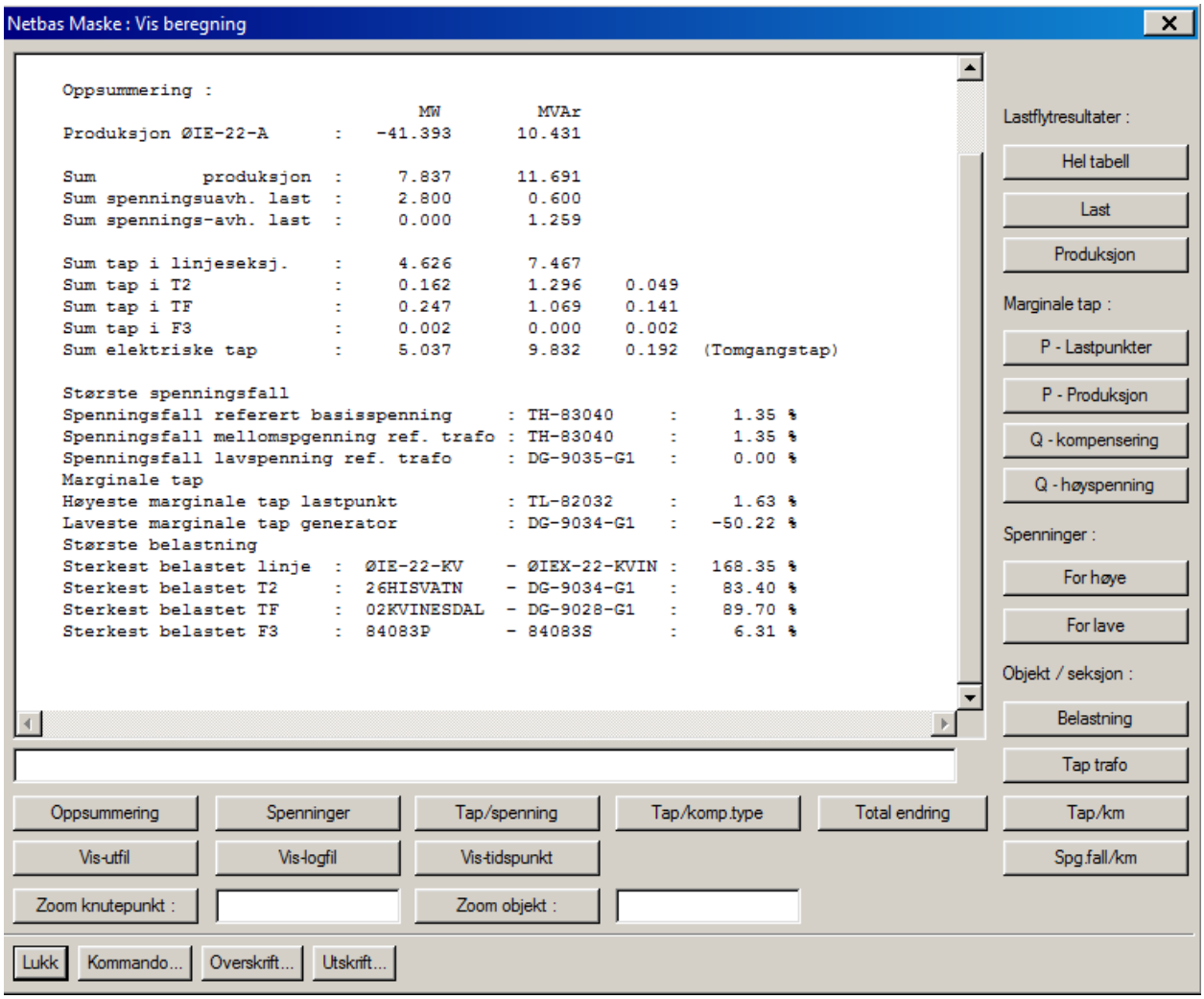

Figure D.3: Case 1C, summary

Appendix E

Case 1D simulation results

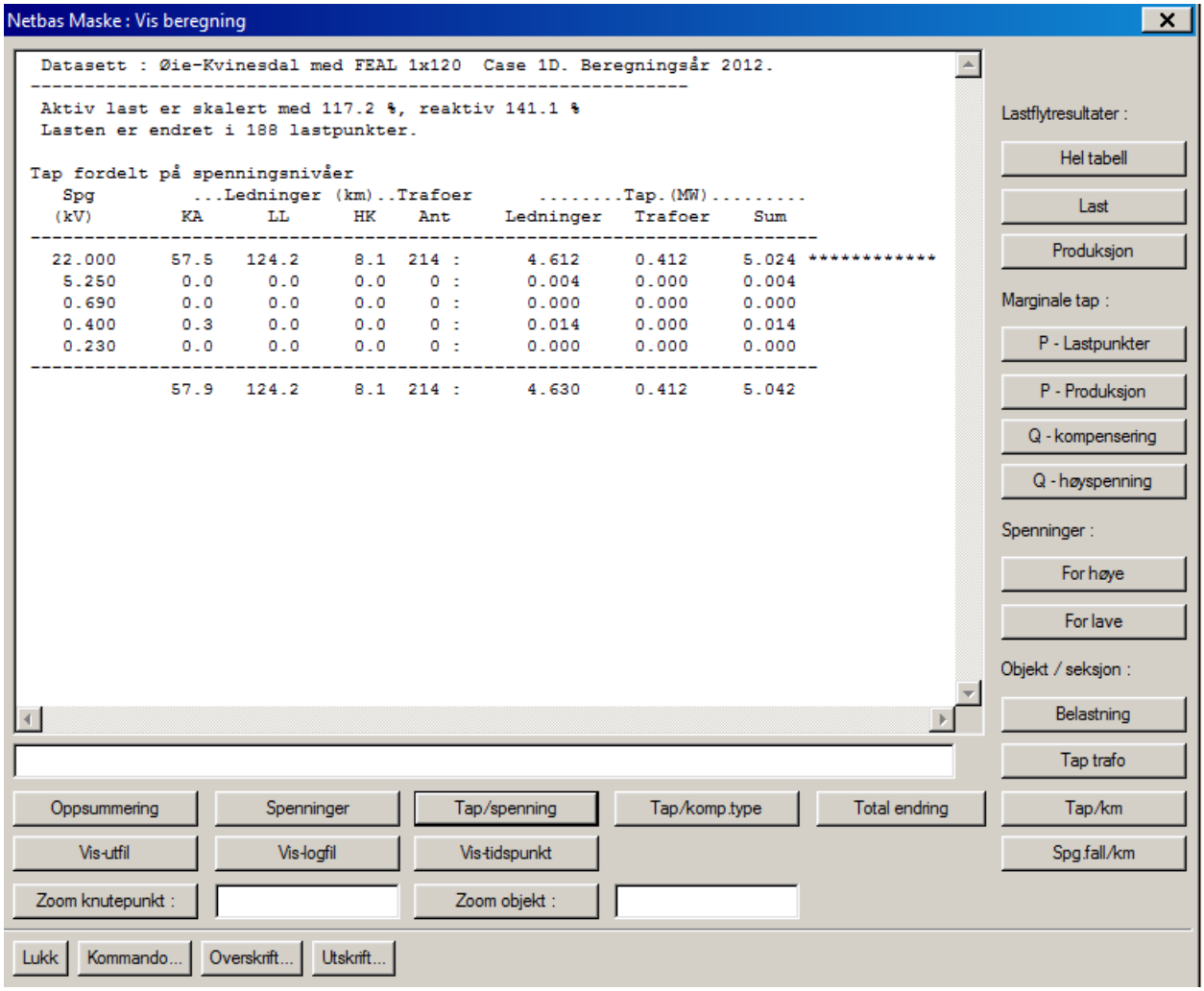

Figure E.1: Case 1D, transmission losses

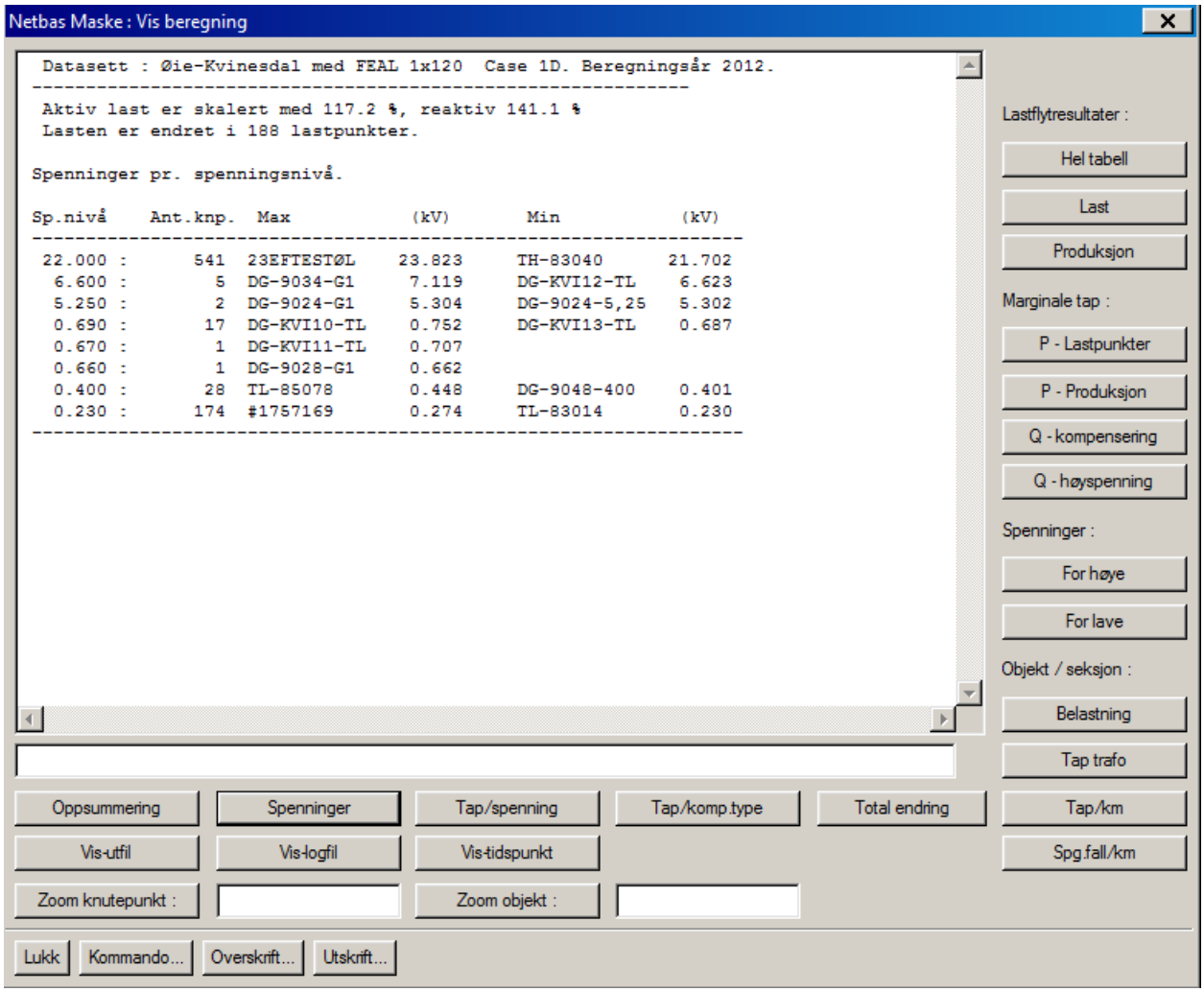

Figure E.2: Case 1D, Max/Min voltage levels

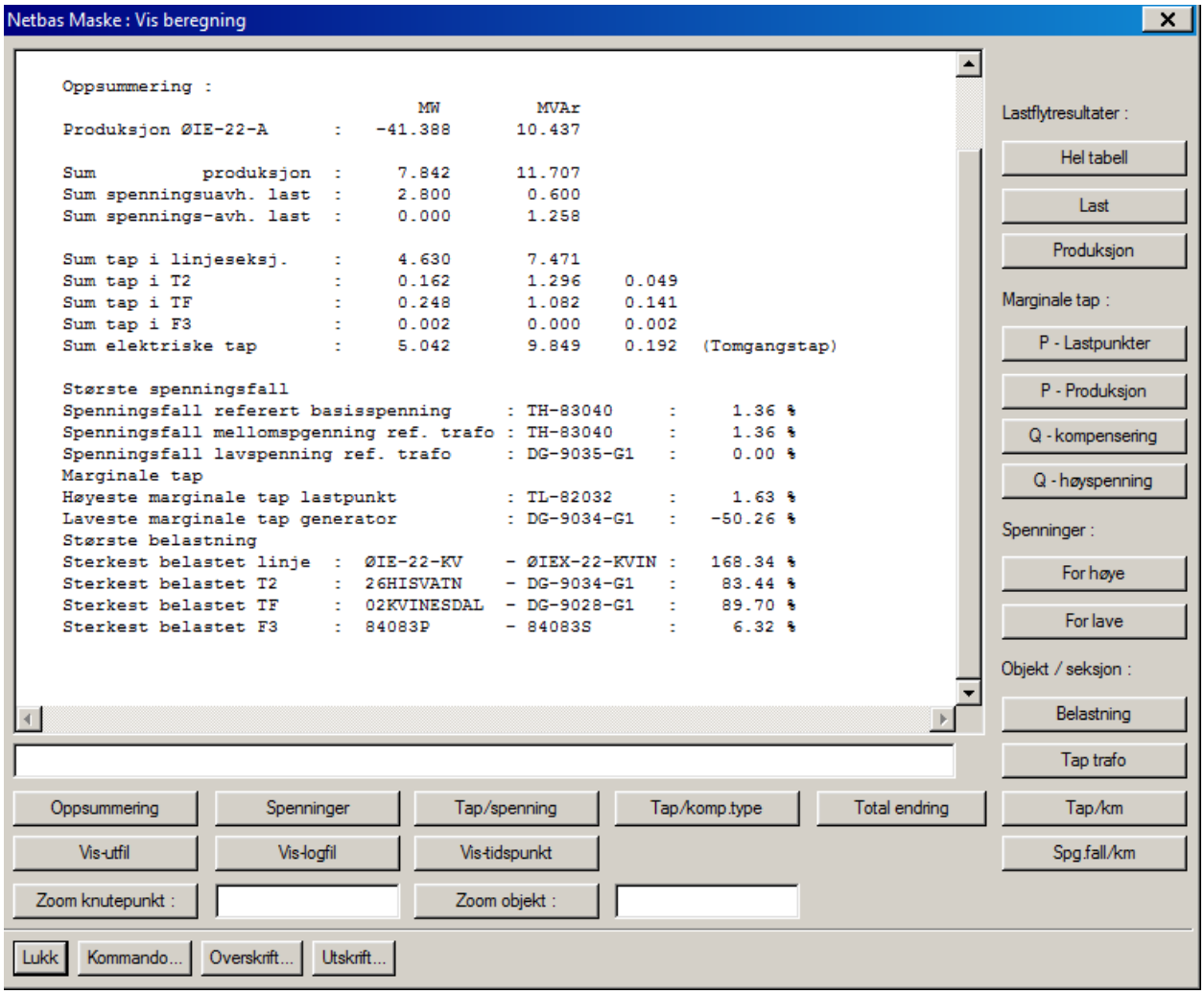

Figure E.3: Case 1D, summary

Appendix F

Case 1E simulation results

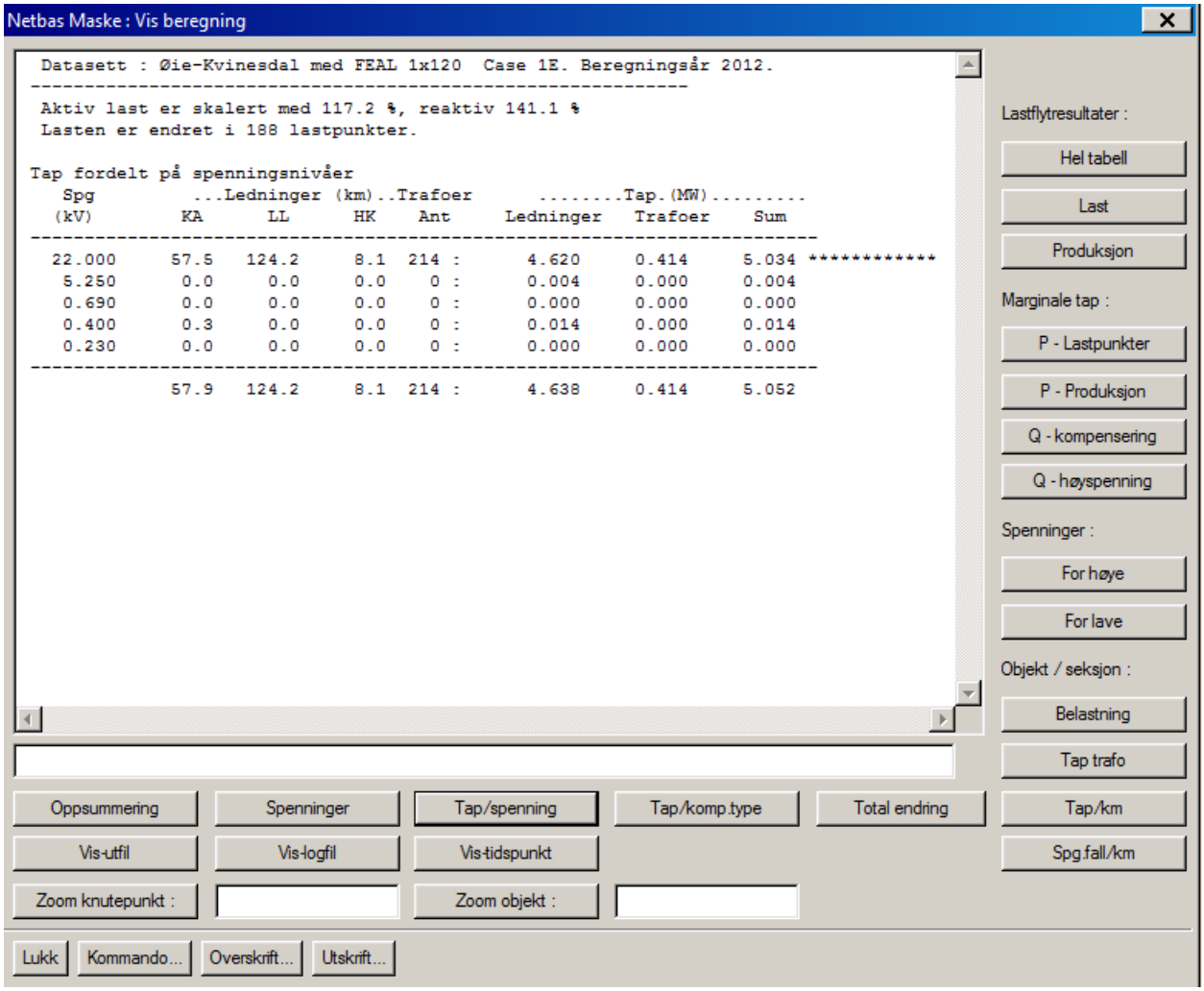

Figure F.1: Case 1E, transmission losses

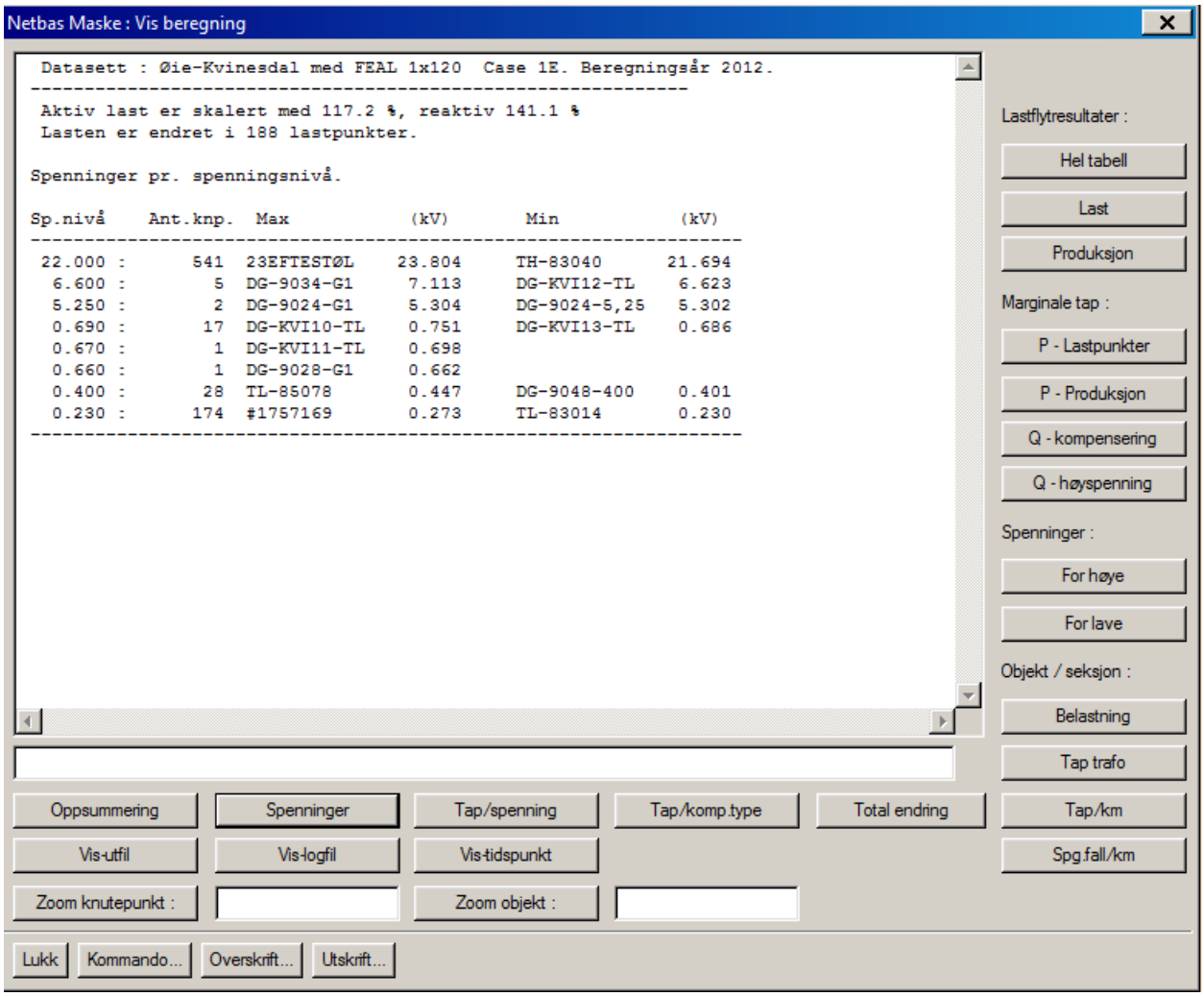

Figure F.2: Case 1E, Max/Min voltage levels

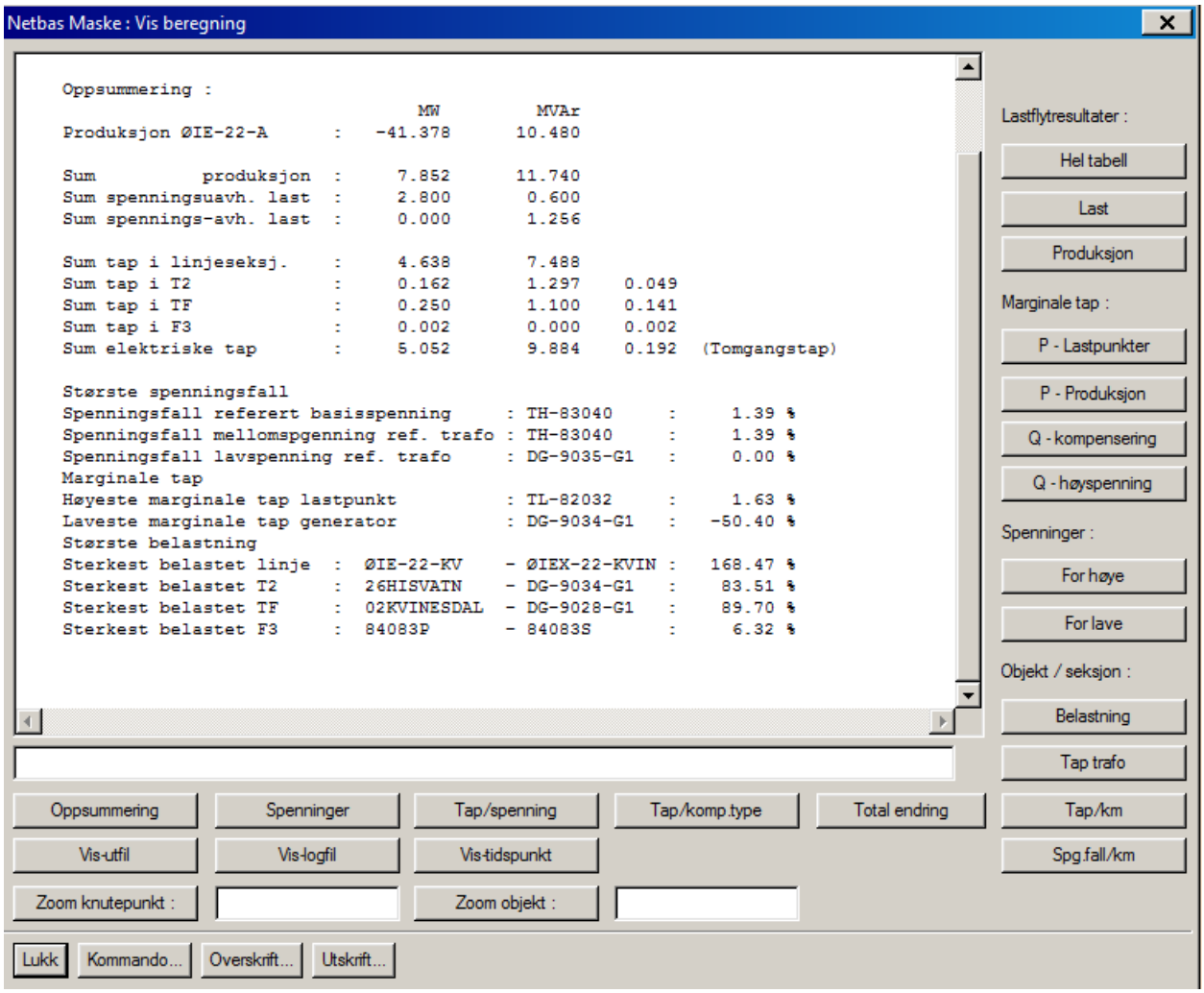

Figure F.3: Case 1E, summary

Appendix G

Case 1F simulation results

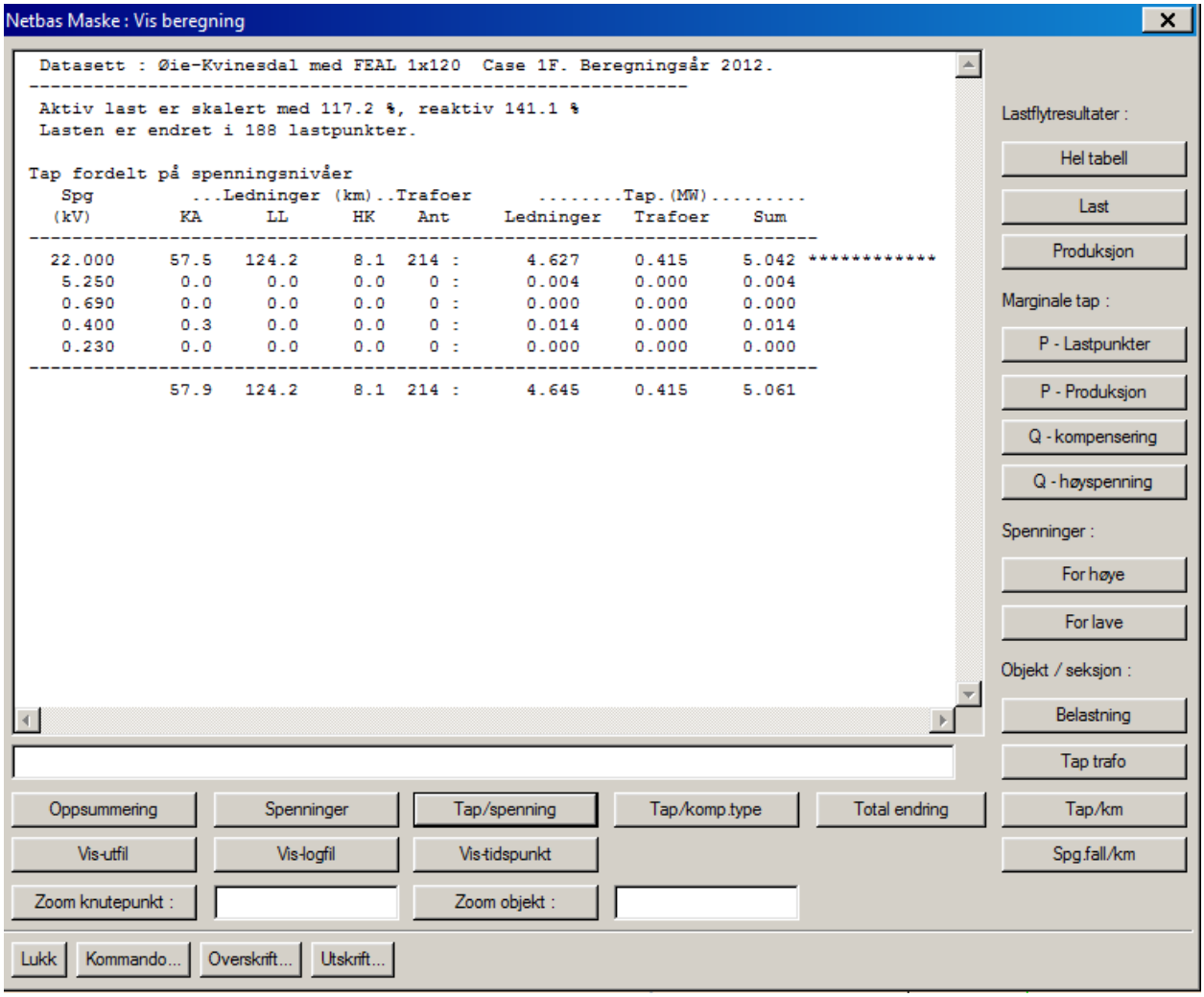

Figure G.1: Case 1F, transmission losses

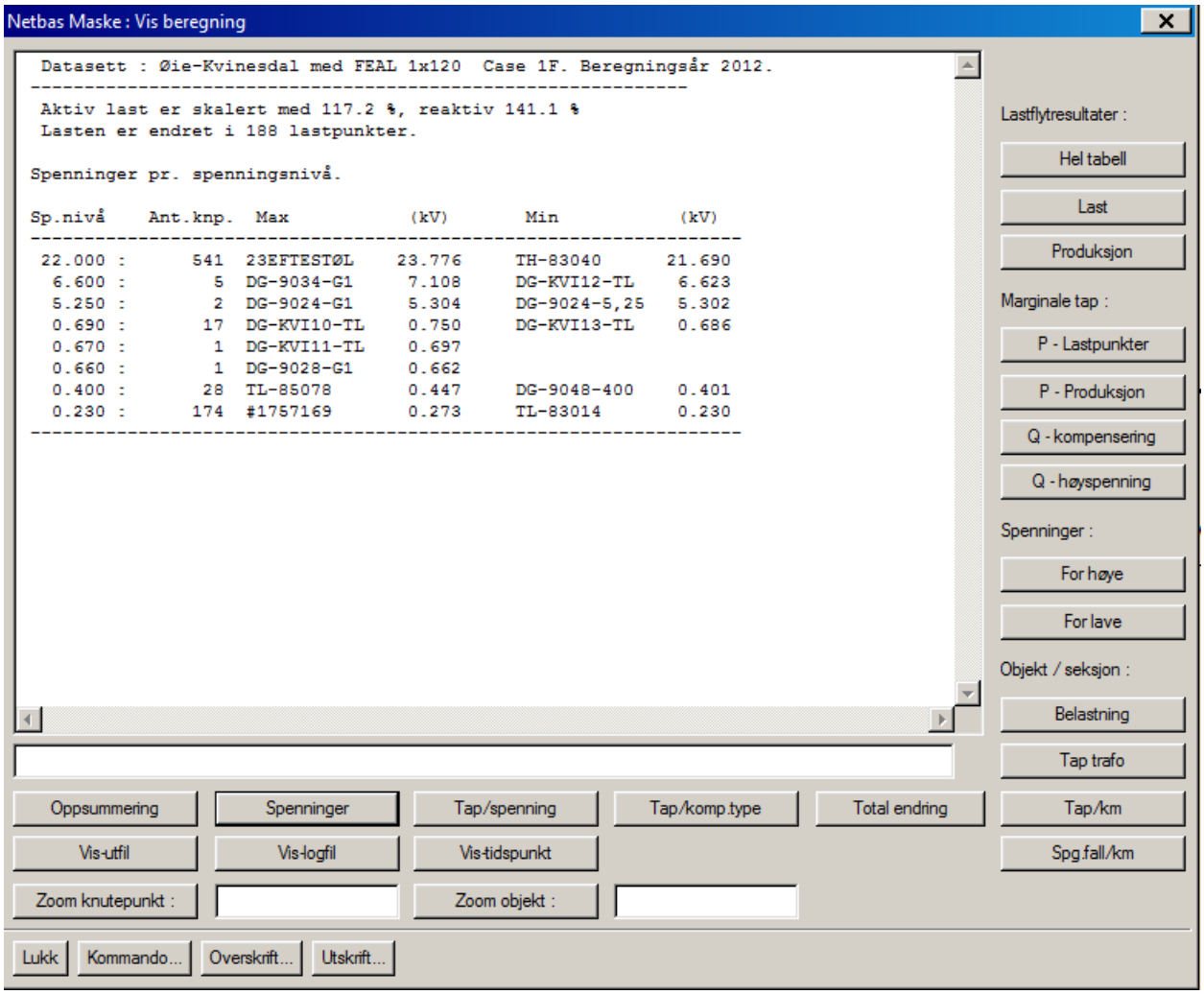

Figure G.2: Case 1F, Max/Min voltage levels

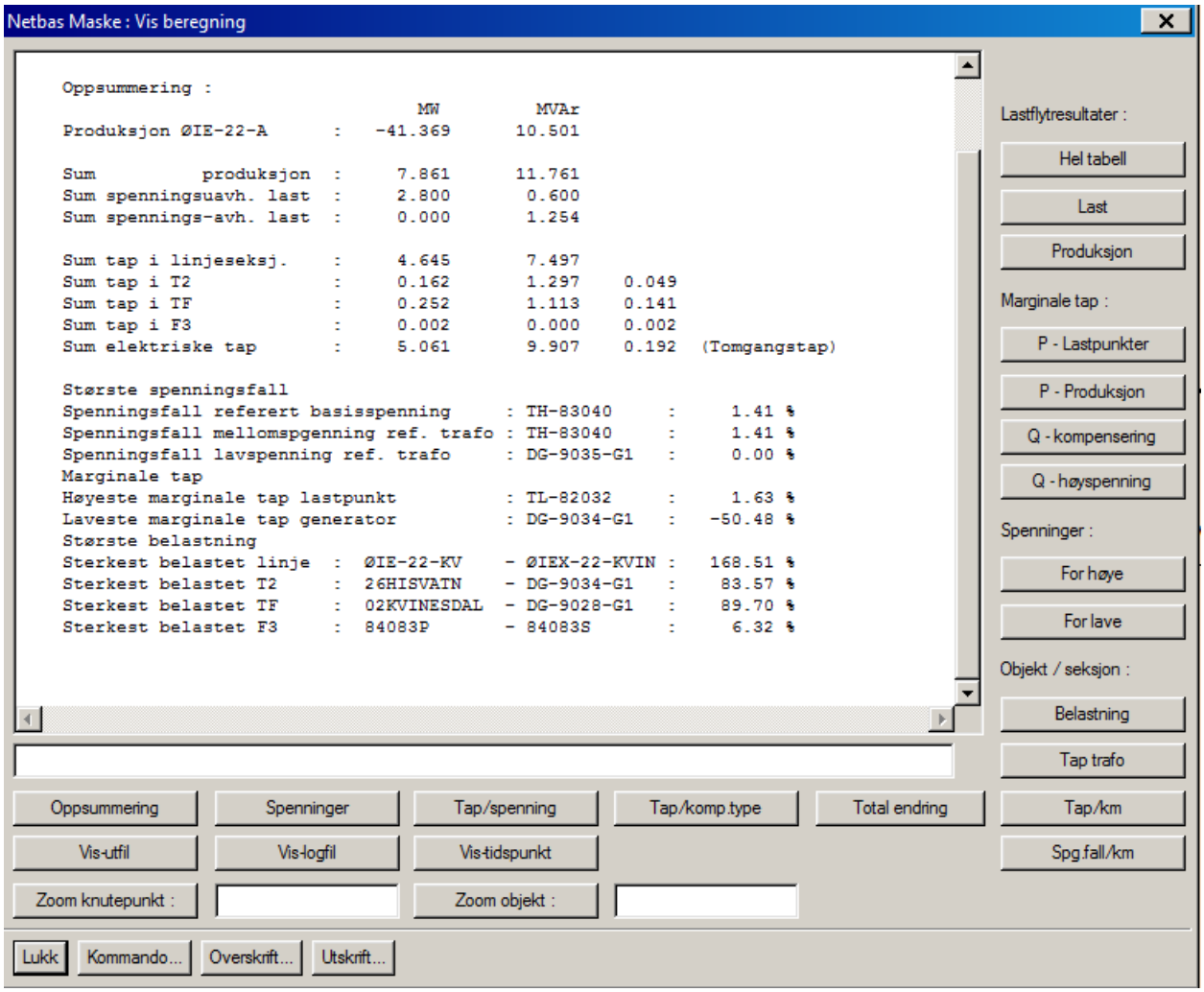

Figure G.3: Case 1F, summary

Appendix H

Case 1G simulation results

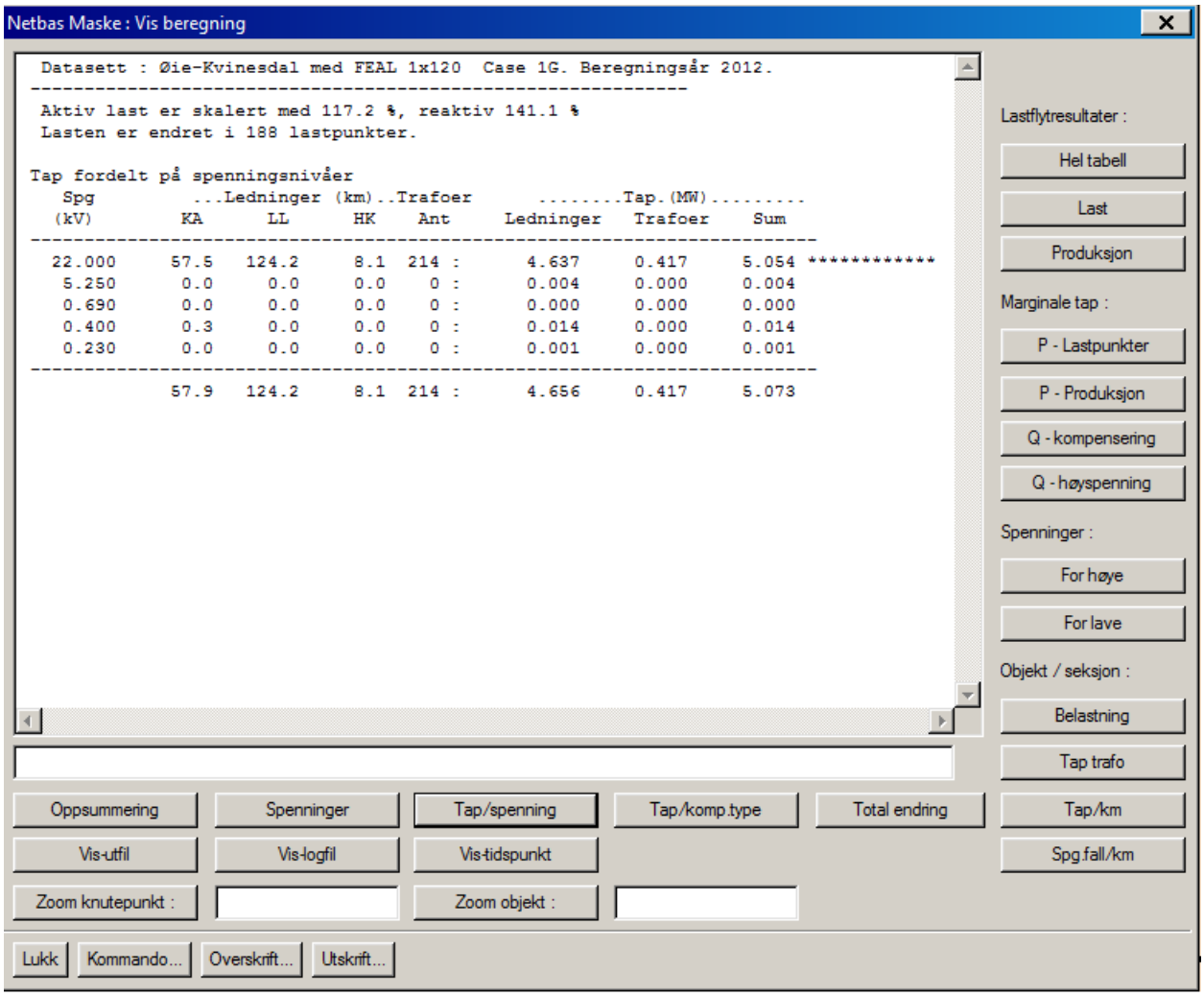

Figure H.1: Case 1G, transmission losses

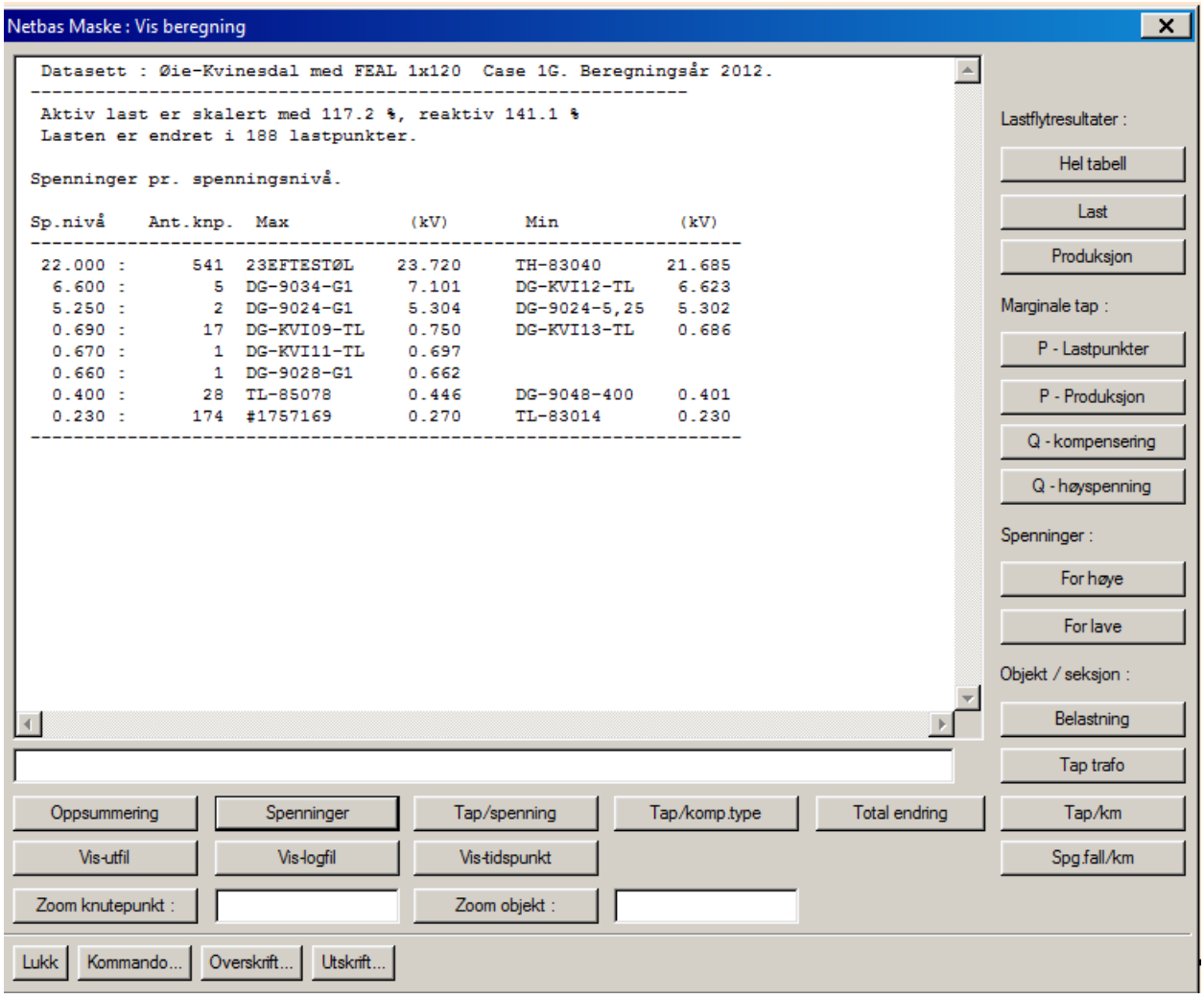

Figure H.2: Case 1G, Max/Min voltage levels

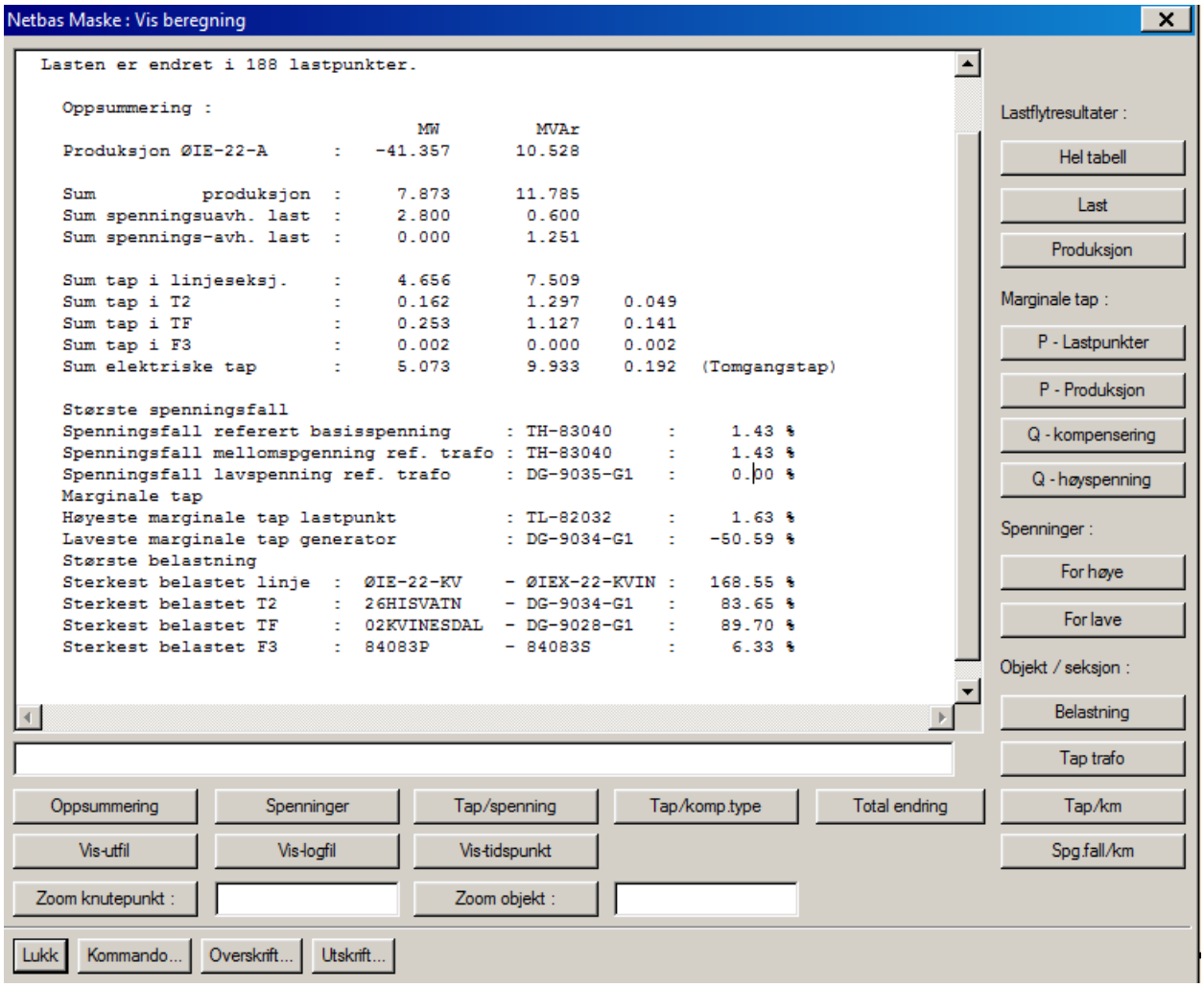

Figure H.3: Case 1G, summary

Appendix I

Case 1H simulation results

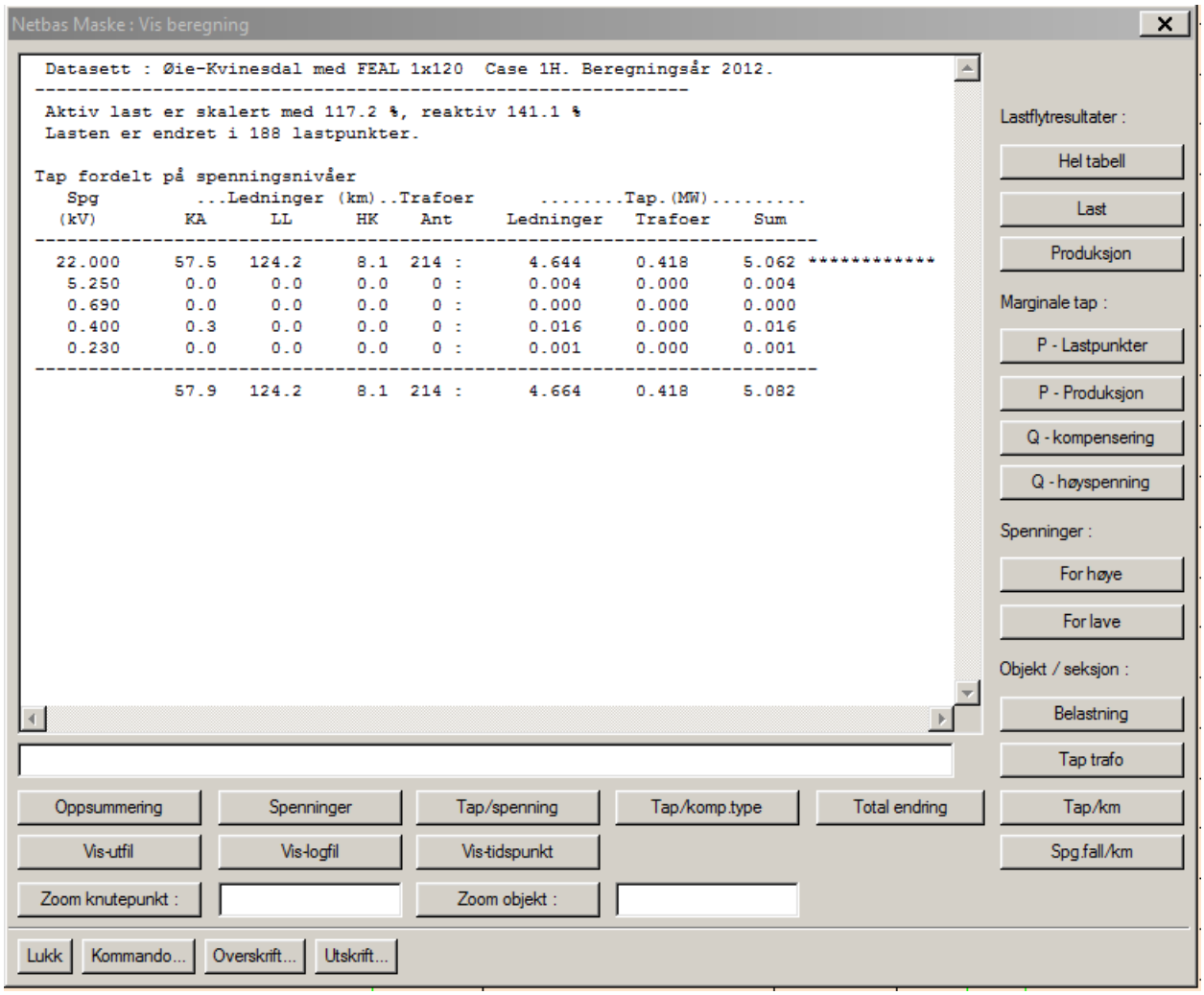

Figure I.1: Case 1H, transmission losses

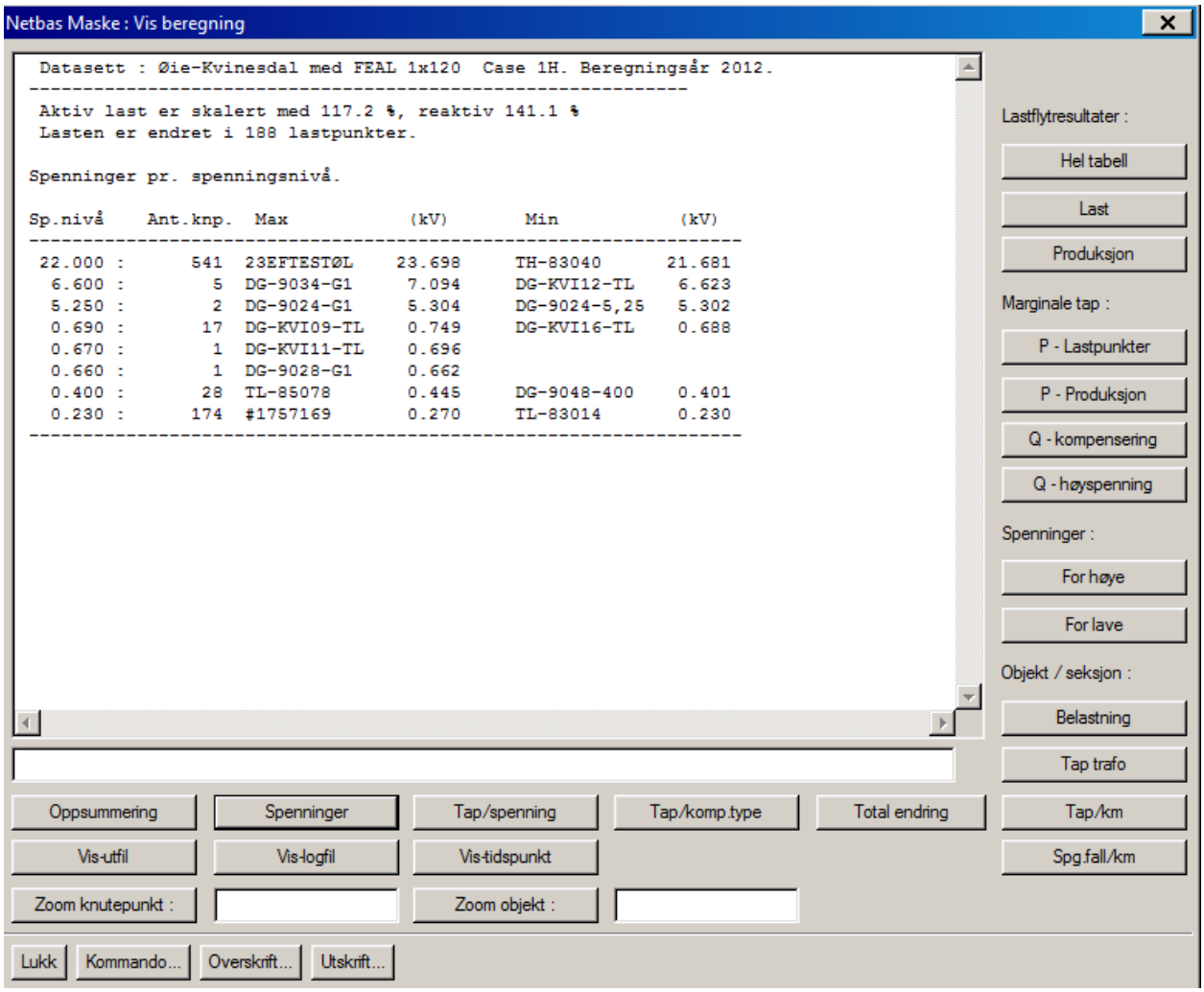

Figure I.2: Case 1H, Max/Min voltage levels

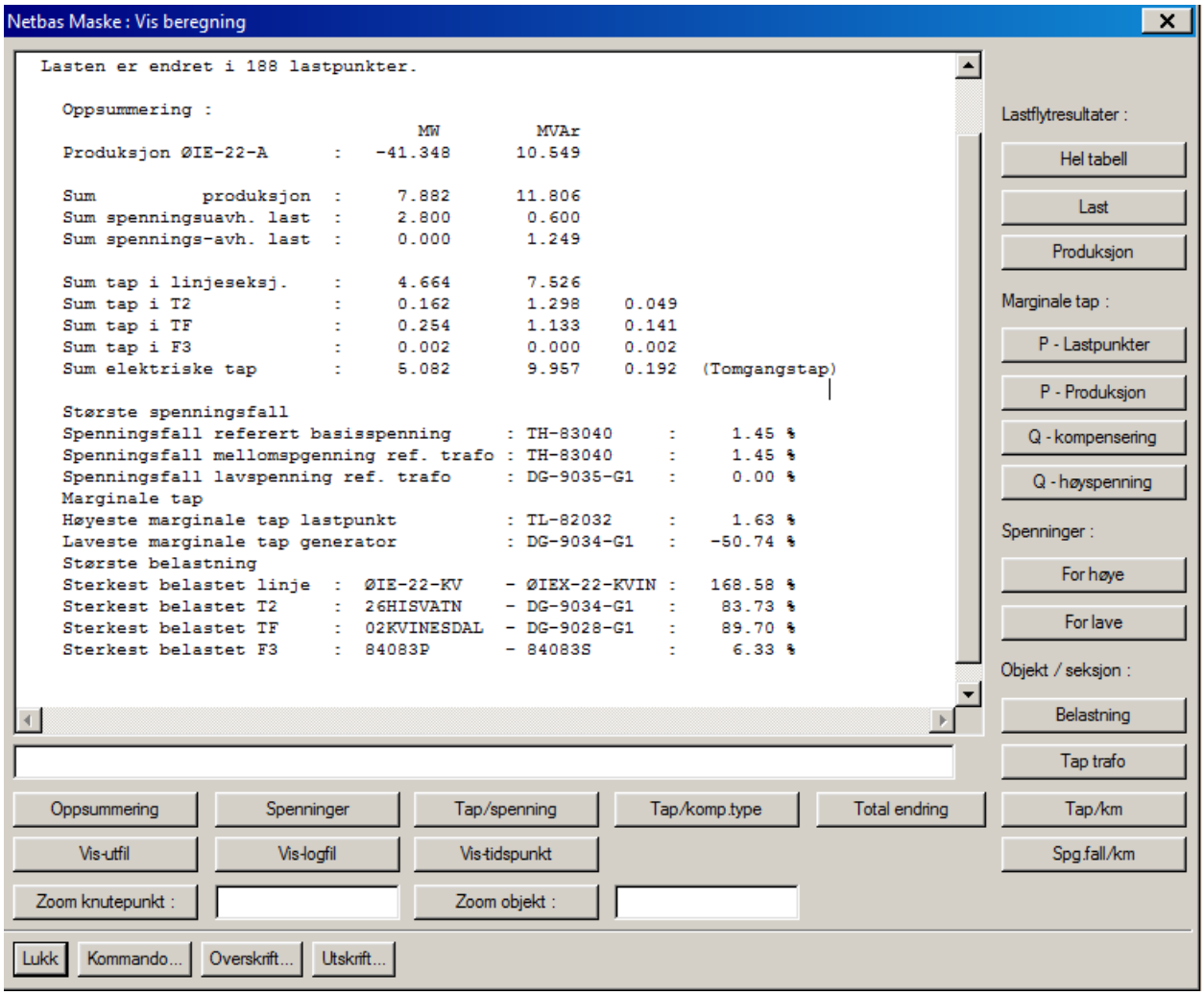

Figure I.3: Case 1H, summary

Appendix J

Case 1I simulation results

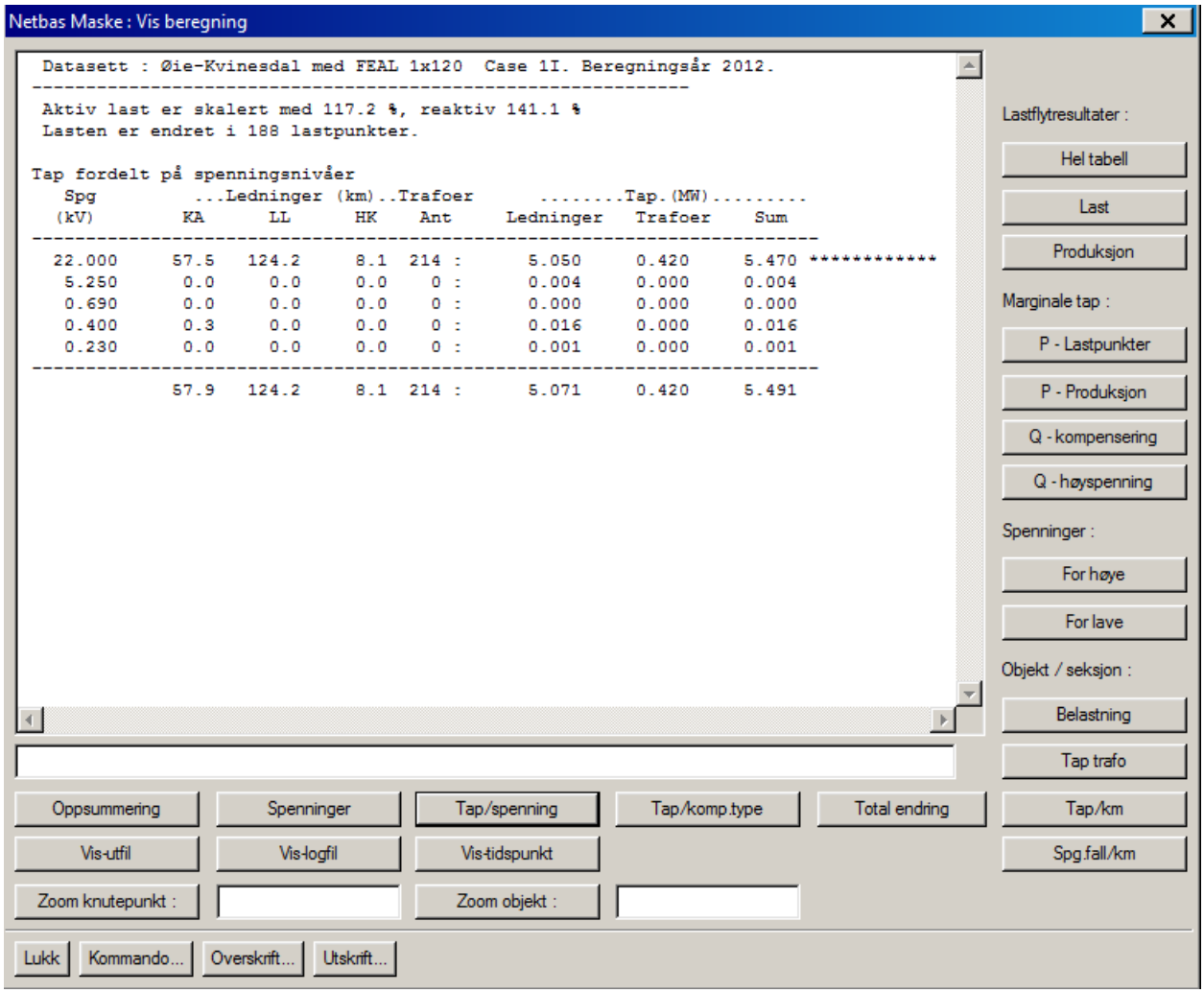

Figure J.1: Case 1I, transmission losses

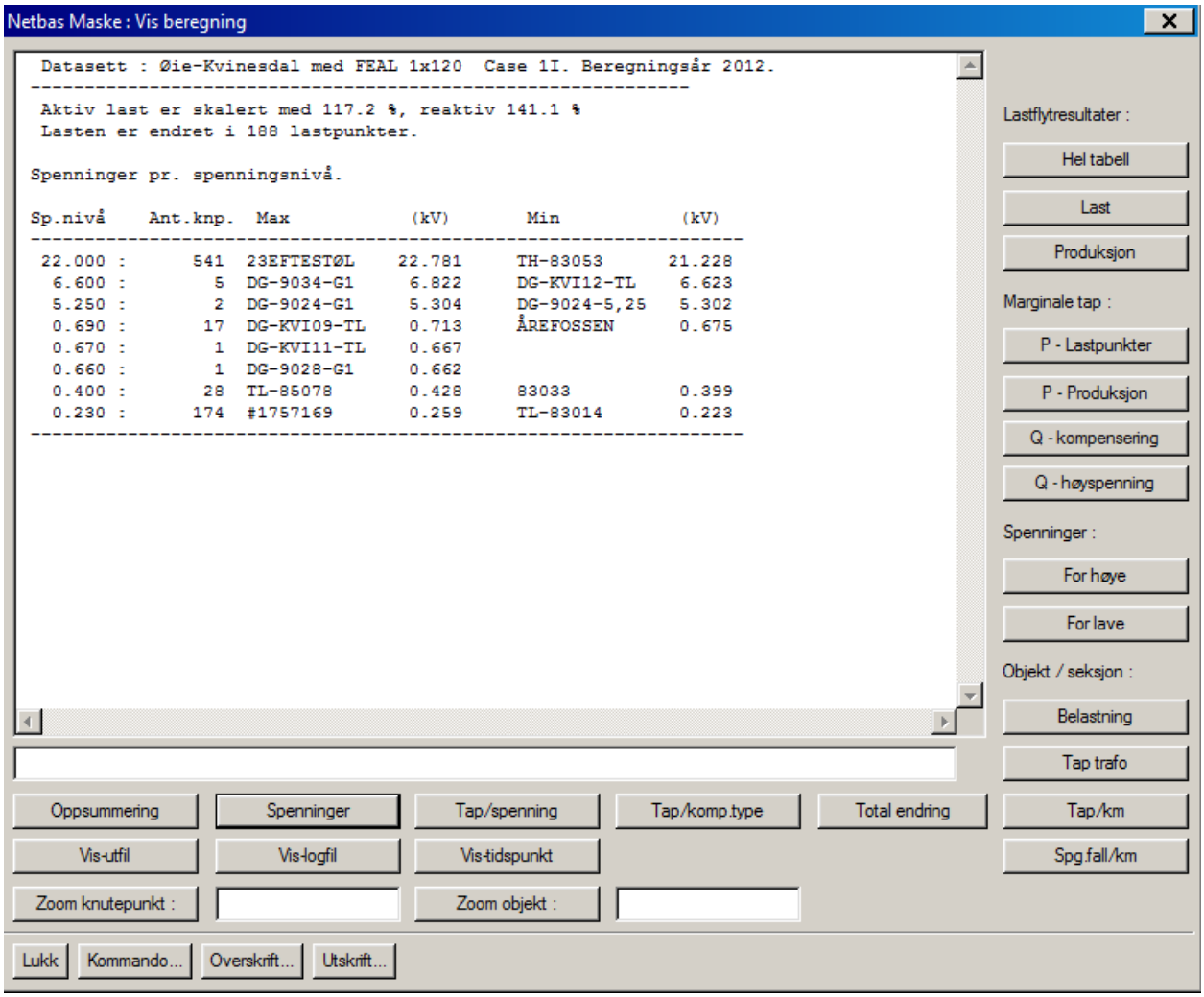

Figure J.2: Case 1I, Max/Min voltage levels

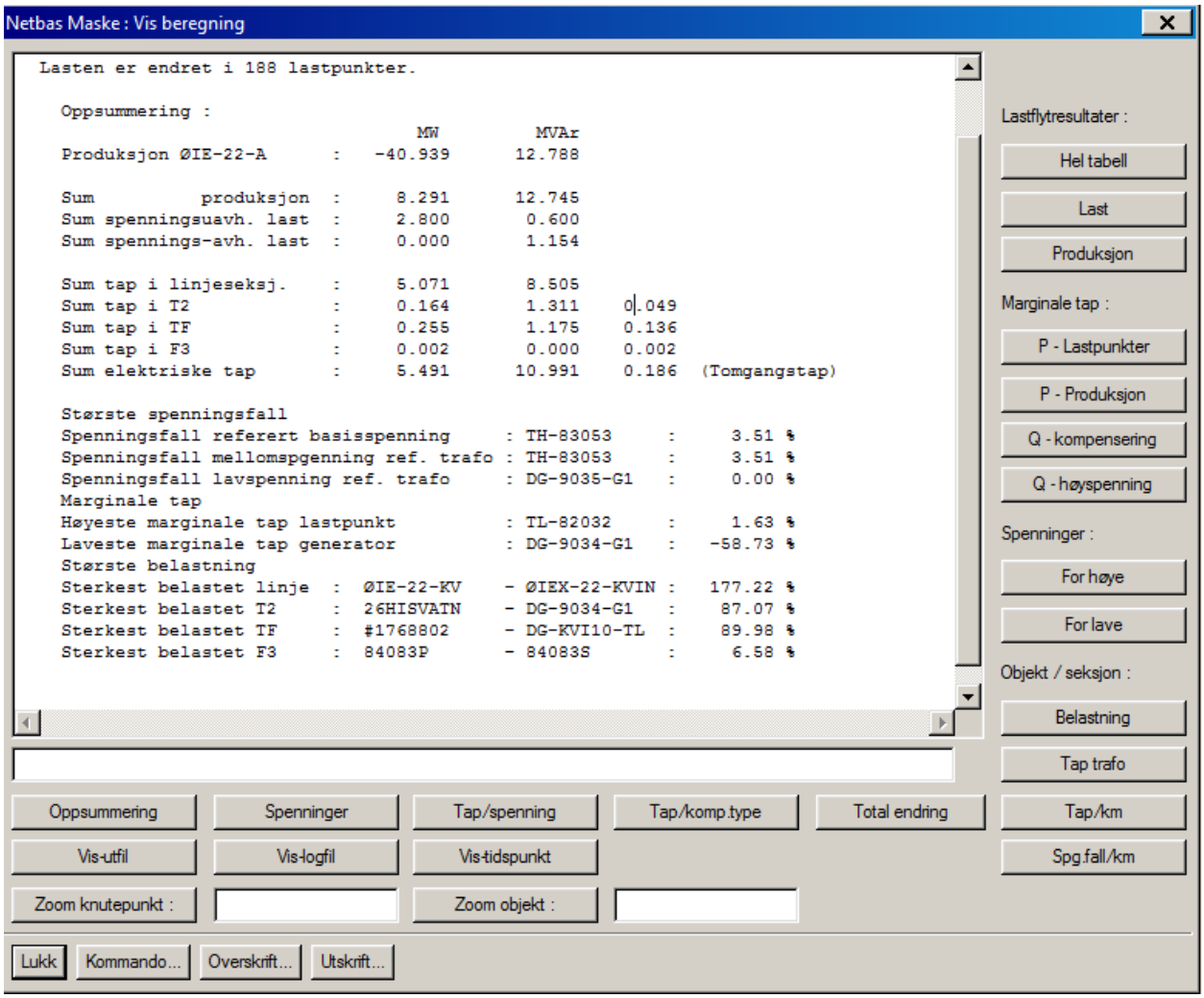

Figure J.3: Case 1I, summary

Appendix K

Case 2A simulation results

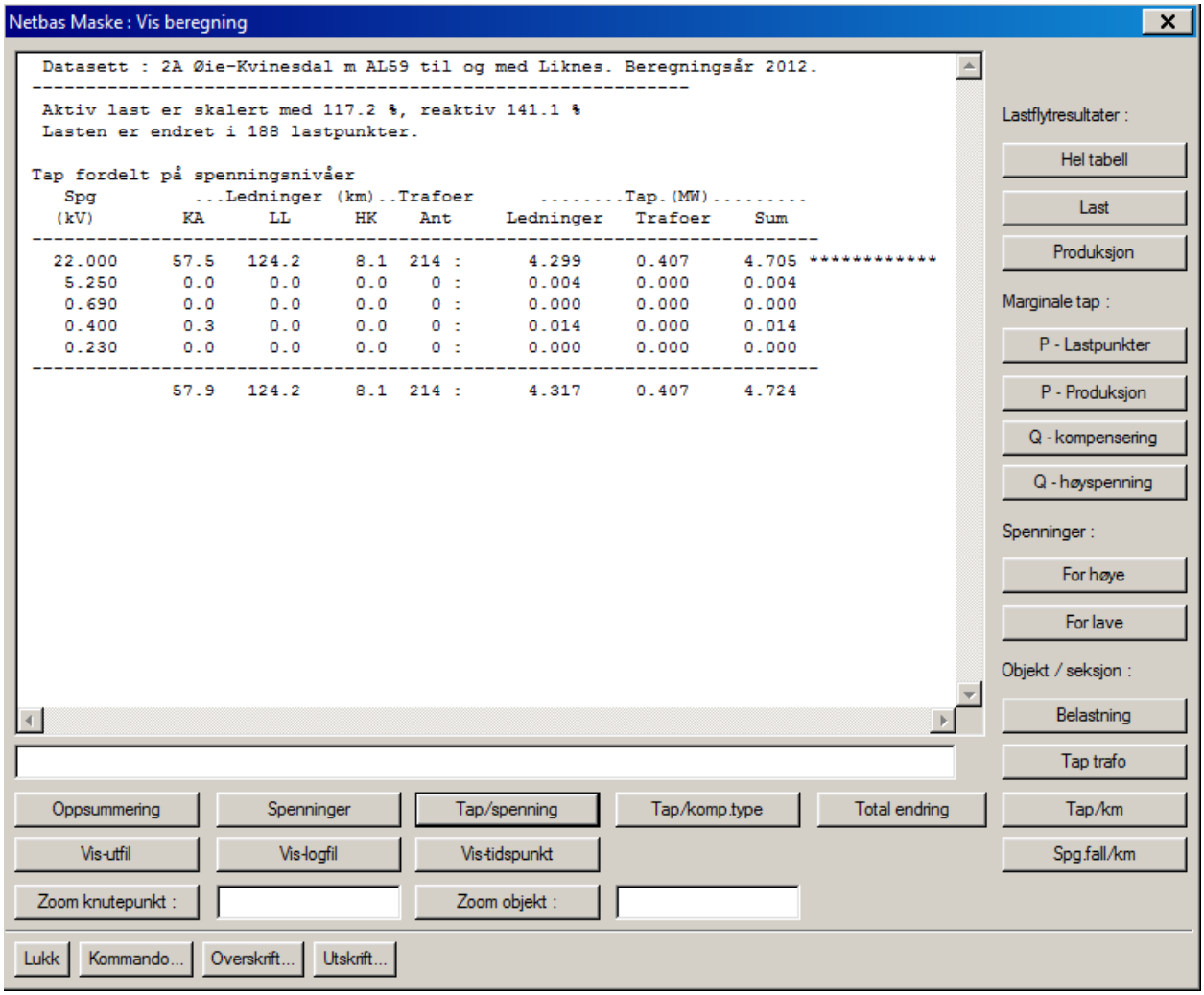

Figure K.1: Case 2A , transmission losses LLHP

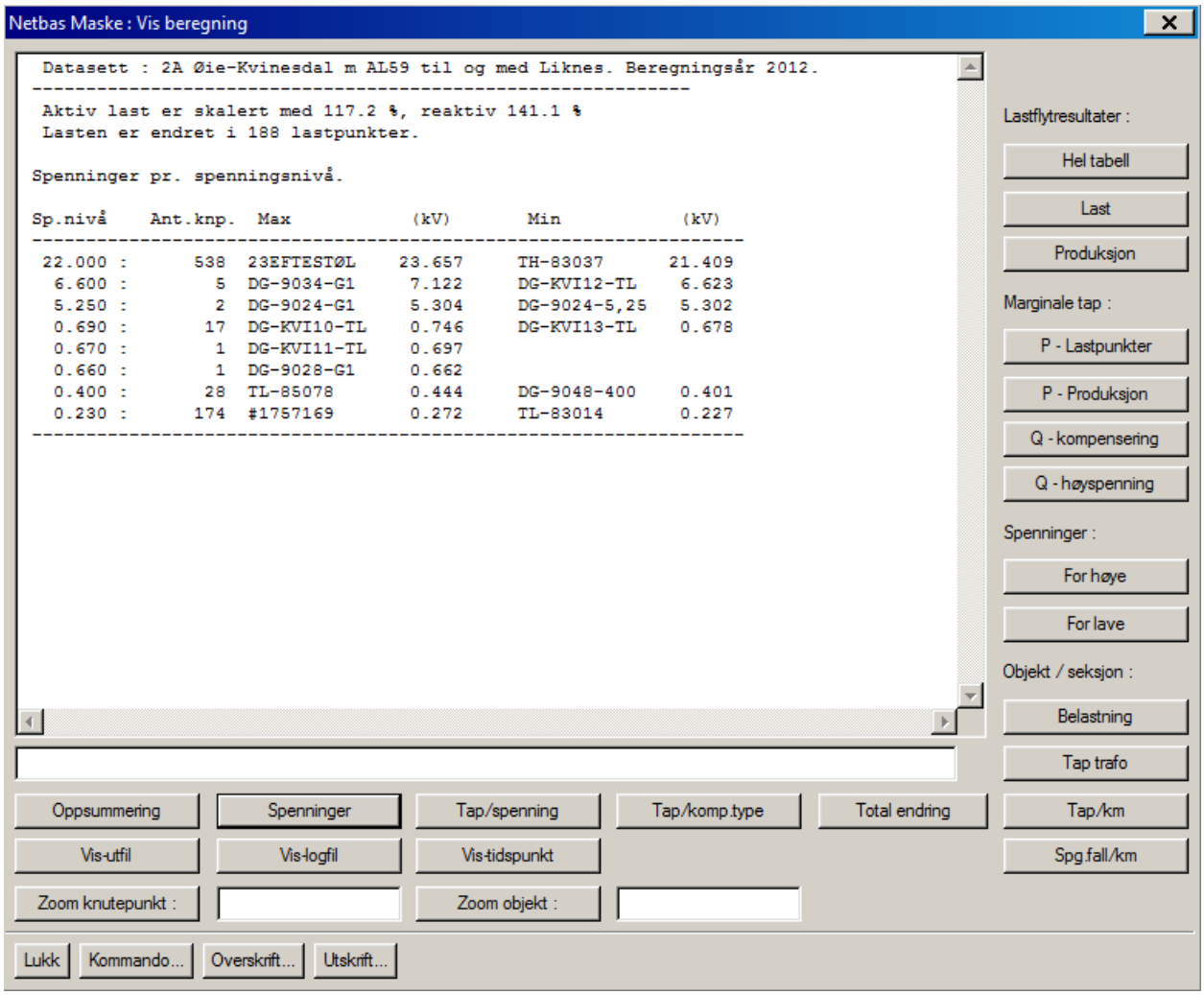

Figure K.2: Case 2A, Max/Min voltage levels LLHP

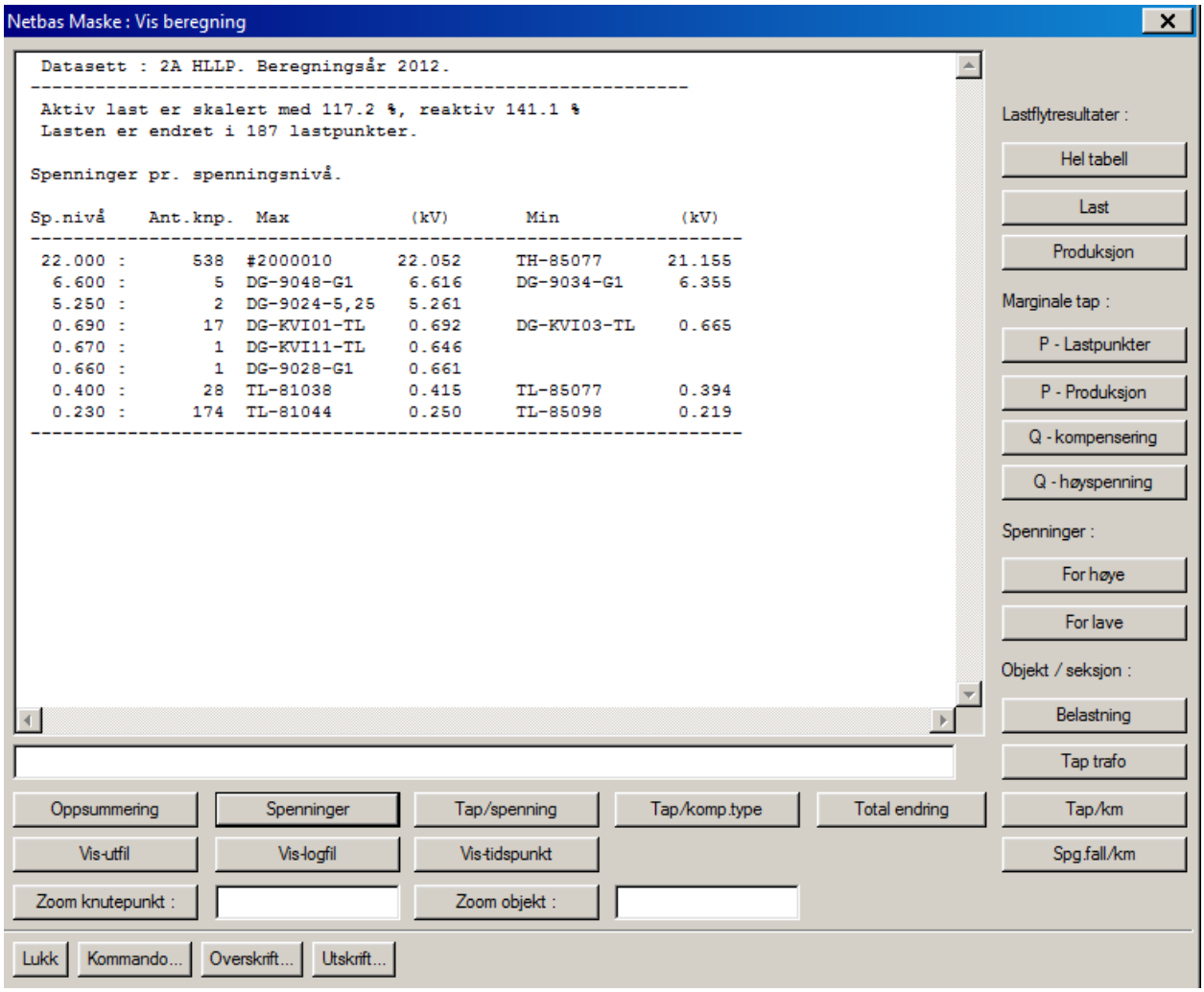

Figure K.3: Case 2A, Max/Min voltage levels HLLP

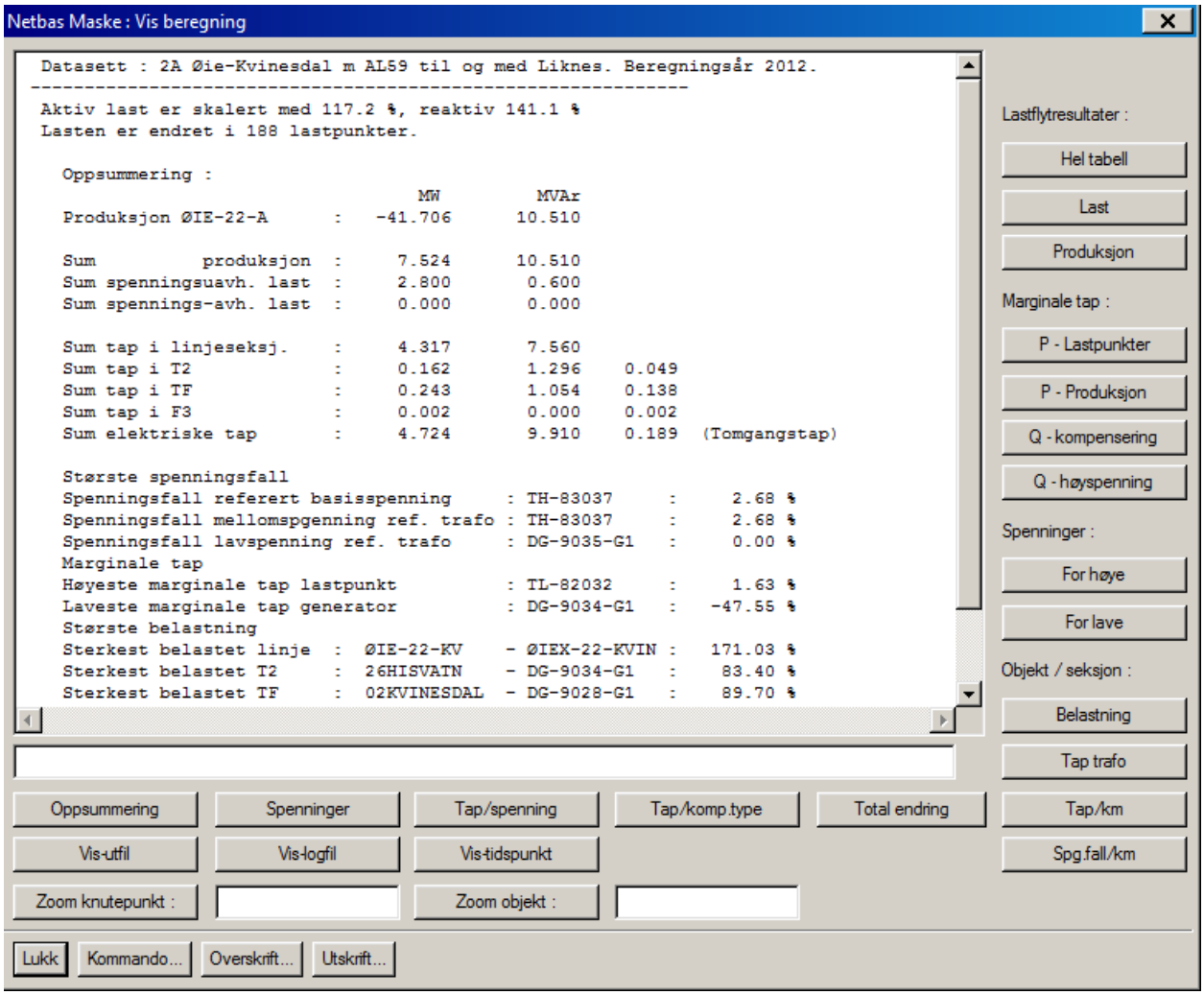

Figure K.4: Case 2A, summary LLHP

Appendix L

Case 2B simulation results

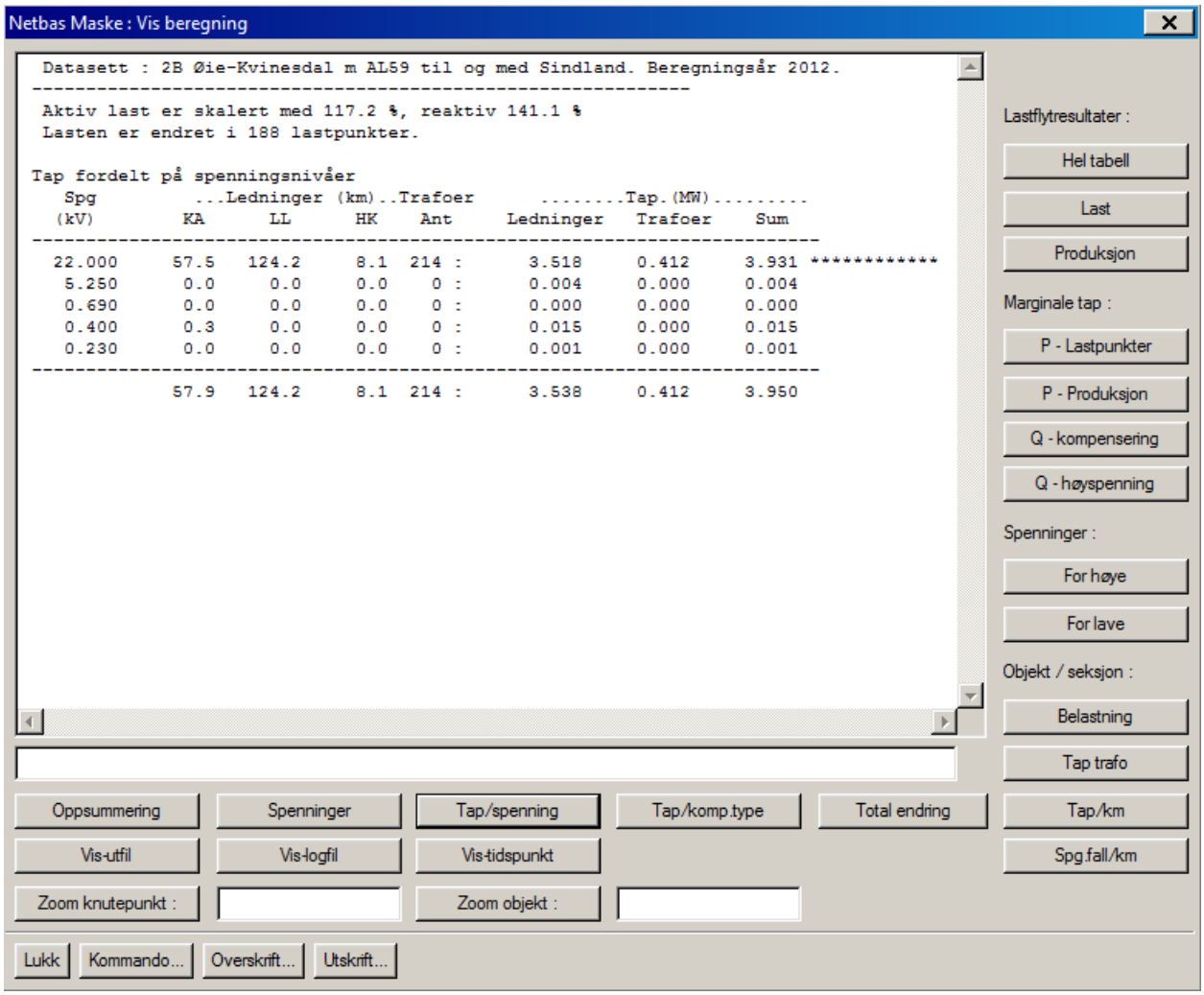

Figure L.1: Case 2B , transmission losses LLHP

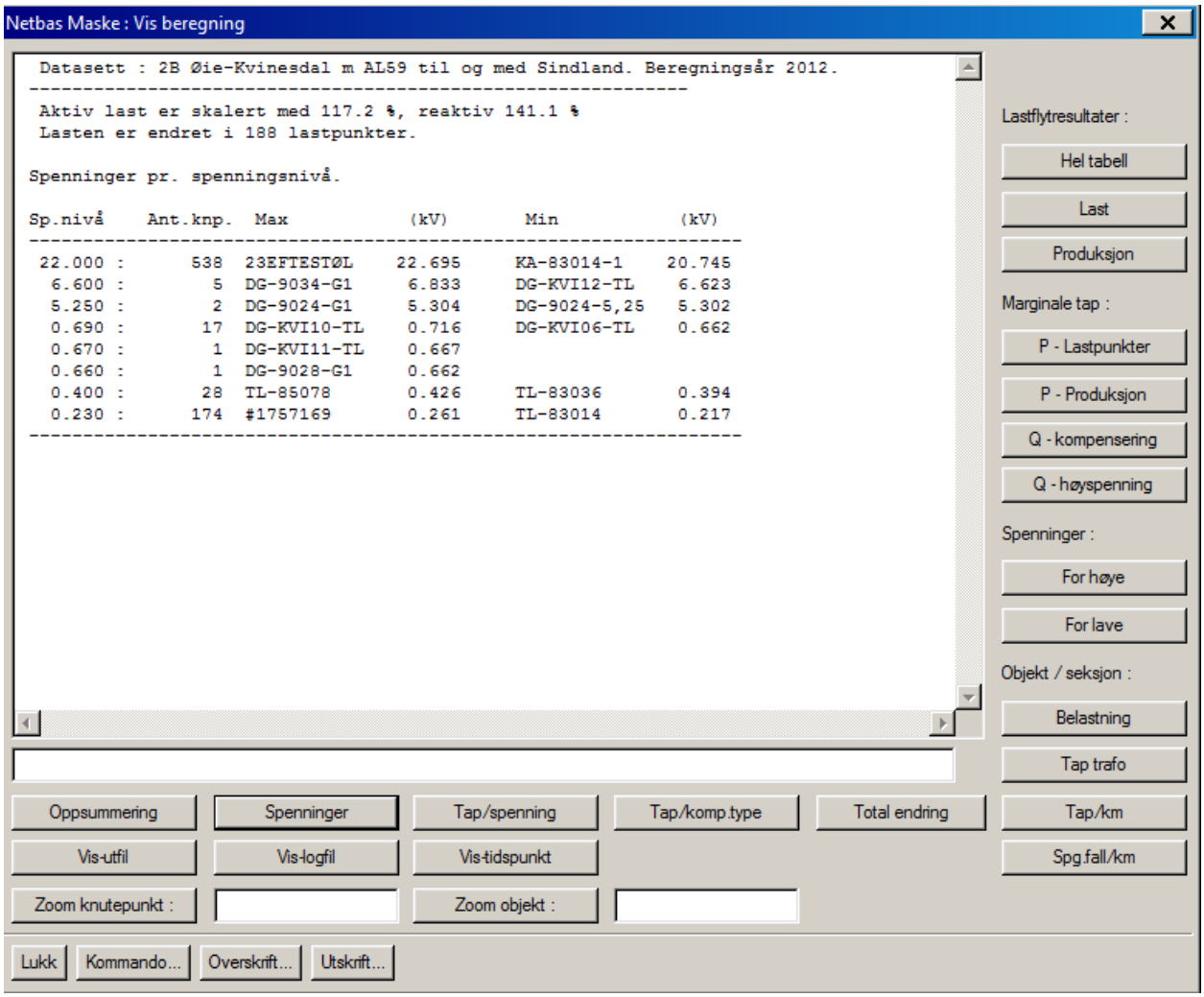

Figure L.2: Case 2B, Max/Min voltage levels LLHP

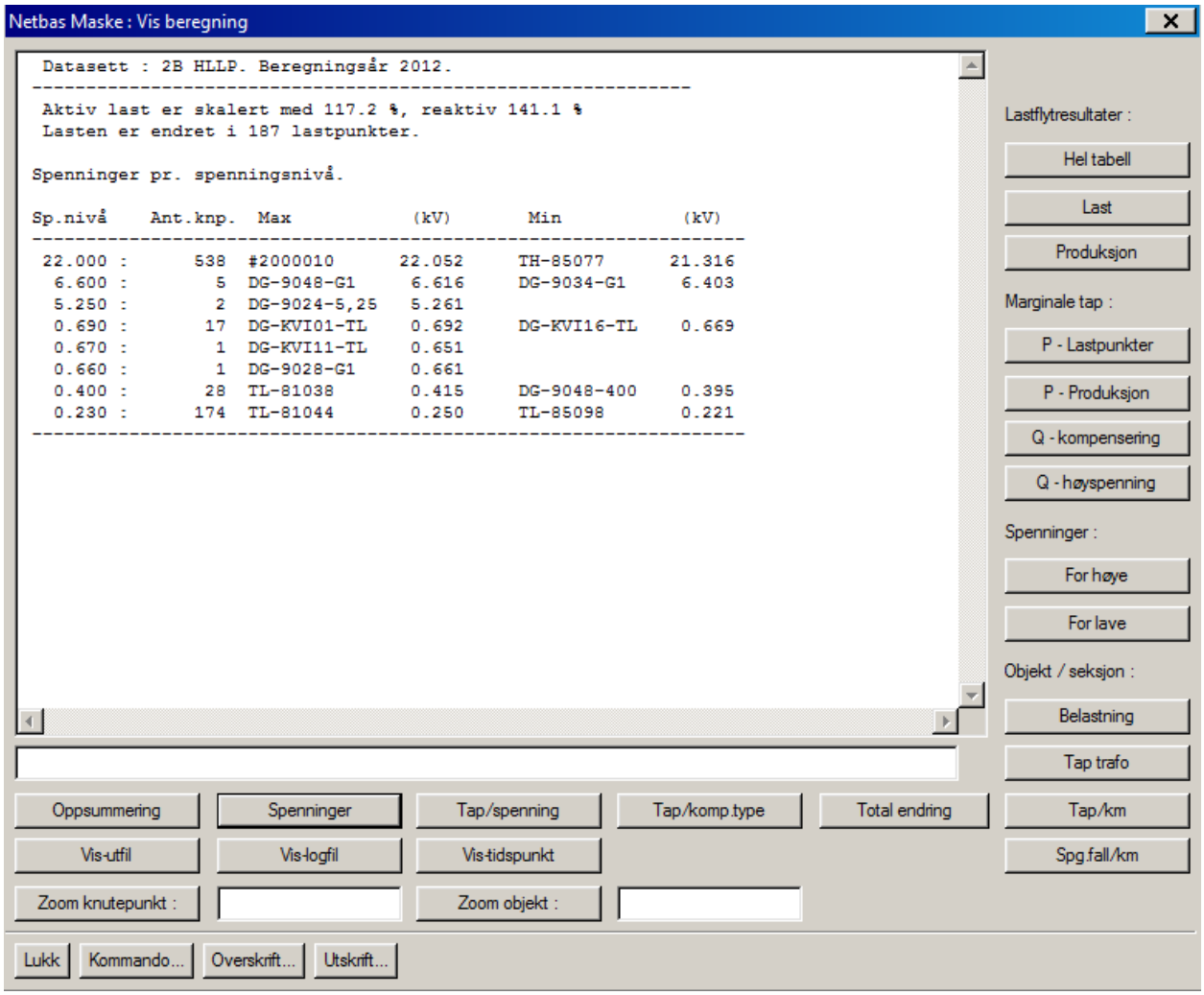

Figure L.3: Case 2B, Max/Min voltage levels HLLP

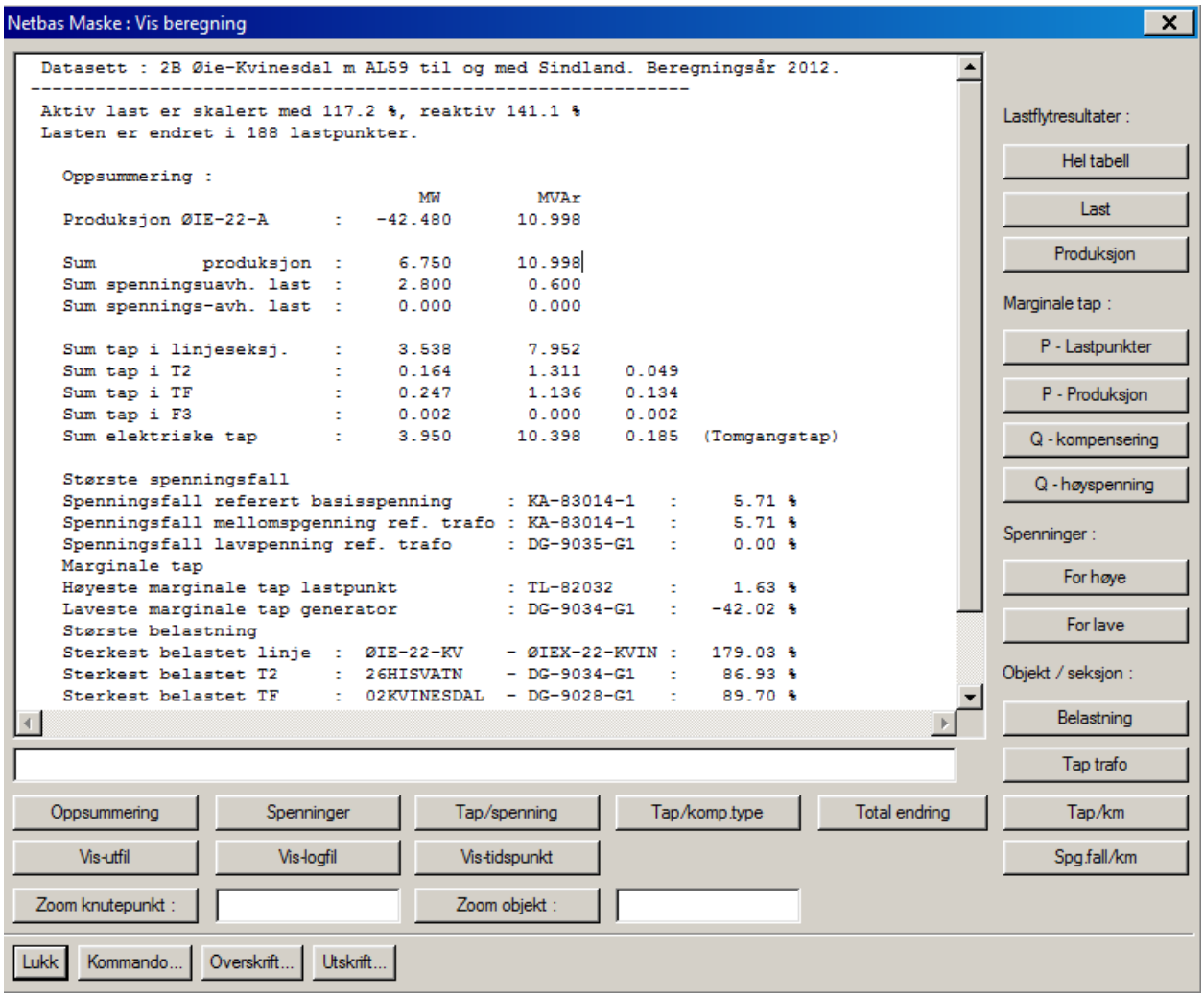

Figure L.4: Case 2B, summary LLHP

Appendix M

Case 2C simulation results

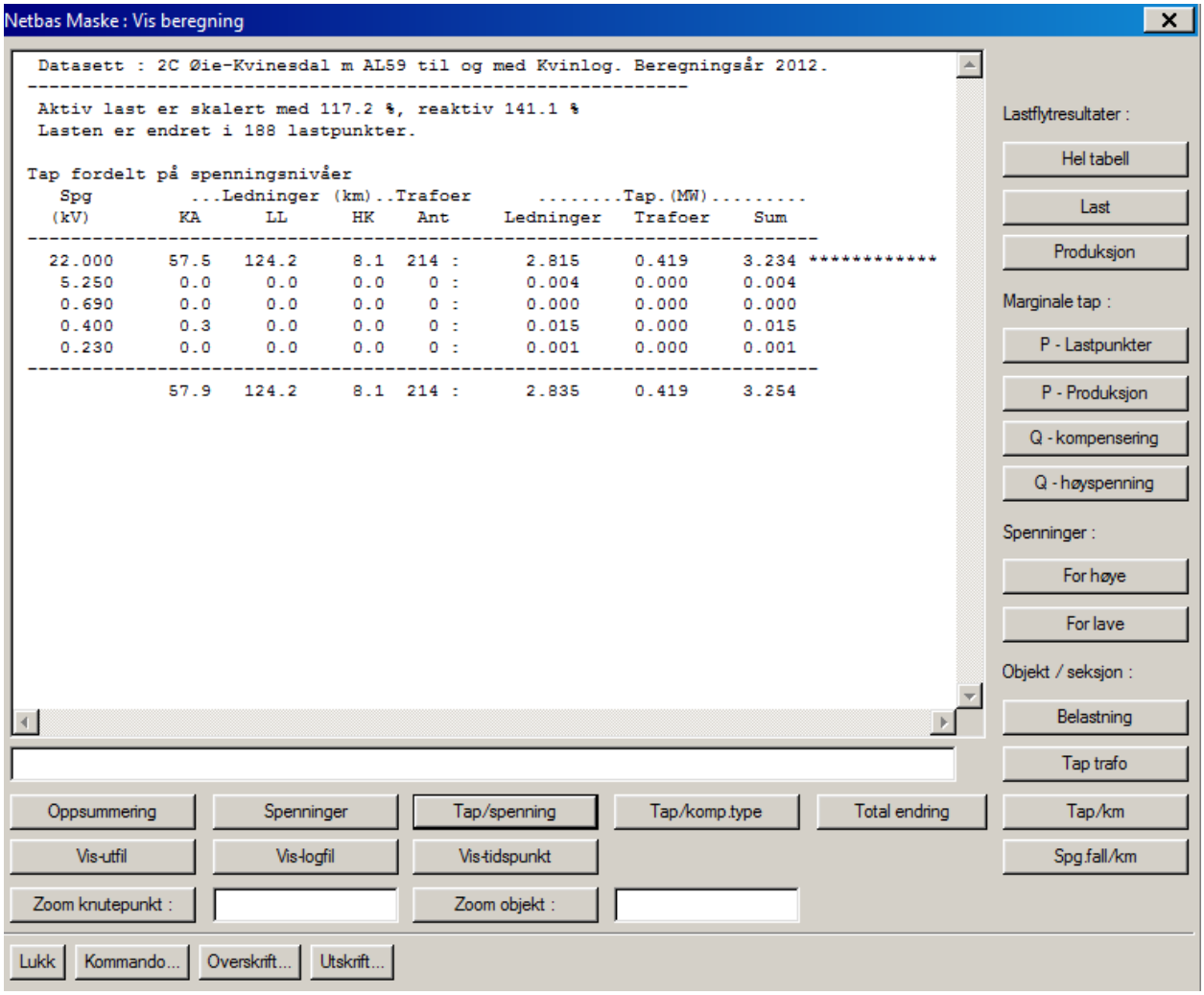

Figure M.1: Case 2C , transmission losses LLHP

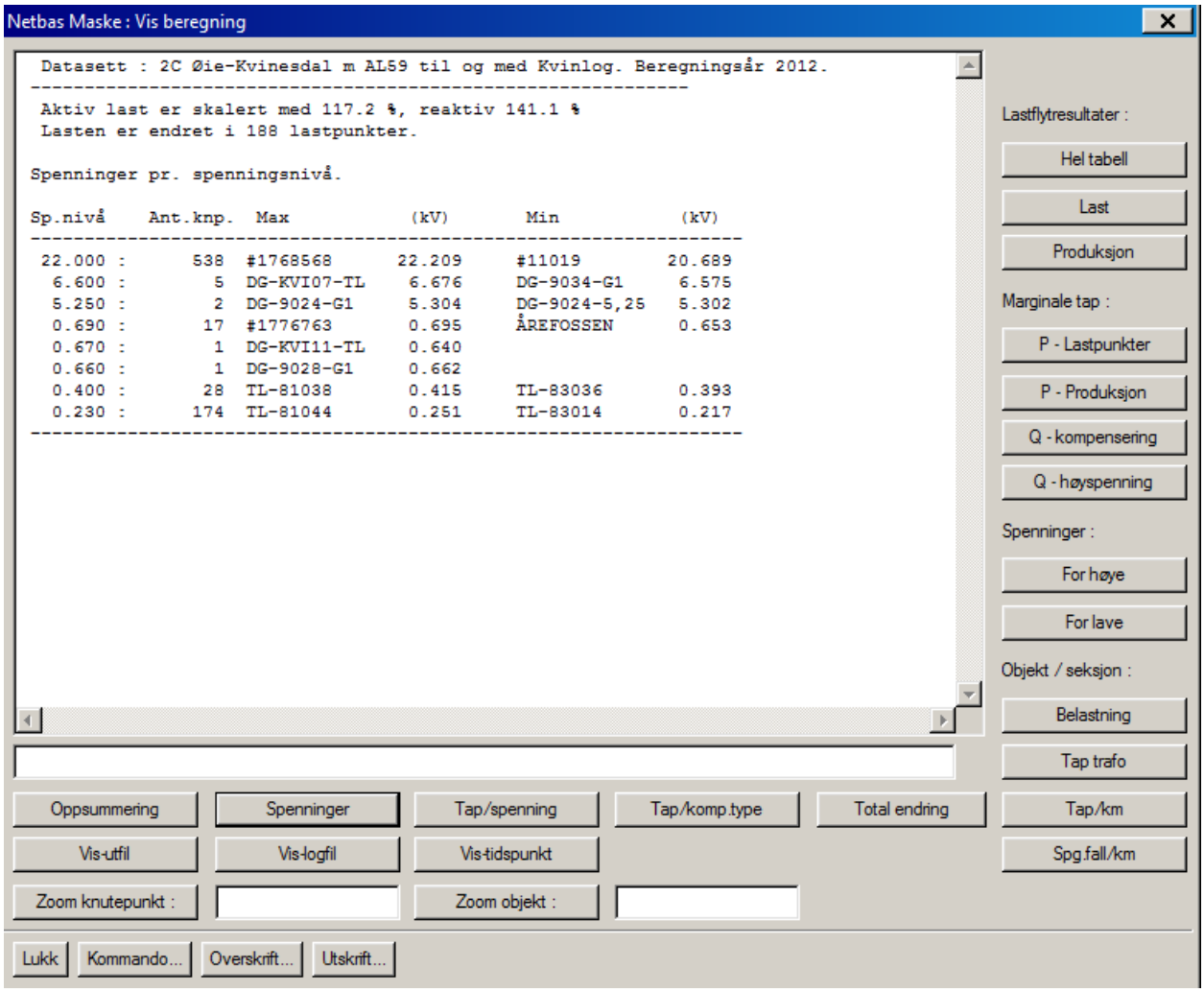

Figure M.2: Case 2C, Max/Min voltage levels LLHP

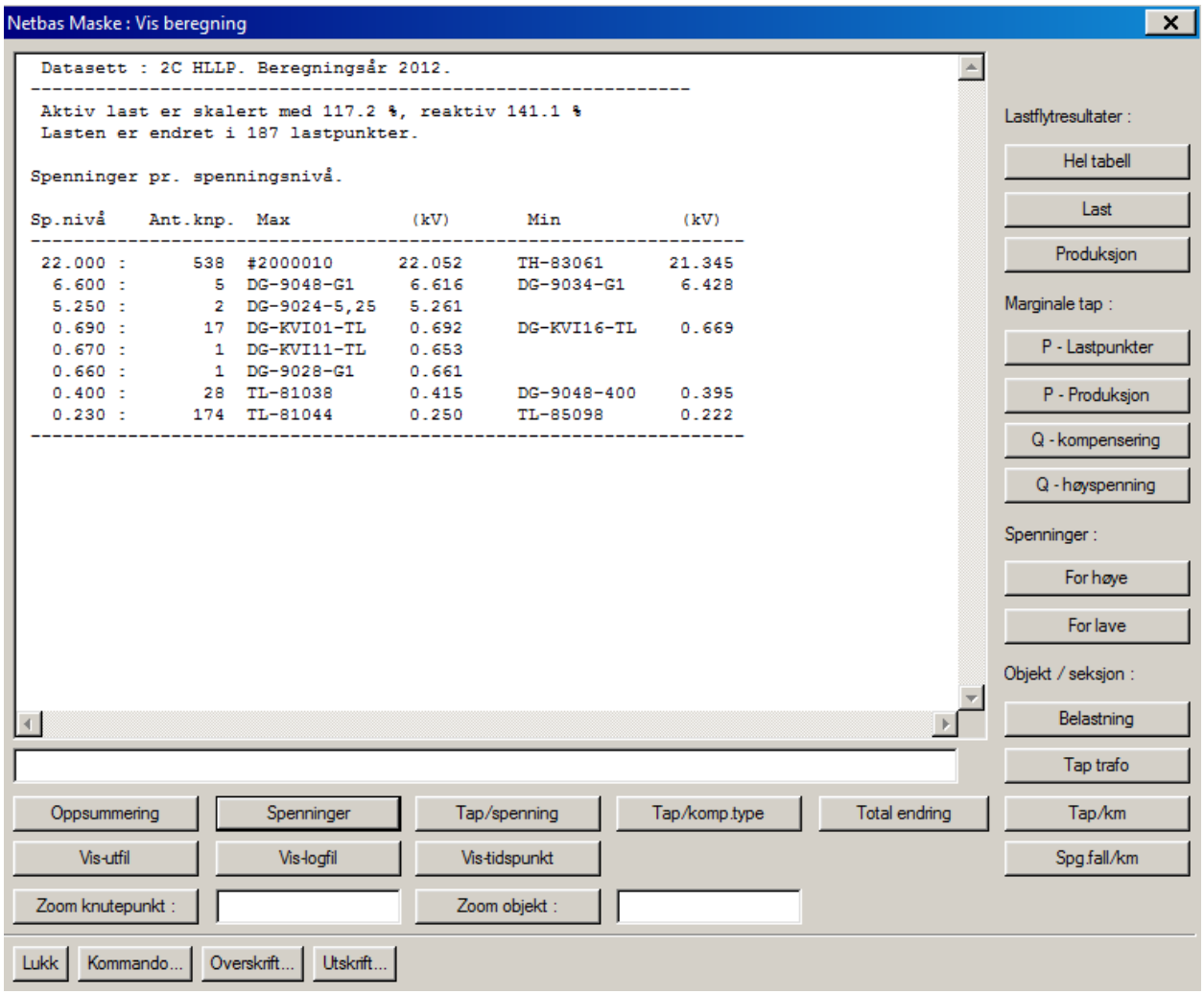

Figure M.3: Case 2C, Max/Min voltage levels HLLP

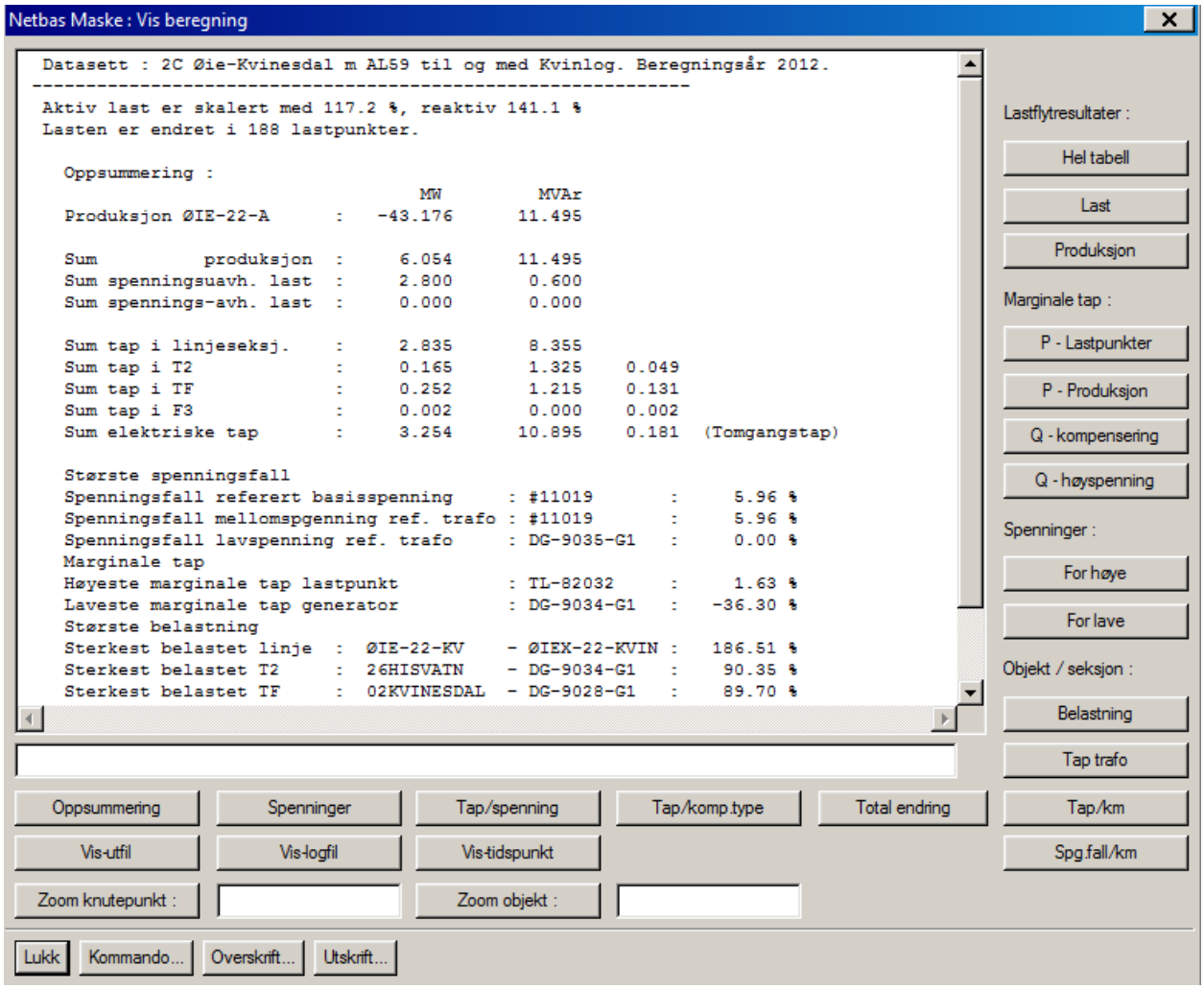

Figure M.4: Case 2C, summary LLHP